Southwest Nova Scotia Resource Assessment

Volume 3:
Acoustic Doppler Current Profiler Results

Final Report Submitted to OERA

by

J. M. McMillan, D. J. Schillinger and A. E. Hay

Department of Oceanography, Dalhousie University

June 25, 2013

Chapter 1:

1.1 Introduction

This document summarizes the ADCP data collected during 2012 in three tidal passages located in the Digby Neck area of the lower Bay of Fundy, Southwest Nova Scotia: Digby Gut (DG), Petit Passage (PP), and Grand Passage (GP). The bathymetry in each passage is shown in Figures 1.1, 1.2 and 1.3, together with the ADCP locations. The bathymetry in Digby Gut is from surveys carried out by the Canadian Hydrographic Service (CHS). The bathymetry in Petit and Grand Passages was acquired as part of this project using the WAASP multibeam sonar system on the fishing vessel *Expectations XL* (Westport). Five ADCPs were deployed in each passage in a semi-coherent array. The array geometry was a compromise among several considerations, including: (a) resolving both along- and cross-channel variations in the model-predicted flow patterns; (b) the bathymetry and overall channel geometry; and (c) locations which Fundy Tidal Inc (FTI) indicated were potential sites for in-stream turbines. In addition, a single ADCP was deployed in Indian Sluice (IS) as part of the reconnaissance component of the project. The ADCP deployment locations and water depths are listed in Table 1.1. The ADCP operating parameters and mooring configuration (see next Section) are listed in Table 1.2.

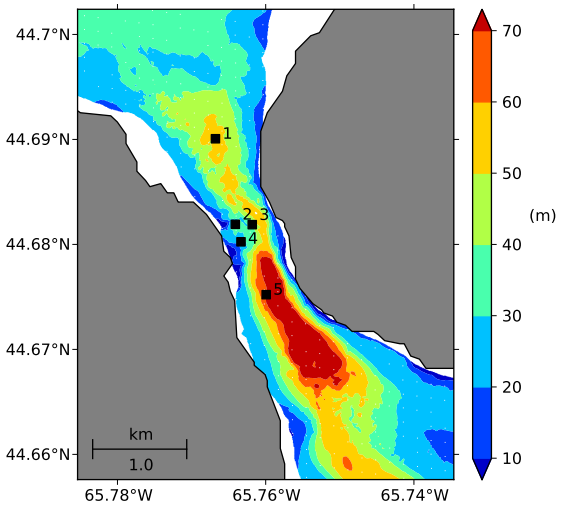

Figure 1.1: Digby Gut ADCP deployment locations and bathymetry, the latter courtesy of the Canadian Hydrographic Service.

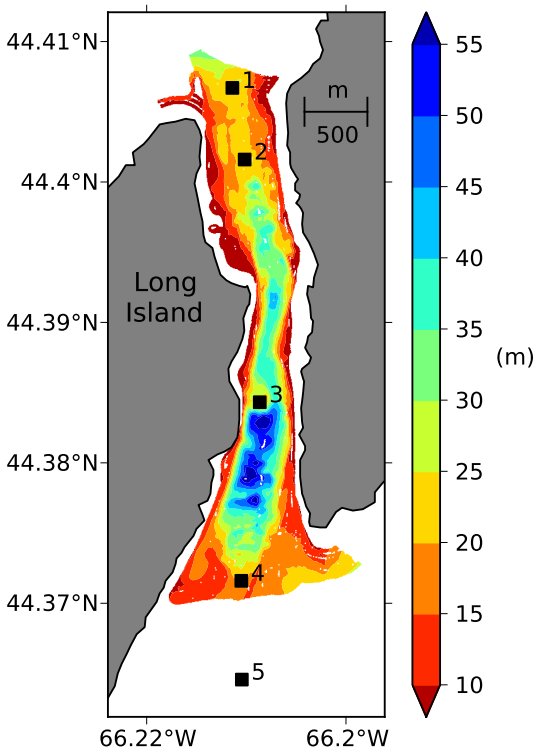

Figure 1.2: Petit Passage ADCP deployment locations and measured bathymetry data.

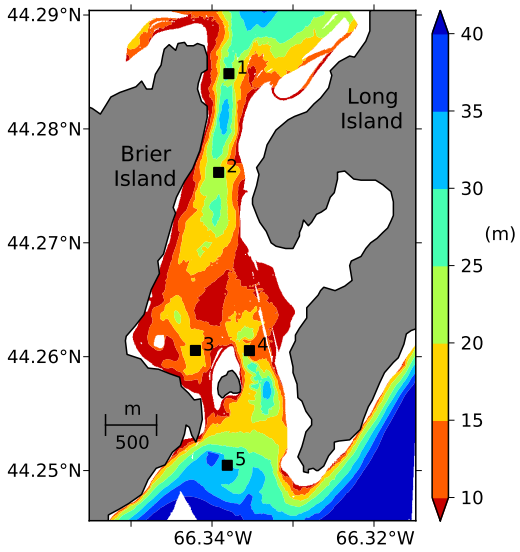

Figure 1.3: Grand Passage ADCP deployment locations and measured bathymetry data.

Site	Longitude	Latitude	Mean Depth (m)	Start Date (2012)	End Date (2012)
DG1	-65.7668	44.6901	55.5‡	Jan 30	Feb 16
DG2	-65.7641	44.6819	34.1*	Jan 30	Mar 5
DG3	-65.7618	44.6819	36.3*	Jan 30	Mar 16
DG4	-65.7633	44.6803	31.6	Jan 30	Mar 16
DG5	-65.7599	44.6752	67.4	Jan 30	Feb 29
GP1	-66.3379	44.2848	†	Jul 26	Aug 27
GP2	-66.3392	44.2762	22.5	Jul 26	Sep 6
GP3	-66.3421	44.2606	17.8	Jul 26	Aug 27
GP4	-66.3354	44.2605	15.4	Jul 26	Aug 27
GP5	-66.3381	44.2505	31.2	Jul 26	Aug 27
PP1	-66.2114	44.4067	35*	Sep 17	Oct 17
PP2	-66.2102	44.4016	23.3	Sep 17	Oct 17
PP3	-66.2087	44.3843	31.4	Sep 17	Oct 17
PP4	-66.2105	44.3716	23.0	Sep 17	Oct 17
PP5	-66.2104	44.3646	31.9	Sep 17	Oct 17
IS1	-65.5686	43.7716	∼6*	Nov 8	Nov 16

Table 1.1: Southwest Nova Scotia ADCP deployment summary. The depths are as measured by the ADCP. The asterisks indicate ADCPs that moved at some point during the deployment, due to ambient currents. The ‡ indicates the mooring that was found floating at the surface, likely having been hauled to the surface by a scallop dragger. The † symbol for GP1 indicates no velocity data from this instrument, due to a firmware problem in the ADCP.

Site	Configuration	Frequency (kHz)	Pings per Ensemble	Ensemble Interval (s)	Bin Size (m)	RBR Sensor
DG1	SUBS	300	75	150	1.0	yes
DG2	Bottom pod	600	40	20	0.5	no
DG3	Bottom pod	600	40	20	0.5	no
DG4	Bottom pod	600	80	120	0.5	yes
DG5	SUBS	300	75	150	1.0	yes
GP1	Bottom pod	600	80	120	0.5	no
GP2	Bottom pod	600	49	20	0.5	no
GP3	Bottom pod	600	49	20	0.5	no
GP4	Bottom pod	600	80	120	0.5	yes
GP5	SUBS	600	80	120	0.5	no
PP1	Bottom pod	600	100	120	0.5	no
PP2	Bottom pod	600	40	20	0.5	yes
PP3	Bottom pod	600	40	20	0.5	no
PP4	Bottom pod	600	100	120	0.5	yes
PP5	SUBS	600	100	120	0.5	no
IS1	Bottom pod	1200	90	60	0.5	no

Table 1.2: ADCP mooring configurations and operating parameters. RBR pressure temperature sensors were deployed with some moorings, as indicated.

1.2 Deployment Methodology

Two types of mooring were implemented for this study. One employed a streamlined underwater buoyancy system (SUBS) to support the upward-looking ADCP. This mooring type was used for deeper locations: i.e. water depths of 50 m or more. Depending on water depth and the ADCP acoustic frequency, the ADCP/SUBS package was located from 5 to 10 meters above the seabed, with an acoustic release between the ADCP and an expendable anchor, as sketched in Figure 1.4.

We have been using SUBS-based ADCP moorings since 2003. However, the method is problematic in the present application for three reasons: (a) the lower part of the bottom boundary layer is not captured; (b) the ballast, typically a railway wheel, is left behind after recovery; and (c) the SUBS package does not provide a sufficiently stable platform for measuring short-term velocity fluctuations in these high speed, high Reynolds number flows. Figure 1.5 illustrates the latter issue. Shown are the time series and probability distributions of the standard deviation of the ADCP pitch. These values, internally recorded in the instrument, are based on values registered during the ensemble-averaging interval, which was 2 minutes in this case (GP5, Table 1.2). The fluctuations are quite large, reaching maximum values approaching 15 degrees. The high standard deviations, occurring roughly twice per day, are associated with the high speed currents which, at this location (see Figure 1.3), are strongest during ebb .

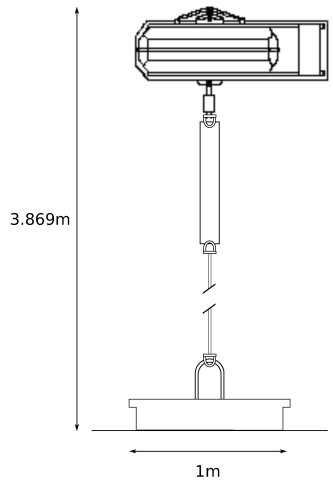

Figure 1.4: SUBS mooring sketch, showing from top to bottom, the SUBS with upward-looking ADCP, the acoustic release, the tether and the train wheel on the seabed.

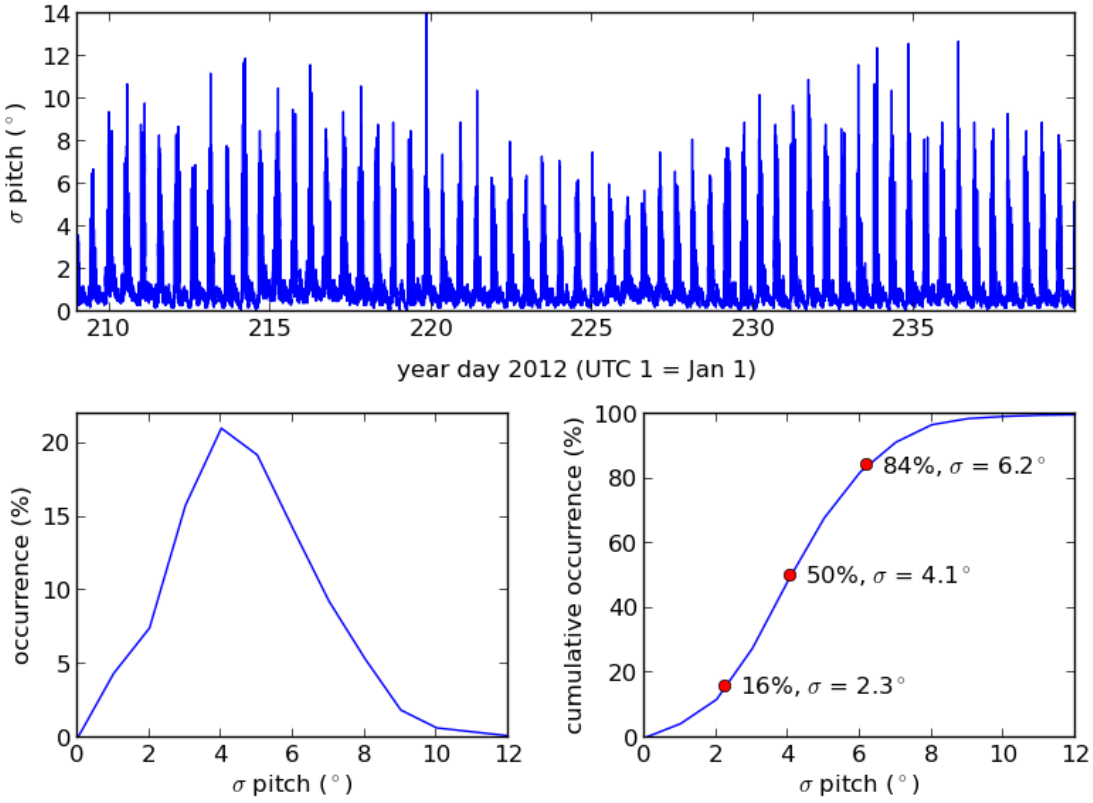

Figure 1.5: Time series of the standard deviation, σ, of the ADCP pitch at GP5 within the 2-minute intervals of the velocity ensembles recorded by the instrument. The corresponding probability density and cumulative probability distribution for flow speeds greater than 0.7 m/s are also shown, the latter indicating the 16, 50 and 84 cumulative percent values.

The statistics of pitch and roll standard deviations (i.e. σ) for all SUBS-based ADCPs are summarized in Table 1.3. Those for the heading are listed in Table 1.4, for flood and ebb tide separately. These standard deviations in the attitude angles of the SUBS-based ADCPs were based on 75 to 100 values measured at every ping during the 2 to 2.5 minute ensemble intervals (Table 1.2). The maximum instantaneous variations were necessarily much higher. Values as high as 30 degrees (i.e. 2 standard deviations) are likely, and well beyond the acceptable limits for obtaining reliable estimates of the short-term velocity variability.

Site	N	**Pitch (°)**				**Roll (°)**			
		P_{16}	P_{50}	P_{84}	P_{95}	P_{16}	P_{50}	P_{84}	P_{95}
DG1	5910	1.5	2.6	4.1	5.4	1.6	2.6	3.9	4.8
DG5	9311	0.6	1.8	3.9	5.4	0.7	1.9	3.9	5.1
GP5	1488	2.3	4.1	6.2	7.7	2.2	3.8	5.9	7.4
PP5	4838	1.5	2.5	3.7	4.6	1.3	2.2	3.2	4.0

Table 1.3: Pitch and roll standard deviations (in degrees) at the indicated percentiles for all SUBS-based ADCPs, for vertically-averaged flow speed greater than 0.7 m/s. The values listed for P_x indicate that $100 - x\%$ of the observed values exceeded the listed value: e.g. for DG1, 5 % of the pitch values exceeded 5.4 degrees. N is the number of data points included in the estimates. One degree bins were used for computing the probability densities and cumulative distributions. See also Figure 1.5.

Site	**Ebb Heading (°)**					**Flood Heading (°)**				
	N	P_{16}	P_{50}	P_{84}	P_{95}	N	P_{16}	P_{50}	P_{84}	P_{95}
DG1	3142	5.9	7.8	10.2	12.6	2768	4.6	6.1	7.6	8.8
DG5	4893	2.1	3.7	5.9	7.5	4418	5.4	9.7	15.5	19.9
GP5	1411	9.5	14.6	23.7	31.7	77	3.5	5.4	13.2	16.8
PP5	4838	5.3	7.6	11.2	14.3	0	-	-	-	-

Table 1.4: Heading standard deviations (in degrees) at the indicated percentiles for all SUBS-based ADCPs, for vertically-averaged flow speed greater than 0.7 m/s. The values listed for P_x indicate that $100 - x\%$ of the observed values exceeded the listed value. N is the number of data points included in the estimates. One degree bins were used for computing the probability densities and cumulative distributions. See also Figure 1.3.

Because of the above issues with the SUBS-based moorings, we implemented a bottom pod mooring with a float-line recovery system for this project. A burn-wire, when activated via an acoustic command, releases a float which carries the recovery line to the surface. The entire package is retrieved, including ballast. Thus littering the seafloor in these relatively confined passages with mooring ballast (issue b above) is avoided, which would otherwise be a potential problem given the multiple future deployments that can be anticipated as tidal power research and development proceeds. Also, by not using SUBS-type moorings a compact low-profile assembly can be achieved (Figure 1.6). The bottom pod is assembled from non-ferromagnetic materials, for ease and accuracy of the ADCP compass calibration procedure. The pod when deployed rests directly on the seabed, and the ADCP velocity

profile spans more of the water column than is possible with the SUBS-based mooring design using a single instrument. In particular, in these high Reynolds number flows enough of the lower part of the bottom boundary layer is captured to obtain reliable estimates of bottom stress.

Due to its low profile, the pod is exposed to the lower speed flow in the inner boundary layer, and therefore reduced drag. (Further drag reduction could be accomplished by adding an outer skirt to the pod frame.) The non-ferrous ballast is in the form of 3 disks bolted to the base of the frame, and serves as the three feet, thereby providing a 3-point stance for maximum stability on an irregular surface. In this study, 150 pounds of ballast was usually used; 300 pounds for locations in which the model-predicted maximum currents were ca. 4 m/s or more.

Figure 1.6: ADCP bottom pod over the side, immediately prior to deployment.

Having had no prior experience with this particular burn-wire release, the bottom pods were deployed with two independent float-line/release systems for redundancy, and in depths less than 20 to 30 m to allow for diver recovery if needed. As it turned out, this precautionary approach was useful, as we did encounter several problems during the course of the experiment, problems which were resolved with minor modifications to the system design.

For the first deployments (in DG), the float lines came loose and the pods moved during deployment due to the increased drag (Table 1.1). After fixing this problem, only two 150-pound pods moved in subsequent deployments. In one case (GP2, Table 1.6) the ADCP tilt sensor and compass indicated that the pod attitude and orientation shifted during the periods of high flow associated with spring tides. In the second case (PP1, Table 1.1), the acoustic range to the release immediately prior to recovery indicated that the pod had moved about 1 km from the deployment location, and into ca. 50 m deep water. This displacement was confirmed after recovery by the pressure record which registered an increase from the initial 25 m mean water depth to 45 m mean depth. We have since opted for 300 pounds minimum ballast on all ADCP bottom pods.

In one instance neither of the two floats was released, and the pod was recovered by SCUBA divers. Each float sits atop the recovery line within its cylindrical cannister. The seabed material at this site consisted of mobile shell hash, and during the deployment pieces of shell remobilized by the current settled into the open mouth of the cannister and became lodged between the float and the cannister wall, jamming the float in place. A lid has since been added to seal the top of the cannister until the release is activated.

Time series of the heading, pitch, and roll at PP3, a bottom pod, are presented in Figure 1.7. The values are not constant. Note in particular the abrupt ca.10 to 20 deg changes in heading shortly after deployment and before recovery. Otherwise the pod remained very stable, with small (2 to 3 deg or less) changes in its attitude relative to vertical and magnetic north, clearly modulated by the tide.

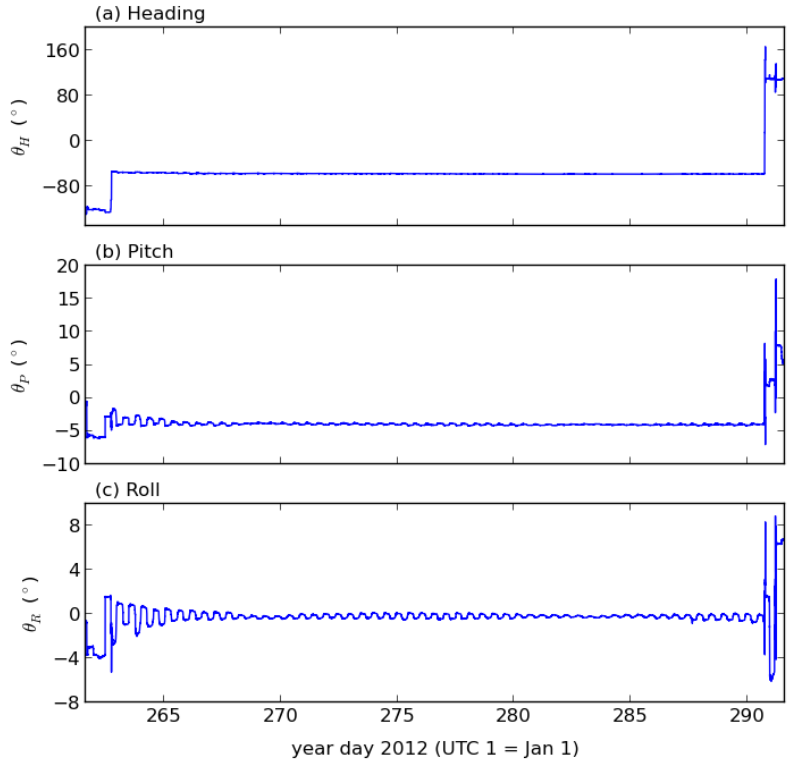

Figure 1.7: PP3 heading, pitch and roll.

Time series of the ADCP orientation parameters at another bottom pod site, GP4, are shown in Figure 1.8. Small amplitude tidally-modulated variability is again present. Also, one major orientation shift occurred, resulting in a 10 degree change in the heading. Both the small and large amplitude changes at this site and at PP3 were associated with the higher speed currents associated with spring tides (see the Appendices).

The mean and standard deviation of the ADCP orientation parameters for all bottom pod moorings are listed in Table 1.5. The mean values are the average over the length of the record of the orientation values recorded with each ensemble. Similarly, the standard deviations are the root mean square deviations from these mean values. With the exception

of DG2 and DG3 (which as described above were dragged when their recovery lines worked free), the mean values of pitch and roll are all quite small (6 degrees or less). One downside of the bottom pod approach is that there is no control over the orientation of the pod once on bottom. Thus, it is encouraging that large tilt angles not arise in these deployments, despite the variable bottom roughness in these passages.

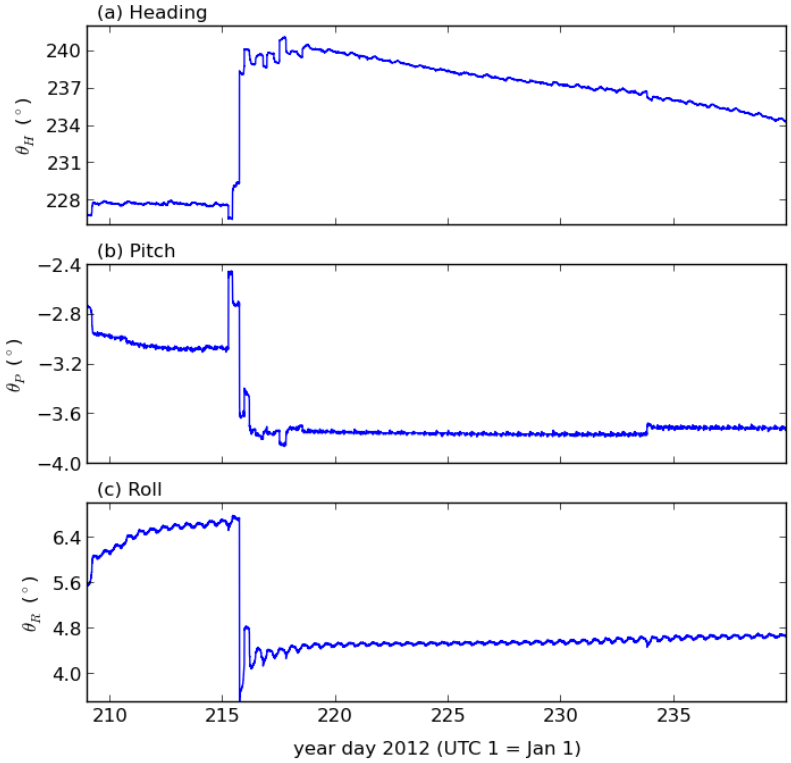

Figure 1.8: PP3 heading, pitch and roll.

Site	Heading (°)		Pitch (°)		Roll (°)	
	Mean	Std. Dev.	Mean	Std. Dev.	Mean	Std. Dev.
DG2	345.7	11.8	-9.0	6.5	-27.2	2.7
DG3	371.0	40.5	4.1	9.0	15.5	6.7
DG4	207.3	0.9	-1.8	0.4	0.0	0.2
GP1	51.0	2.1	-0.6	0.4	-3.6	0.1
GP2	267.0	6.0	1.4	3.6	-0.5	1.3
GP3	83.6	4.7	6.0	0.0	-2.2	0.0
GP4	235.6	4.4	-3.6	0.3	5.0	0.8
PP1	232.7	30.4	-1.6	2.0	2.6	2.8
PP2	314.1	28.2	0.1	1.7	-1.2	1.2
PP3	-55.1	31.0	-3.7	1.5	-0.2	1.1
PP4	79.3	4.3	-4.0	1.1	-3.1	0.6
IS1	219.8	49.2	0.8	2.8	0.7	2.1

Table 1.5: Attitude parameter statistics for all bottom-mounted ADCPs

1.3 Analysis

Principal ebb and flood flow directions were computed from the vertically-averaged velocity components: i.e. averaging from the first ADCP range bin to within 95% of the range to the sea surface. (For the 20-degree tilt from vertical of the acoustic beam axes for RDInstruments Workhorse ADCPs, interference from the sea surface return via the transducer beam pattern sidelobes contaminates the velocities in the range bins within 5% of the vertical range to the sea surface.) Figure 1.9 shows the flow directions at GP3 and GP4. The distributions at the two sites are quite different: the flow at GP3 is both weaker and the direction more variable than at GP4. These differences are due to the narrow constriction immediately south of GP3 (Figure 1.3).

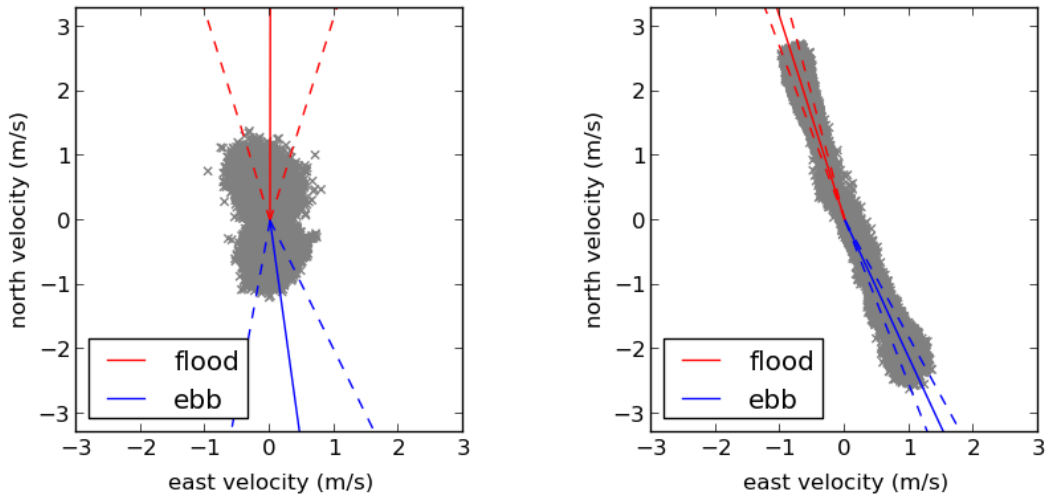

Figure 1.9: The principal flow directions at GP3 and GP4 are shown by the solid red and blue lines for the flood and ebb tides, respectively. The dashed lines indicate ±1 standard deviation from the mean. Individual values are the grey markers.

Tidal constituents were estimated from the pressure and vertically-averaged velocity time series using TTide. As an example, the best-fit parameters for the principal constituents at GP4 are listed in Table 1.6. The RMS residuals in this case were 9.5 cm for elevation, and 21 cm/s for speed, roughly 5% and 10% of the respective maximum constituent amplitude. An example of the measured and best-fit time series is shown in Figure 1.10, together with the residual time series.

Constituent	Period	Elevation		Velocity			
	(hr)	Amplitude (m)	Phase (°)	Major (m/s)	Minor (m/s)	Inclination (°)	Phase (°)
M2	12.42	2.14	77	2.53	-0.00	111	331
N2	12.66	0.36	44	0.30	0.04	109	293
S2	12.00	0.32	123	0.32	0.02	112	25
K1	23.93	0.14	206	0.03	0.00	109	95
O1	25.82	0.12	163	0.02	-0.00	112	64
M4	6.21	0.07	112	0.07	-0.05	118	199

Table 1.6: GP4 tidal constituents, from the 31-day ADCP pressure and velocity records.

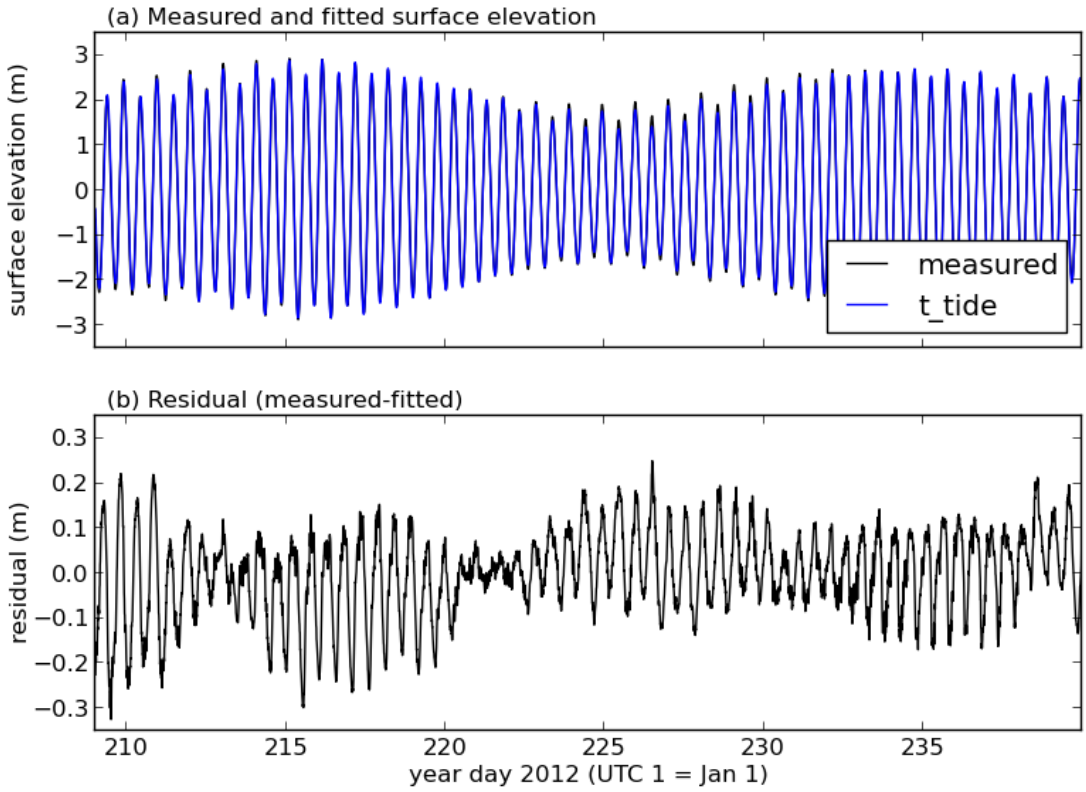

Figure 1.10: Observed and best-fit surface elevations at GP4 (top panel). The residual is shown in the lower panel.

The bottom drag coefficient, C_d, was computed from the ADCP speed profiles using the law-of-the-wall:

$$u(z) = \frac{u_*}{\kappa} \ln \frac{z}{z_o} \tag{1.1}$$

where u is the current speed, z the height above bottom, u_* the friction velocity, $\kappa = 0.4$ von Karman's constant, and z_0 the bed roughness parameter. The currents were averaged in 10 minute intervals and separated into ebb and flood. For each phase of the tide, the profiles

were grouped into 0.25 m/s speed bins (except 0.1 m/s for GP3) based on the vertically-averaged speed. The average profile was obtained for each bin. A non-linear least squares best fit to Equation 1.1 over the lower 3 to 6 m of each of the resulting profiles (Figure 1.11) yielded estimates for u_* and z_o. C_d and u_* are related via

$$u_*^2 = C_d U^2 \tag{1.2}$$

where U is a representative mean flow speed. For the present study, two values for U were used: the vertically-averaged speed as defined above, and the speed at 1 m height above bottom. C_d was then obtained from the least-squares best fit between u_* and U (Figure 1.12).

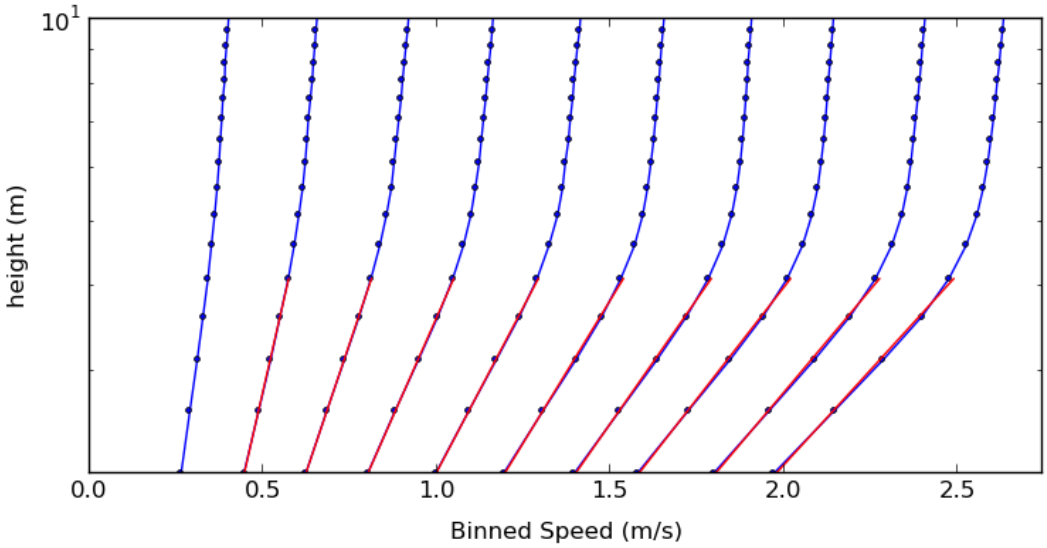

Figure 1.11: Binned speed profiles for GP4. The red lines indicate the best fit to Equation 1.1.

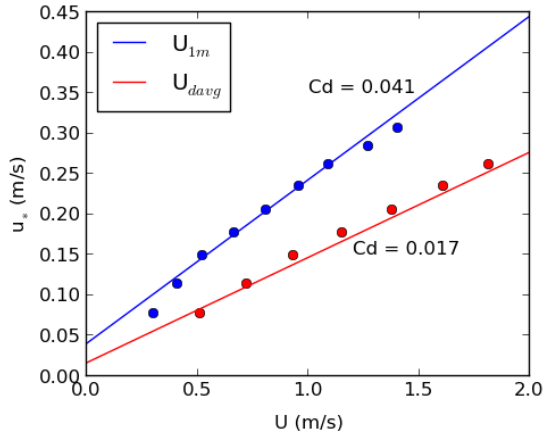

Figure 1.12: Determination of C_d from law of the wall fits. As per the legend, the colours indicate the two different reference speeds, U.

Potential power production for a typical TEC device was estimated using a water-to-wire efficiency of 0.4. It was assumed that the devices were passive yaw: i.e. the device would always align itself optimally with the flow. Both of these conditions likely result in overestimates of power output. The hub height was taken to be half the mean water depth. Power production estimates were made for three different turbine configurations, varying in diameter (capture area) and cut-in speed. These parameters along with the average energy production per day, maximum power output, and operating times for both unlimited peak power and 500 kW maximum allowable power, are summarized in Table 1.7 for the PP3 site.

	A	**B**	**C**	**D**	**E**	**F**
Diameter (m)	8.0	10.0	12.0	8.0	10.0	12.0
Cut-in Speed (m/s)	1.0	1.0	1.0	1.0	1.0	1.0
Rated Power (kW)	-	-	-	500	500	500
Max Power Output (kW)	537	839	1208	500	500	500
Avg. Energy Production (kWh/day)	2800	4375	6300	2800	4217	5364
Operating Time (%)	82.0	82.0	82.0	82.0	82.0	82.0

Table 1.7: Power production estimates at PP3 for four possible turbine configurations.

1.4 Results

The primary results of the study are summarized in Table 1.8. (Detailed data products from each ADCP mooring location are summarized in the Appendices.) Listed in Table 1.8 are the mean and maximum observed speeds at each site, the mean power density, the mean flood and ebb directions, and the flood and ebb drag coefficients. The values are based on the vertically-averaged flow speed, as defined in the previous section. (Note to the reader: the C_d values listed in the Table are not final. As can be seen from the log profile fits and the u_* vs. U plots in the Appendix, further refinement in these estimates, such as the choice of height interval over which the log-fit is implemented, are indicated in some cases.)

Excluding the locations outside the passage entrances (see Figures 1.1 and 1.3), the observed maximum speeds range from a low of 2.2 m/s to a high of 4.1 m/s. At Indian Sluice the maximum speed was 5.7 m/s.

A result worthy of note are the several instances in which the drag coefficients on the flood and ebb phases of the tide differ significantly, by a factor of 2 to 3. This result is consistent with ADCP measurements obtained in GP in 2010 under an NSERC Engage grant, and in GP in the fall of 2012 in another OERA-funded project, an investigation of turbulence in high Reynolds number tidal passages.

Site	**Mean Speed** (m/s)	**Max Speed** (m/s)	**Mean Power Density** (kW/m^2)	**Direction** Flood (°)	Ebb (°)	**Drag Coefficient,** C_d Flood (10^{-3})	Ebb (10^{-3})
DG1	0.9	2.2	0.7	172	-41	-	-
DG2	1.2	2.6	1.6	153	-17	3.7	2.5
DG3	1.4	3.0	2.3	161	-16	2.2	2.7
DG4	1.2	2.6	1.6	142	-33	17.5	10.9
DG5	0.7	1.5	0.3	146	-16	-	-
GP2	1.4	2.4	1.9	-	-	3.0	6.3
GP3	0.4	1.4	0.0	-1	172	2.2	5.6
GP4	1.7	2.7	3.5	-18	155	15.6	4.8
GP5	0.4	1.6	0.1	34	157	-	-
PP1	1.1	3.2	1.7	-7	181	2.5	3.1
PP2	1.8	3.5	4.2	-17	169	4.2	4.8
PP3	1.9	4.0	6.0	1	185	5.4	3.7
PP4	1.1	2.8	1.2	5	192	5.8	2.0
PP5	0.5	1.8	0.2	20	208	-	-
IS1	2.0	4.6	7.6	445	268	4.9	3.8

Table 1.8: Summary of analysis results. The values listed are based on the flow speed that has been depth averaged below 95% of the range to the sea surface. The estimates of C_d for PP1 and IS1, the two bottom pods which underwent significant horizontal displacements during deployment, are preliminary.

Acknowledgments:
We thank the following people without whose efforts this work would not have been possible: Greg Trowse (FTI) for assistance in the field, input regarding the power extraction calculations, and for catching some important errors in the original version of tabulated results; Richard Cheel and Walter Judge (Dalhousie University) for technical and field support, including with the design and assembly of the ADCP bottom pods; John Lindley and Adam Harding (Dalhousie University) and Mike Huntley (Huntley's Sub-Aqua Construction) and his team, for dive support; and last but not least, Daniel Kenney III and Vance Hazelton, the skippers of the *MV Expectations XL* (Westport) and *MV Branntelle* (Digby) and their crews.

Appendix A

Acoustic Doppler Current Profiler Results

A.1 DG1

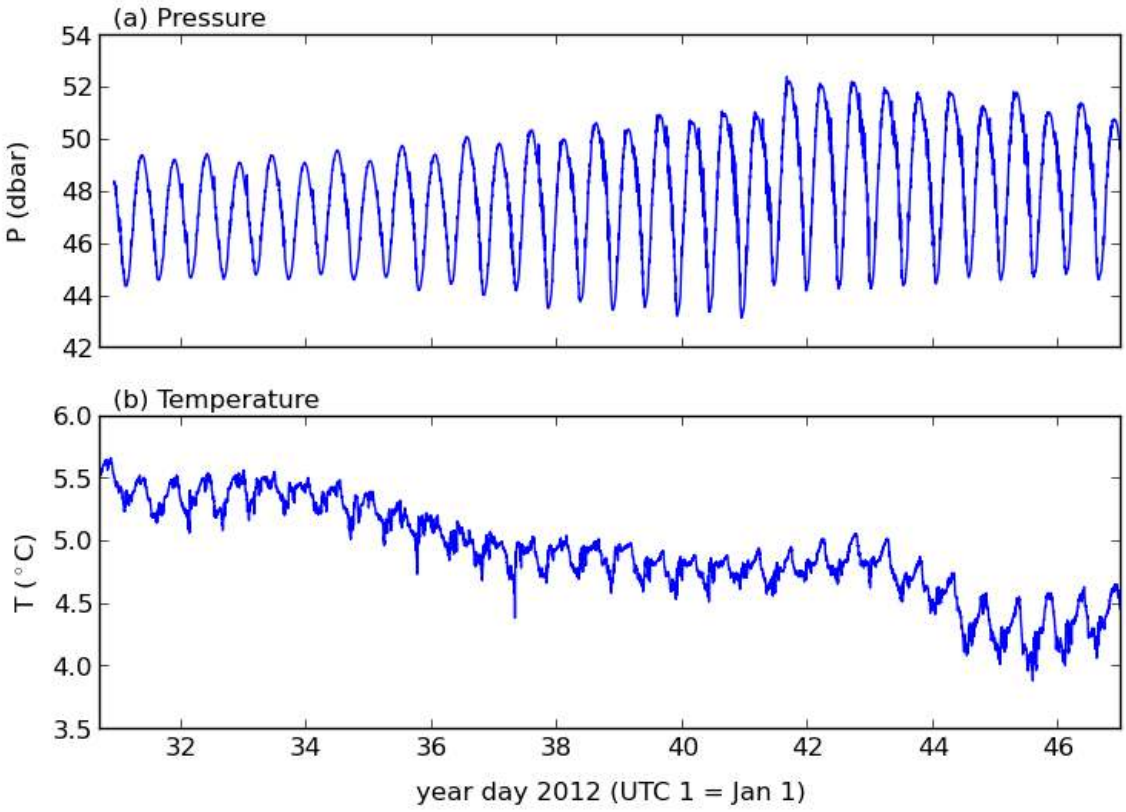

Figure A.1.1: Measurements of pressure and temperature at DG1.

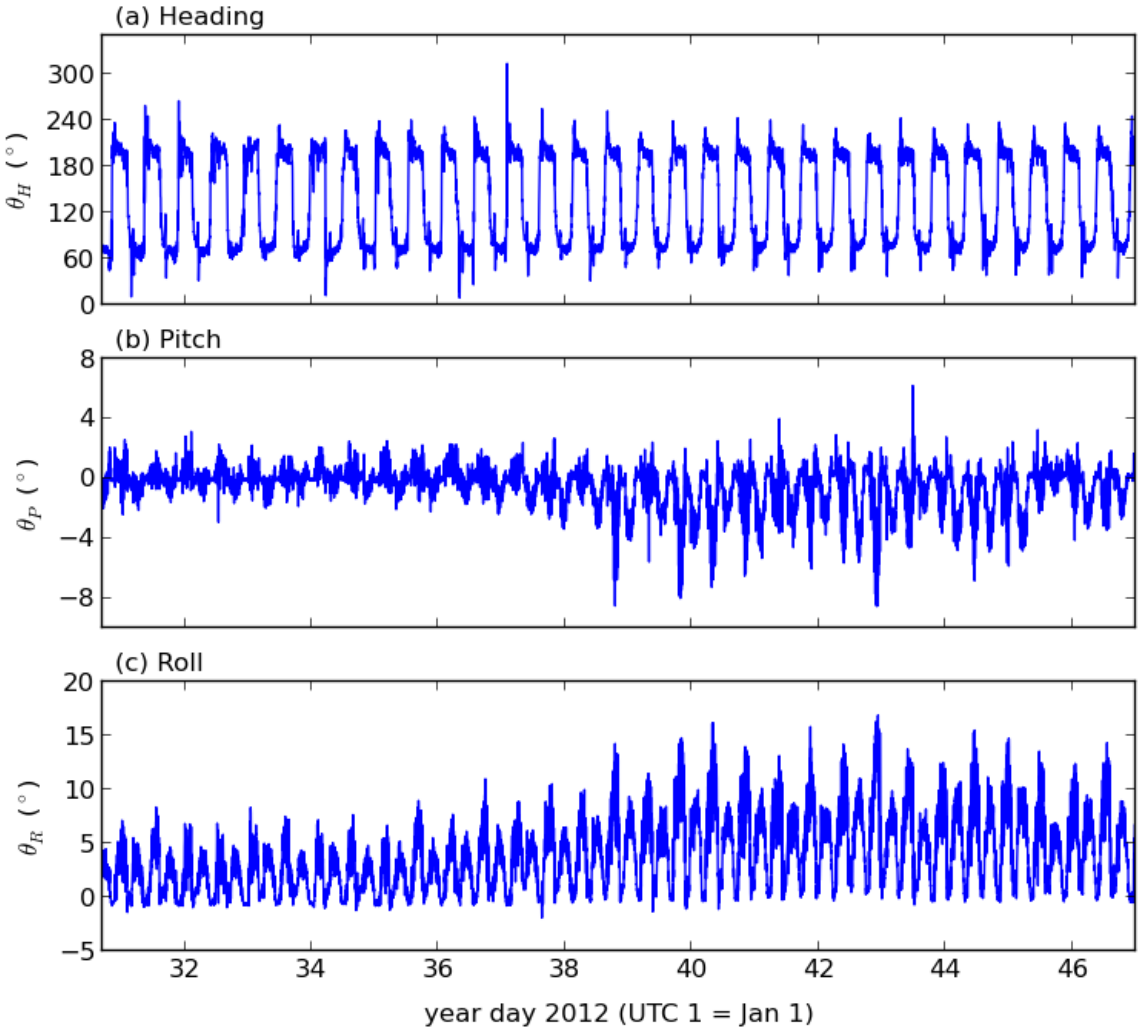

Figure A.1.2: Measurements of heading, pitch and roll at DG1.

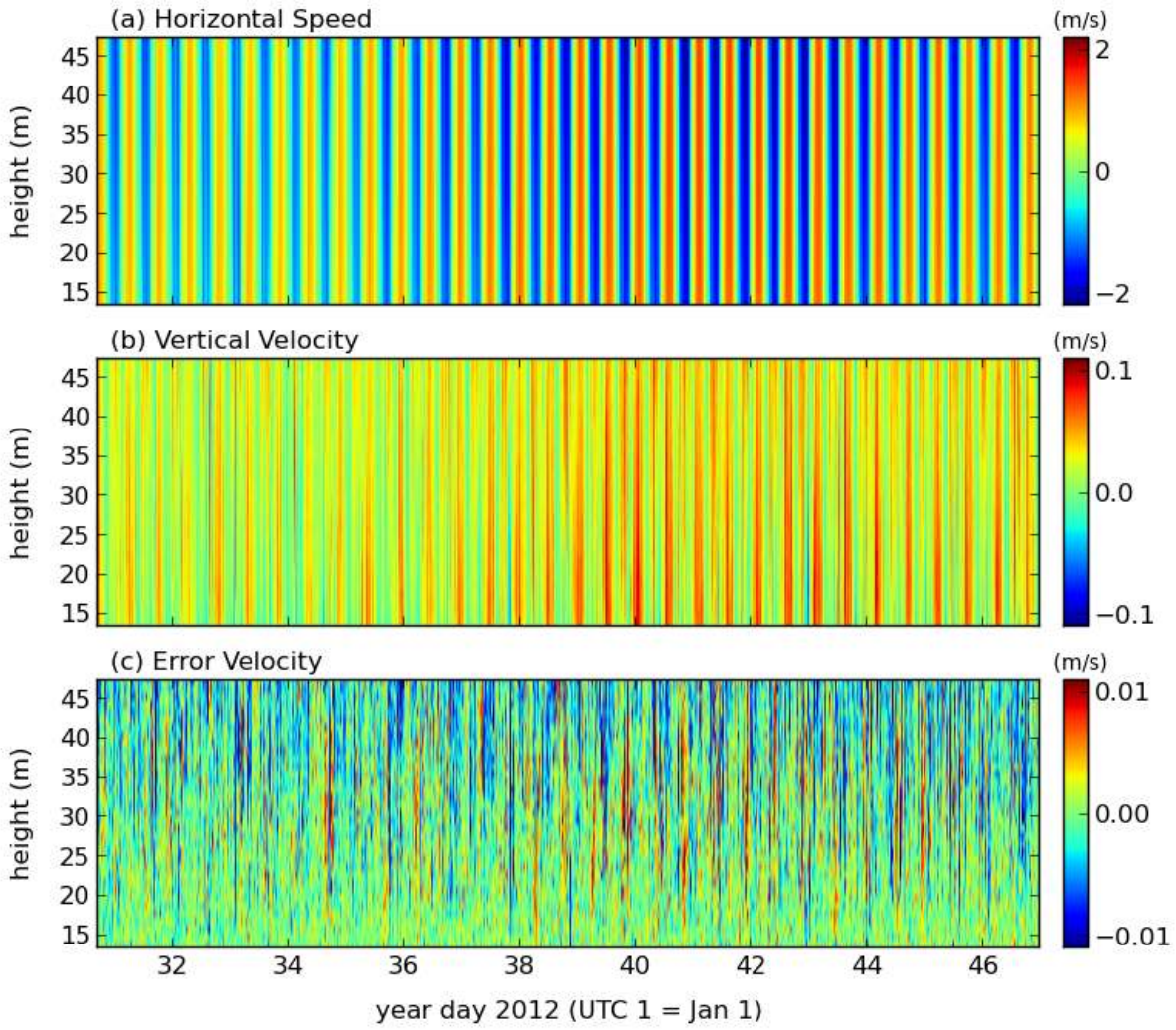

Figure A.1.3: Ten minute ensemble averaged horizontal current speeds, vertical velocities and error velocities for DG1. In panel (a), positive velocities correspond to the flood direction and negative velocities correspond to the ebb direction. The maximum depth is equivalent to 95% of the lowest low water.

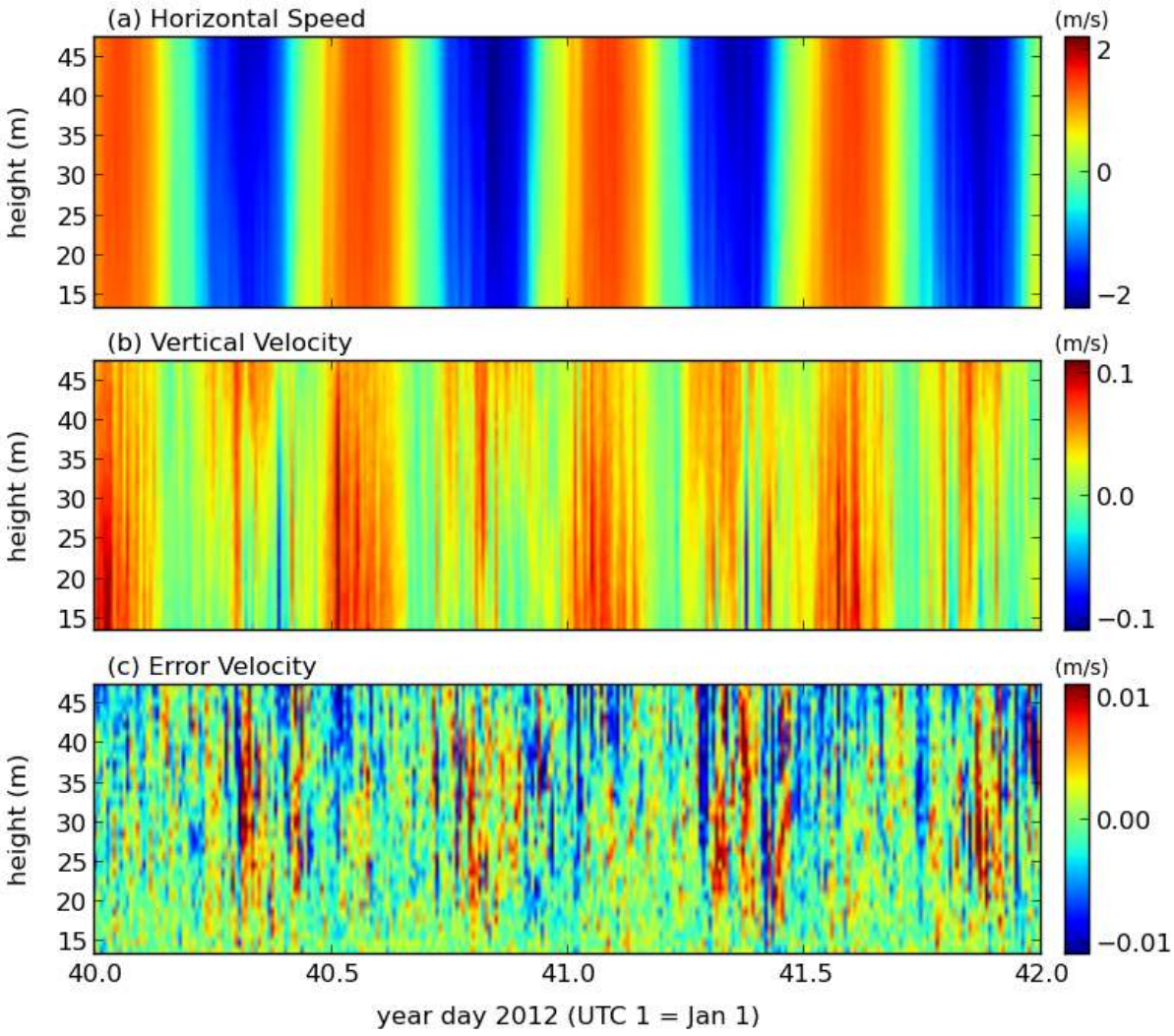

Figure A.1.4: As above, but during a 2-day period.

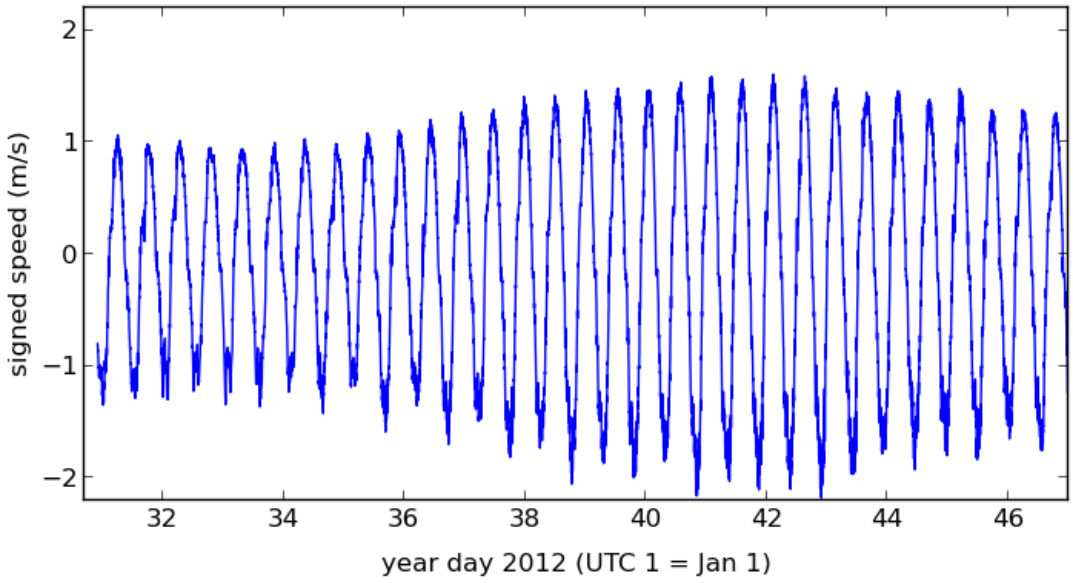

Figure A.1.5: Time series of the depth averaged velocity at DG1. The averages were computed to 95% of the surface signal. Positive velocities correspond to the flood direction and negative velocities correspond to the ebb direction.

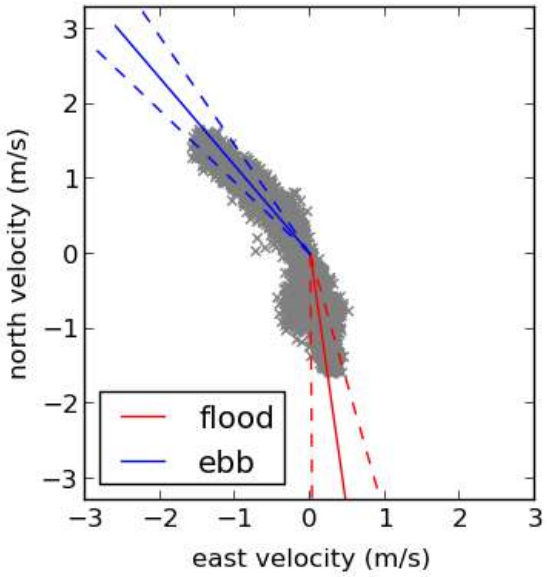

Figure A.1.6: The principal flow directions at DG1 are shown by the solid red and blue lines for the flood and ebb tides, respectively. The dashed lines indicate ±1 standard deviation from the mean. Individual values are plotted as grey x markers.

	A	B	C	D	E	F
Diameter (m)	8.0	10.0	12.0	8.0	10.0	12.0
Cut-in Speed (m/s)	1.0	1.0	1.0	1.0	1.0	1.0
Rated Power (kW)	-	-	-	500	500	500
Max Power Output (kW)	69	108	155	69	108	155
Avg. Energy Production (kWh/day)	197	307	442	197	307	442
Operating Time (%)	35.2	35.2	35.2	35.2	35.2	35.2

Table A.1.1: Turbine statistics for six configurations at DG1. All turbines are assumed to have a hub height of 10 m and a water-wire efficiency of 0.4.

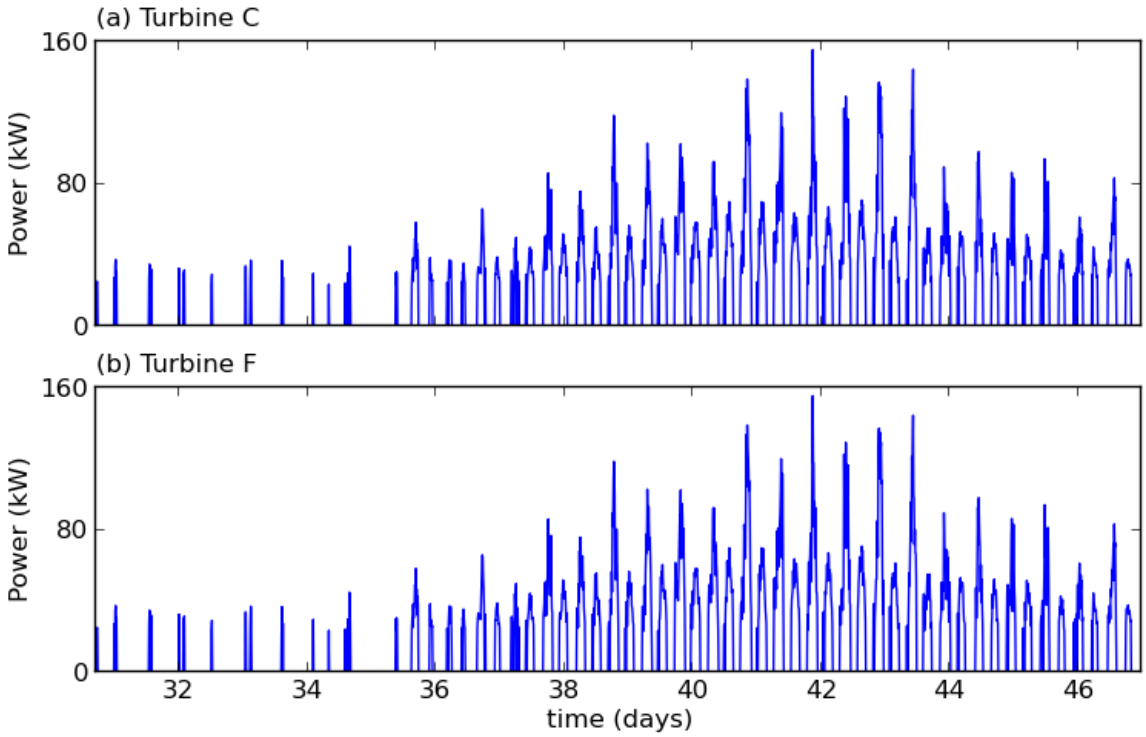

Figure A.1.7: A time series of the power output DG1 for the six turbine configuations listed in Table A.1.1. The power output was computed at a hub height of 10 m using the ten minute ensembled data.

A.2 DG2

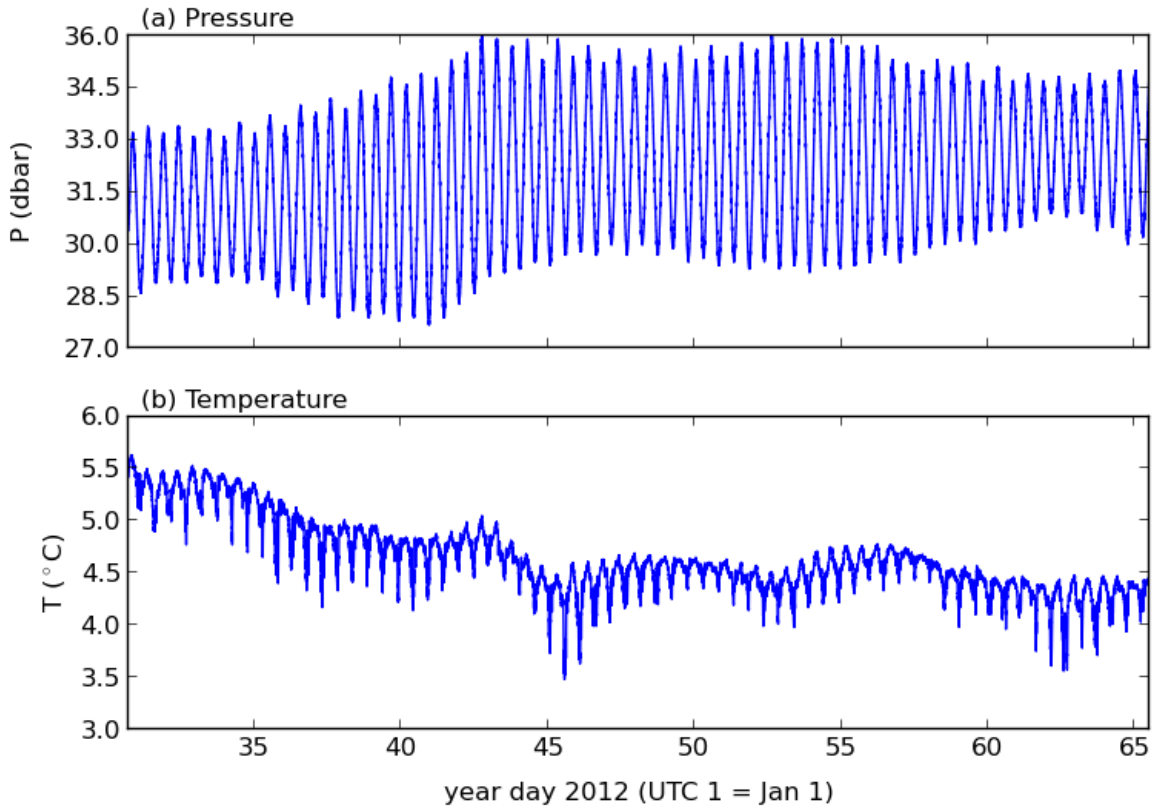

Figure A.2.1: Measurements of pressure and temperature at DG2.

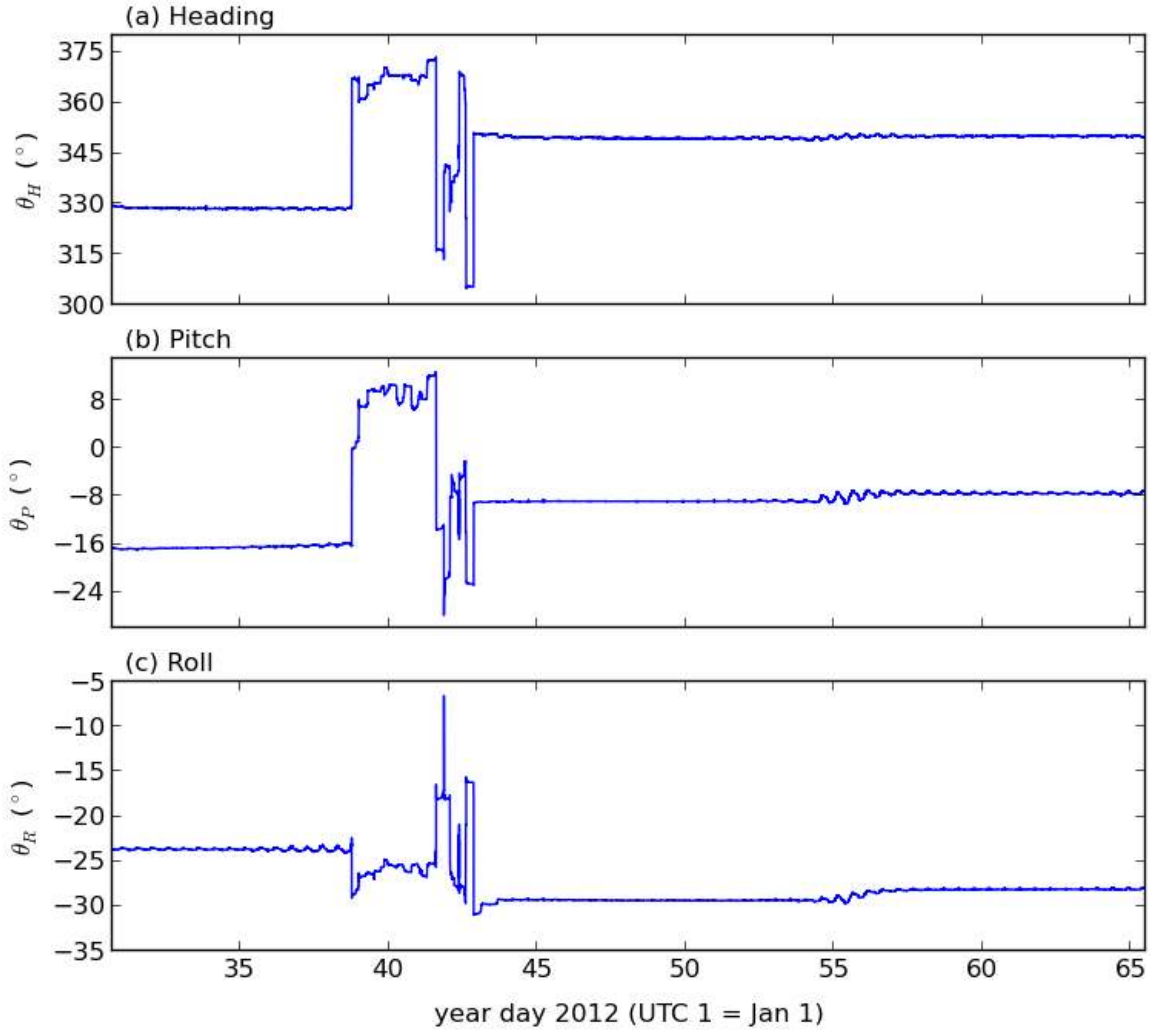

Figure A.2.2: Measurements of heading, pitch and roll at DG2.

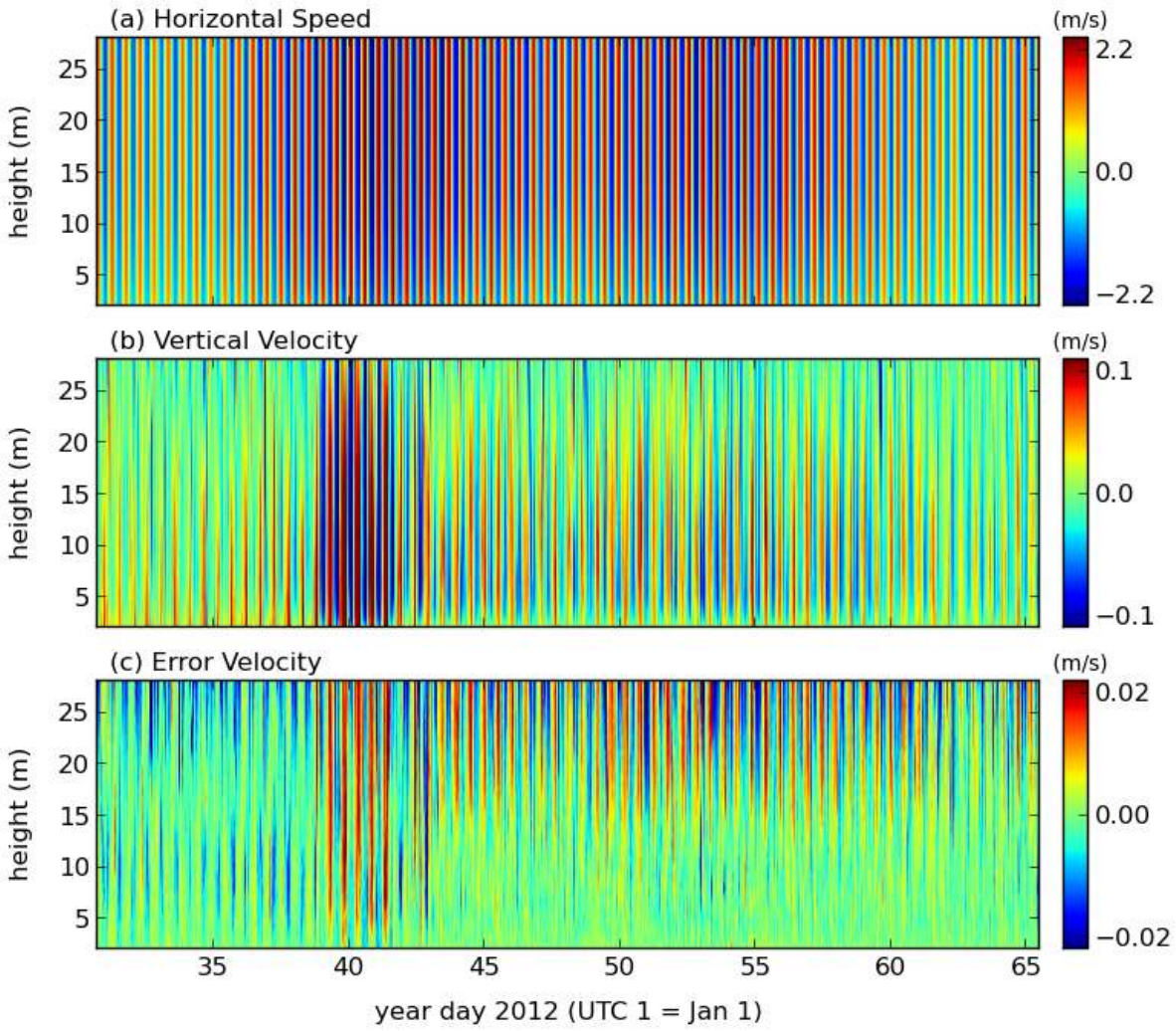

Figure A.2.3: Ten minute ensemble averaged horizontal current speeds, vertical velocities and error velocities for DG2. In panel (a), positive velocities correspond to the flood direction and negative velocities correspond to the ebb direction. The maximum depth is equivalent to 95% of the lowest low water.

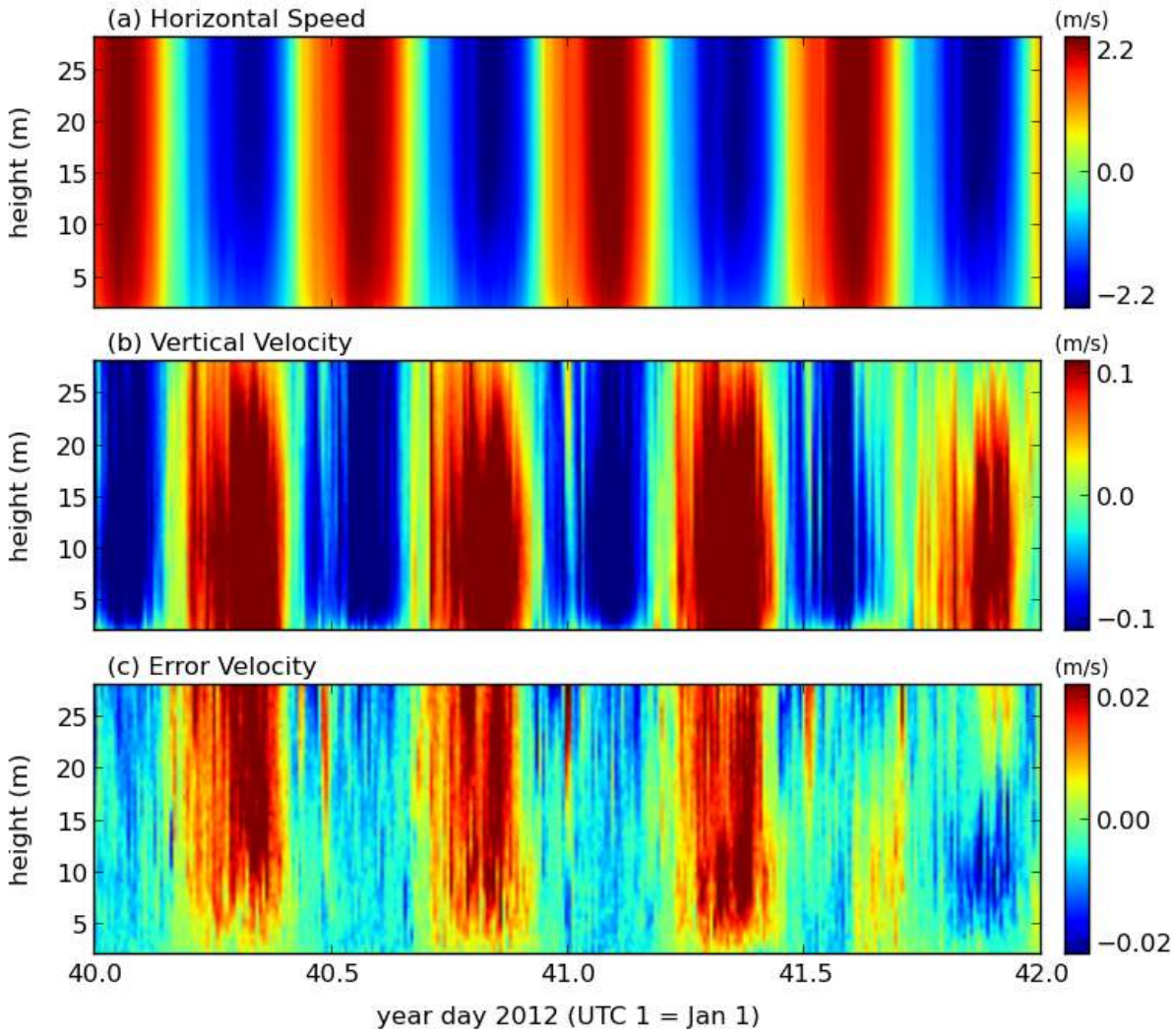

Figure A.2.4: As above, but during a 2-day period.

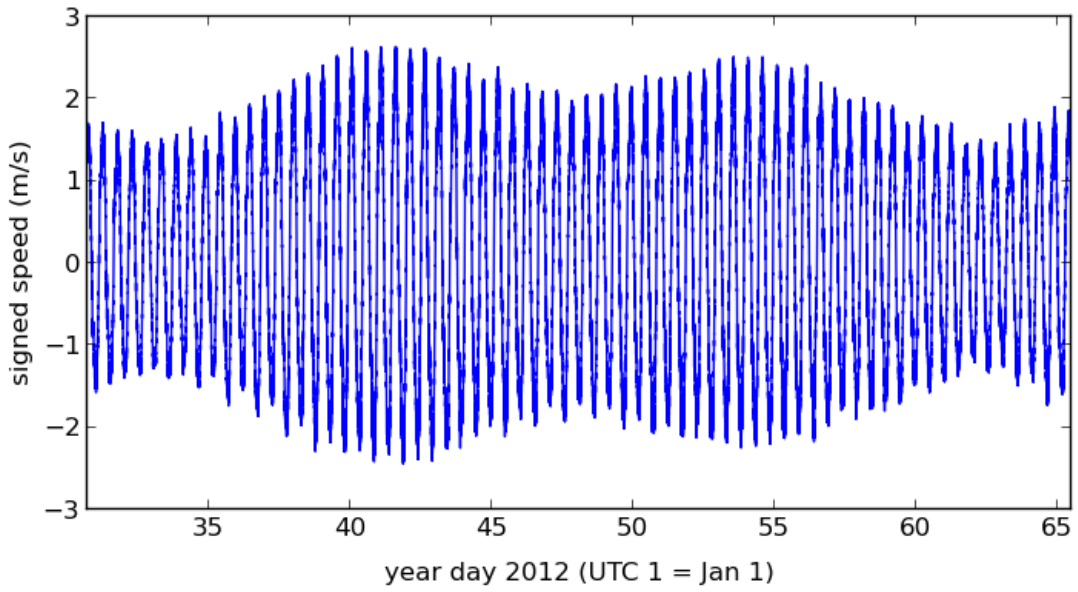

Figure A.2.5: Time series of the depth averaged velocity at DG2. The averages were computed to 95% of the surface signal. Positive velocities correspond to the flood direction and negative velocities correspond to the ebb direction.

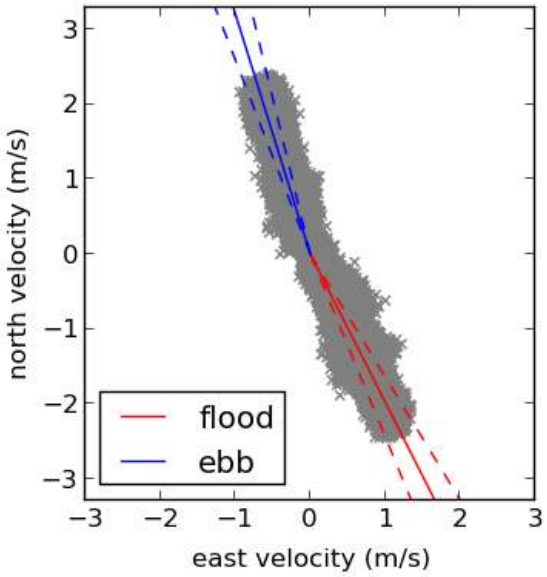

Figure A.2.6: The principal flow directions at DG2 are shown by the solid red and blue lines for the flood and ebb tides, respectively. The dashed lines indicate ±1 standard deviation from the mean. Individual values are plotted as grey x markers.

Constituent	Period (hr)	Elevation		Velocity			
		Amplitude (m)	Phase (°)	Major (m/s)	Minor (m/s)	Inclination (°)	Phase (°)
M2	12.42	2.72	32	1.88	-0.01	112	180
S2	12.00	0.60	126	0.43	-0.01	111	233
N2	12.66	0.51	191	0.34	-0.01	112	170
K1	23.93	0.13	189	0.04	0.00	114	299
O1	25.82	0.07	150	0.02	0.00	113	288
M6	4.14	0.06	69	0.14	0.01	111	308

Table A.2.1: Harmonic Analysis at DG2. The elevation fits were done over a period of 22 days and the velocity fits were done over a period of 22 days. The RMS amplitude of the residual elevation was 14 cm and the RMS amplitude of the residual current speed was 14 cm/s.

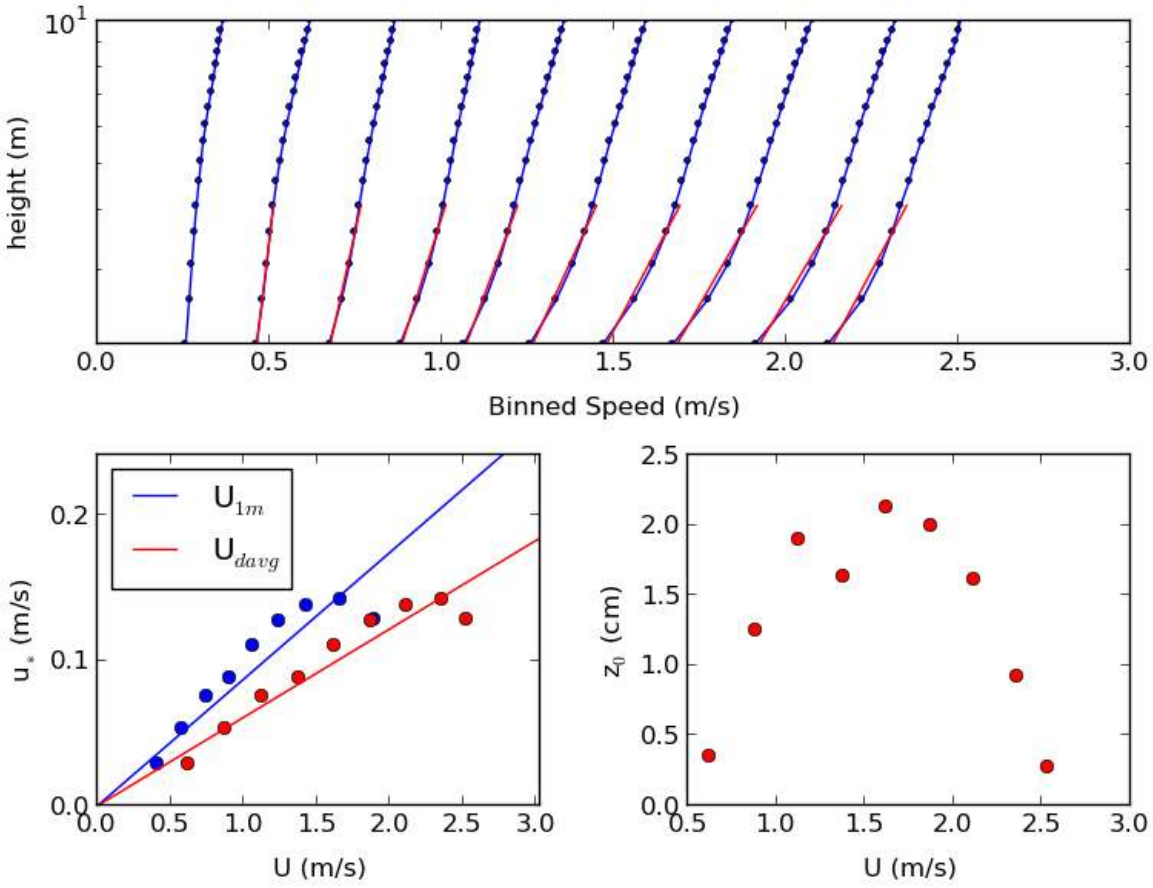

Figure A.2.7: The top panel shows the binned speed profiles during the flood tide at DG2. The red lines correspond to the law of the wall fits. The lower left panel plots u_* as determined from the law of the wall versus a reference speed. Since $u_*^2 = C_d U^2$, C_d is the is the square of the slope of the fitted line. These values are given in the table below. The lower right panel shows the estimates of z_0 from the law of the wall fits.

	Flood	**Ebb**
C_d $(U = V_{1m})$	0.0076	0.0074
C_d $(U = V_{davg})$	0.0037	0.0025
Mean z_0 (cm)	1.3	0.9

Table A.2.2: Drag coefficient, C_d, values at DG2. The values are separated into flood and ebb phases of the tide. Two different reference speeds were used – a theoretical estimate at $z = 1$ m (V_{1m}) and a depth averaged speed which was computed to 95 percent of the surface signal.

	A	**B**	**C**	**D**	**E**	**F**
Diameter (m)	8.0	10.0	12.0	8.0	10.0	12.0
Cut-in Speed (m/s)	1.0	1.0	1.0	1.0	1.0	1.0
Rated Power (kW)	-	-	-	500	500	500
Max Power Output (kW)	174	271	390	174	271	390
Avg. Energy Production (kWh/day)	675	1055	1519	675	1055	1519
Operating Time (%)	64.1	64.1	64.1	64.1	64.1	64.1

Table A.2.3: Turbine statistics for six configurations at DG2. All turbines are assumed to have a hub height of 10 m and a water-wire efficiency of 0.4.

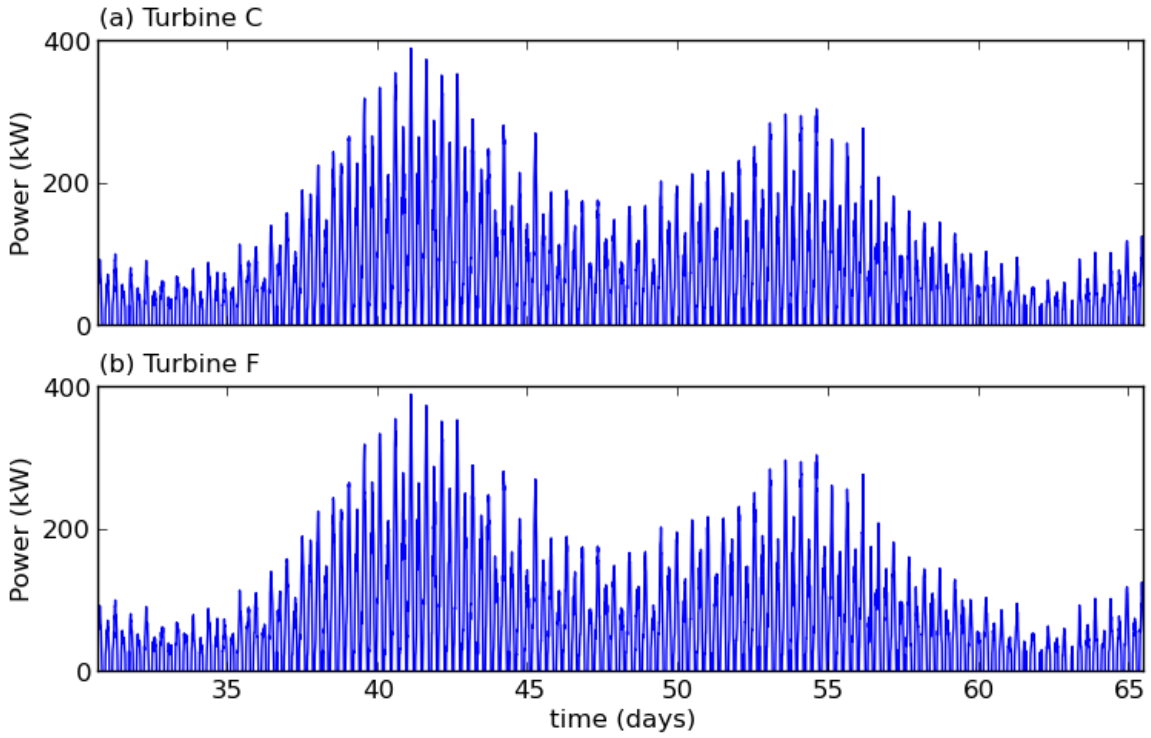

Figure A.2.8: A time series of the power output DG2 for the six turbine configuations listed in Table A.2.3. The power output was computed at a hub height of 10 m using the ten minute ensembled data.

A.3 DG3

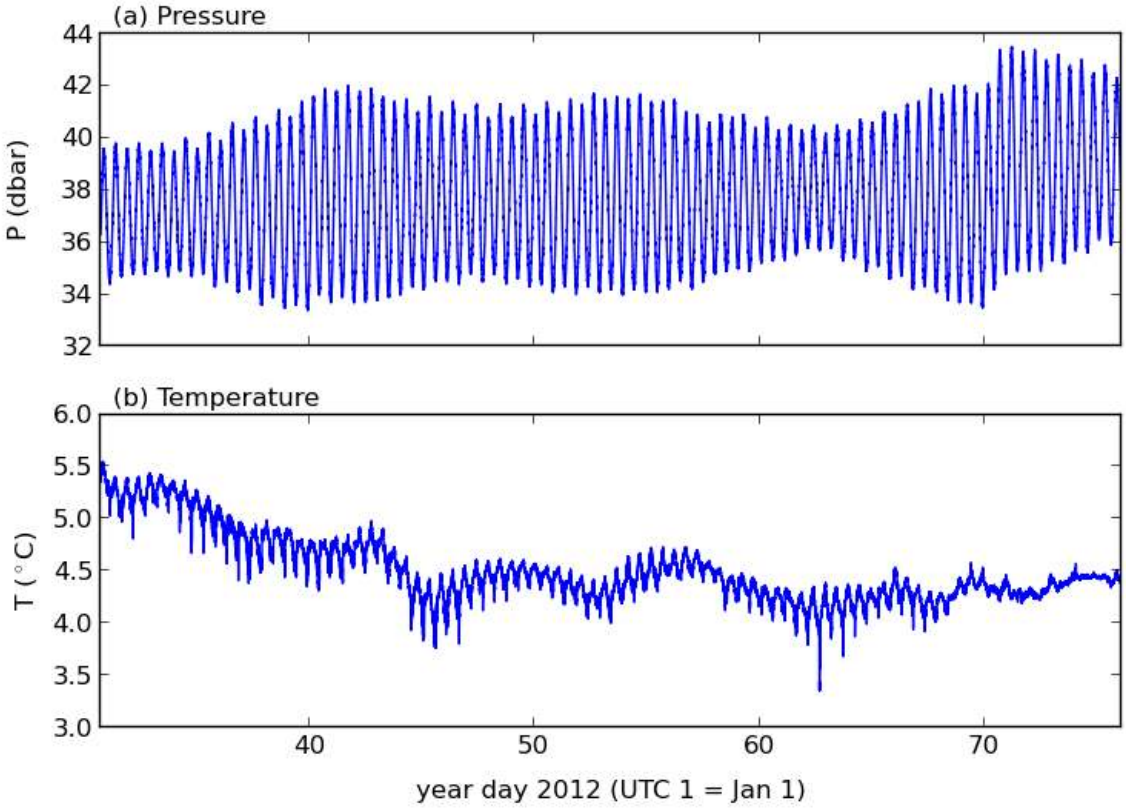

Figure A.3.1: Measurements of pressure and temperature at DG3.

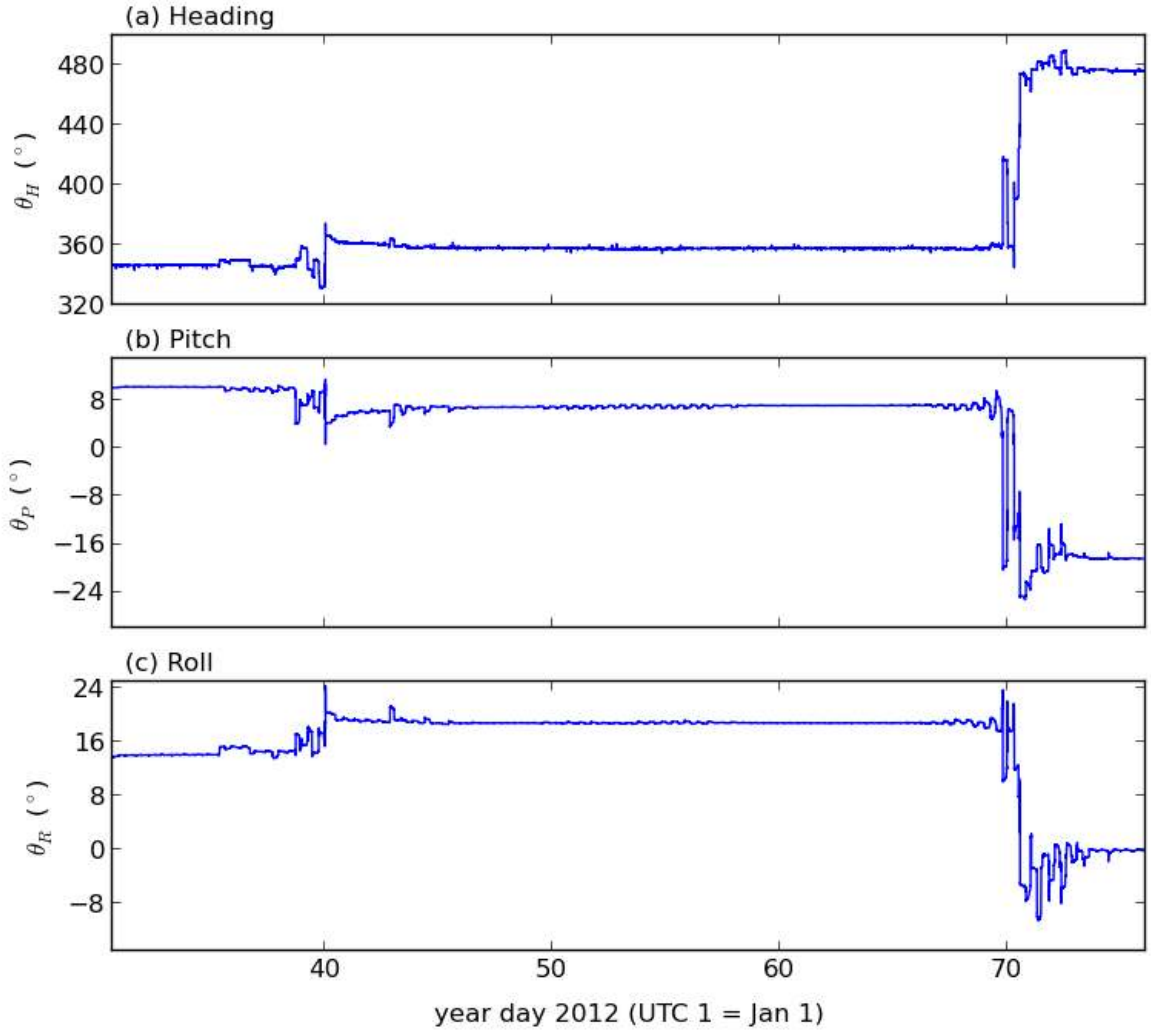

Figure A.3.2: Measurements of heading, pitch and roll at DG3.

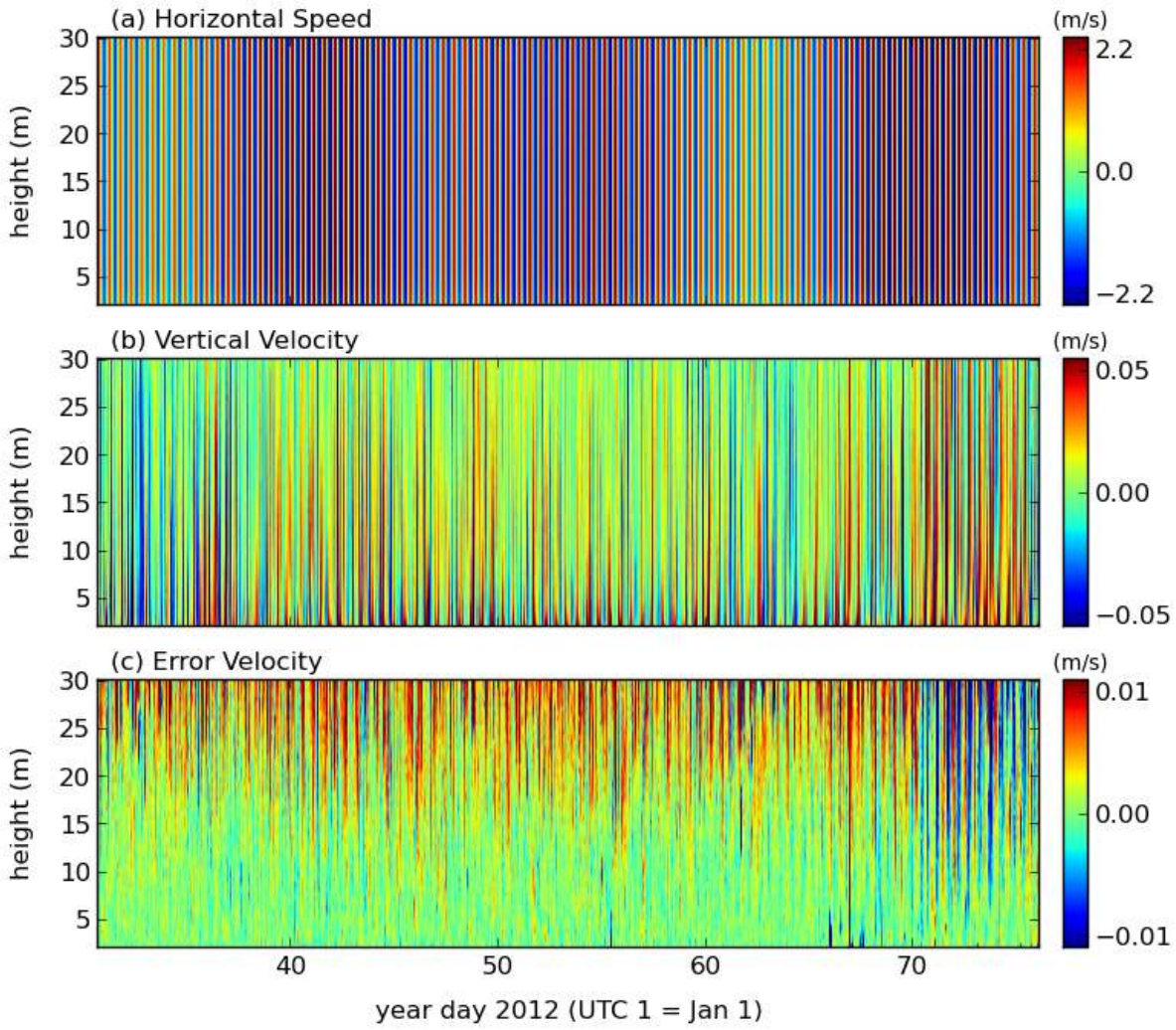

Figure A.3.3: Ten minute ensemble averaged horizontal current speeds, vertical velocities and error velocities for DG3. In panel (a), positive velocities correspond to the flood direction and negative velocities correspond to the ebb direction. The maximum depth is equivalent to 95% of the lowest low water.

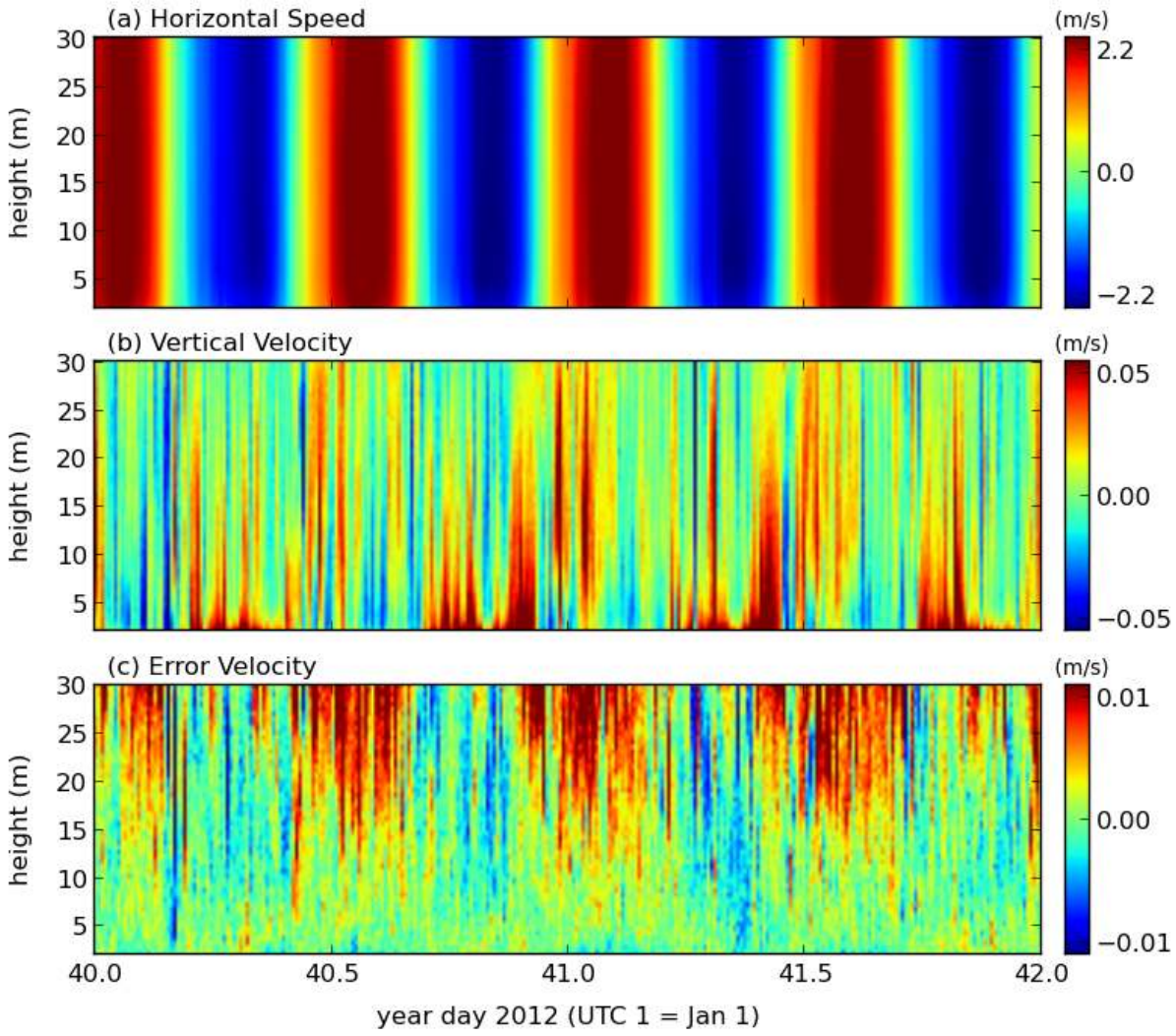

Figure A.3.4: As above, but during a 2-day period.

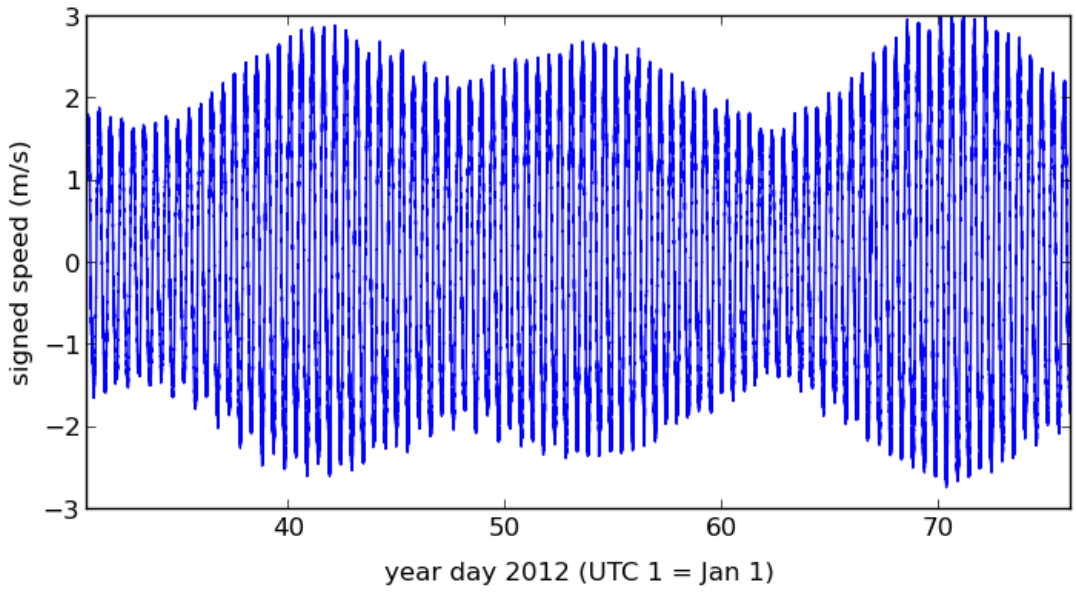

Figure A.3.5: Time series of the depth averaged velocity at DG3. The averages were computed to 95% of the surface signal. Positive velocities correspond to the flood direction and negative velocities correspond to the ebb direction.

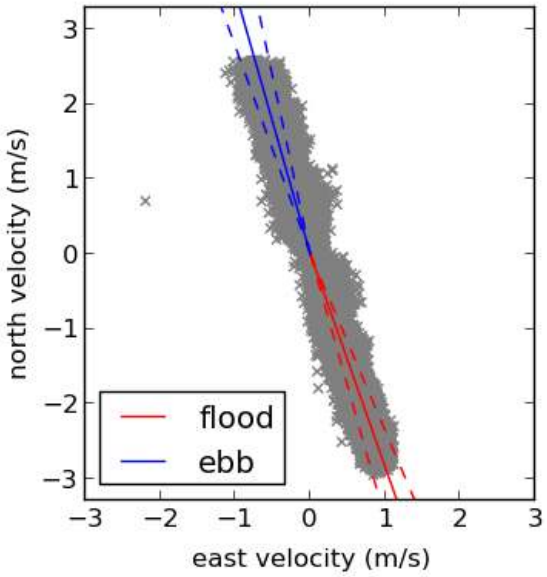

Figure A.3.6: The principal flow directions at DG3 are shown by the solid red and blue lines for the flood and ebb tides, respectively. The dashed lines indicate ±1 standard deviation from the mean. Individual values are plotted as grey x markers.

Constituent	Period	Elevation		Velocity			
	(hr)	Amplitude (m)	Phase (°)	Major (m/s)	Minor (m/s)	Inclination (°)	Phase (°)
M2	12.42	3.18	88	2.07	-0.00	107	181
S2	12.00	0.60	137	0.40	-0.00	106	232
N2	12.66	0.55	73	0.35	0.01	107	166
K1	23.93	0.16	212	0.05	0.00	107	308
O1	25.82	0.09	173	0.03	0.00	104	267
M4	6.21	0.08	173	0.07	0.00	105	156

Table A.3.1: Harmonic Analysis at DG3. The elevation fits were done over a period of 39 days and the velocity fits were done over a period of 39 days. The RMS amplitude of the residual elevation was 30 cm and the RMS amplitude of the residual current speed was 15 cm/s.

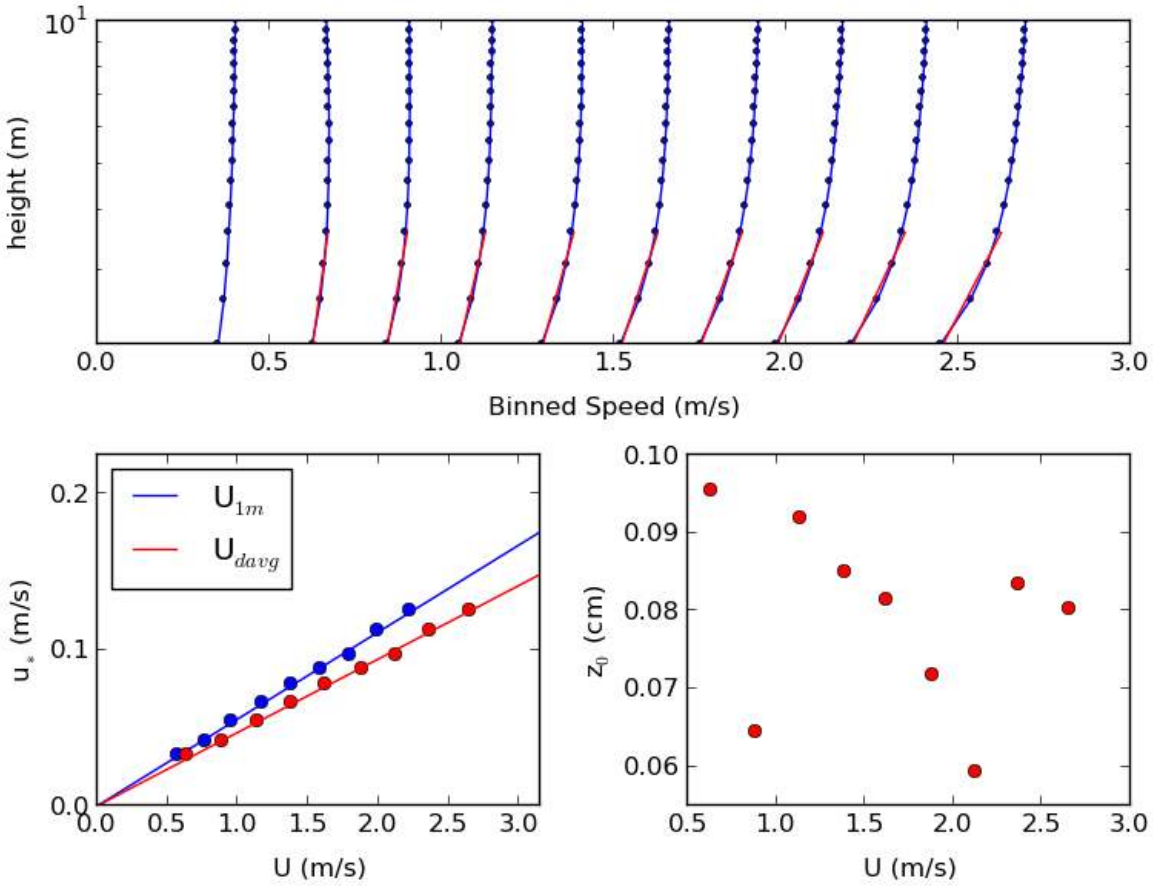

Figure A.3.7: The top panel shows the binned speed profiles during the flood tide at DG3. The red lines correspond to the law of the wall fits. The lower left panel plots u_* as determined from the law of the wall versus a reference speed. Since $u_*^2 = C_d U^2$, C_d is the is the square of the slope of the fitted line. These values are given in the table below. The lower right panel shows the estimates of z_0 from the law of the wall fits.

	Flood	**Ebb**
C_d $(U = V_{1m})$	0.0031	0.0044
C_d $(U = V_{davg})$	0.0022	0.0027
Mean z_0 (cm)	0.1	0.2

Table A.3.2: Drag coefficient, C_d, values at DG3. The values are separated into flood and ebb phases of the tide. Two different reference speeds were used – a theoretical estimate at $z = 1$ m (V_{1m}) and a depth averaged speed which was computed to 95 percent of the surface signal.

	A	**B**	**C**	**D**	**E**	**F**
Diameter (m)	8.0	10.0	12.0	8.0	10.0	12.0
Cut-in Speed (m/s)	1.0	1.0	1.0	1.0	1.0	1.0
Rated Power (kW)	-	-	-	500	500	500
Max Power Output (kW)	270	422	608	270	422	500
Avg. Energy Production (kWh/day)	1162	1816	2615	1162	1816	2608
Operating Time (%)	70.6	70.6	70.6	70.6	70.6	70.6

Table A.3.3: Turbine statistics for six configurations at DG3. All turbines are assumed to have a hub height of 10 m and a water-wire efficiency of 0.4.

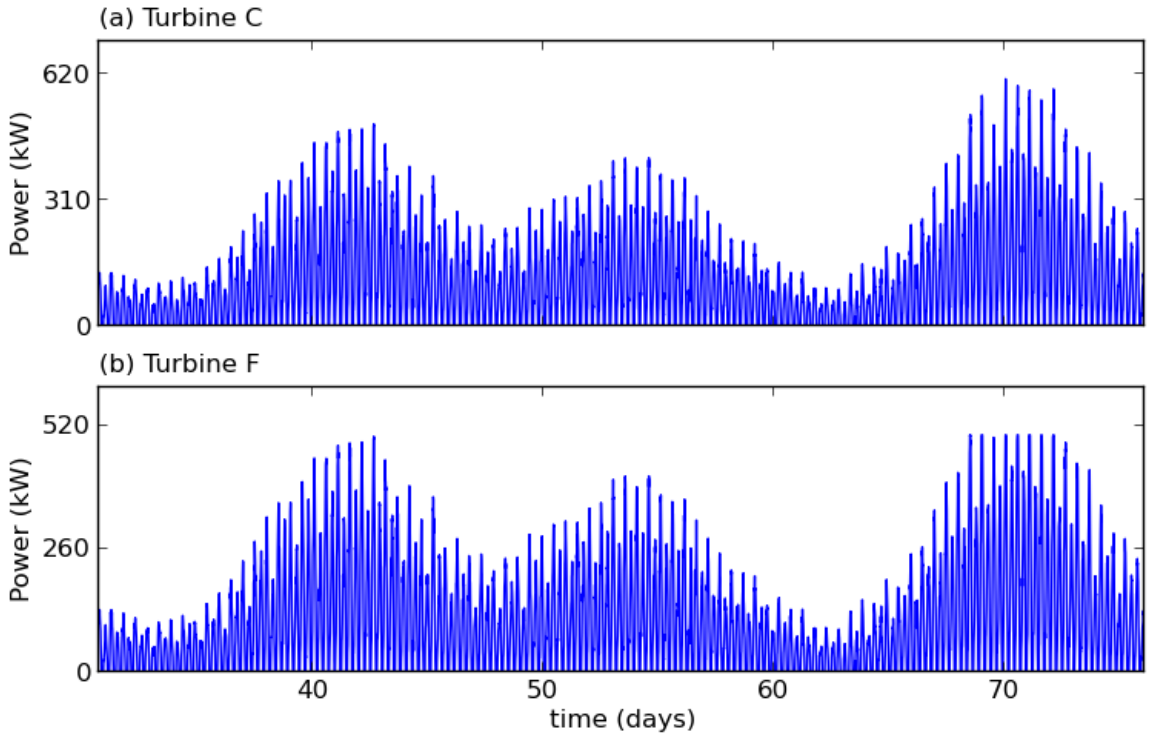

Figure A.3.8: A time series of the power output DG3 for the six turbine configuations listed in Table A.3.3. The power output was computed at a hub height of 10 m using the ten minute ensembled data.

A.4 DG4

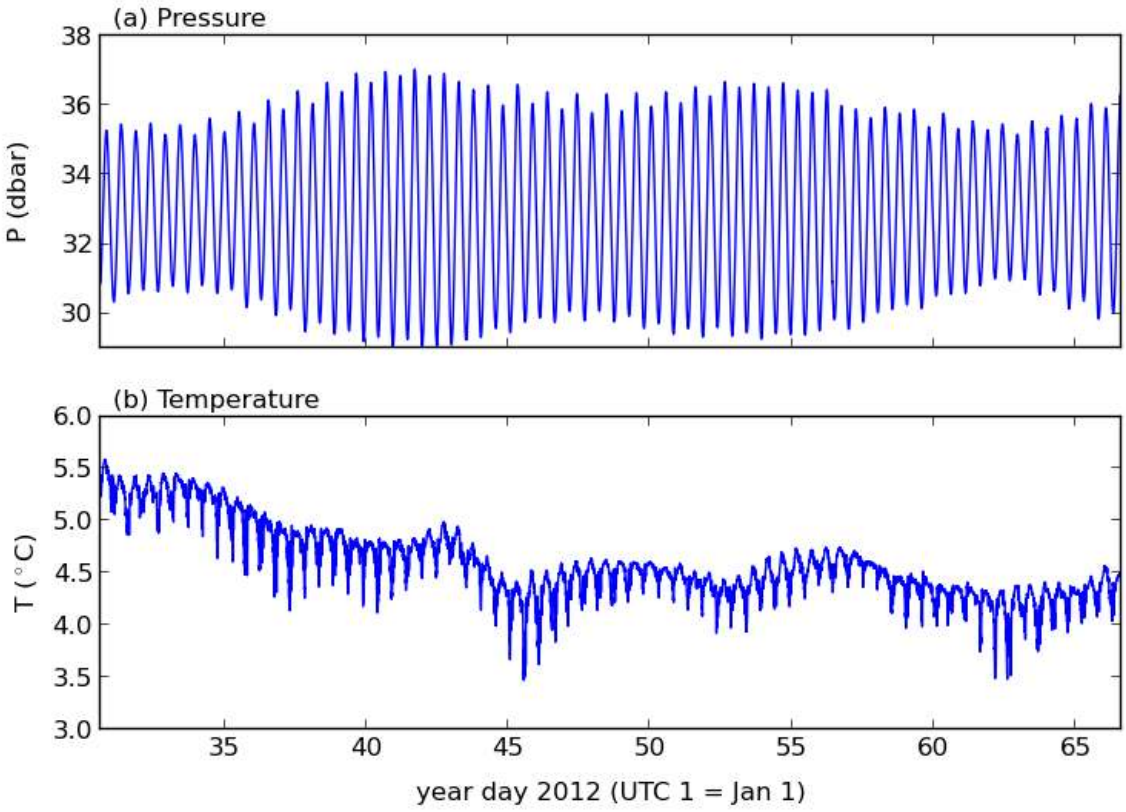

Figure A.4.1: Measurements of pressure and temperature at DG4.

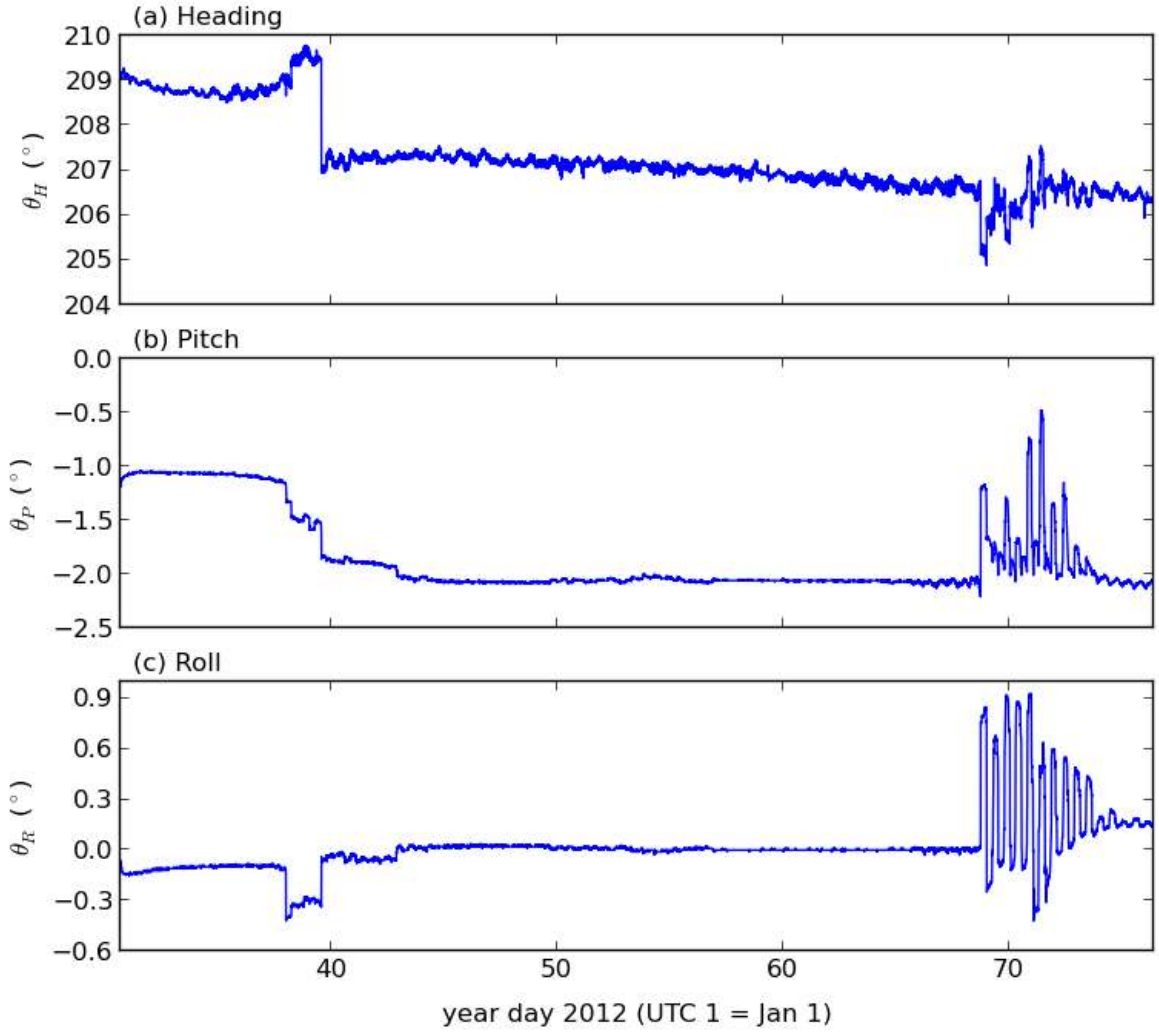

Figure A.4.2: Measurements of heading, pitch and roll at DG4.

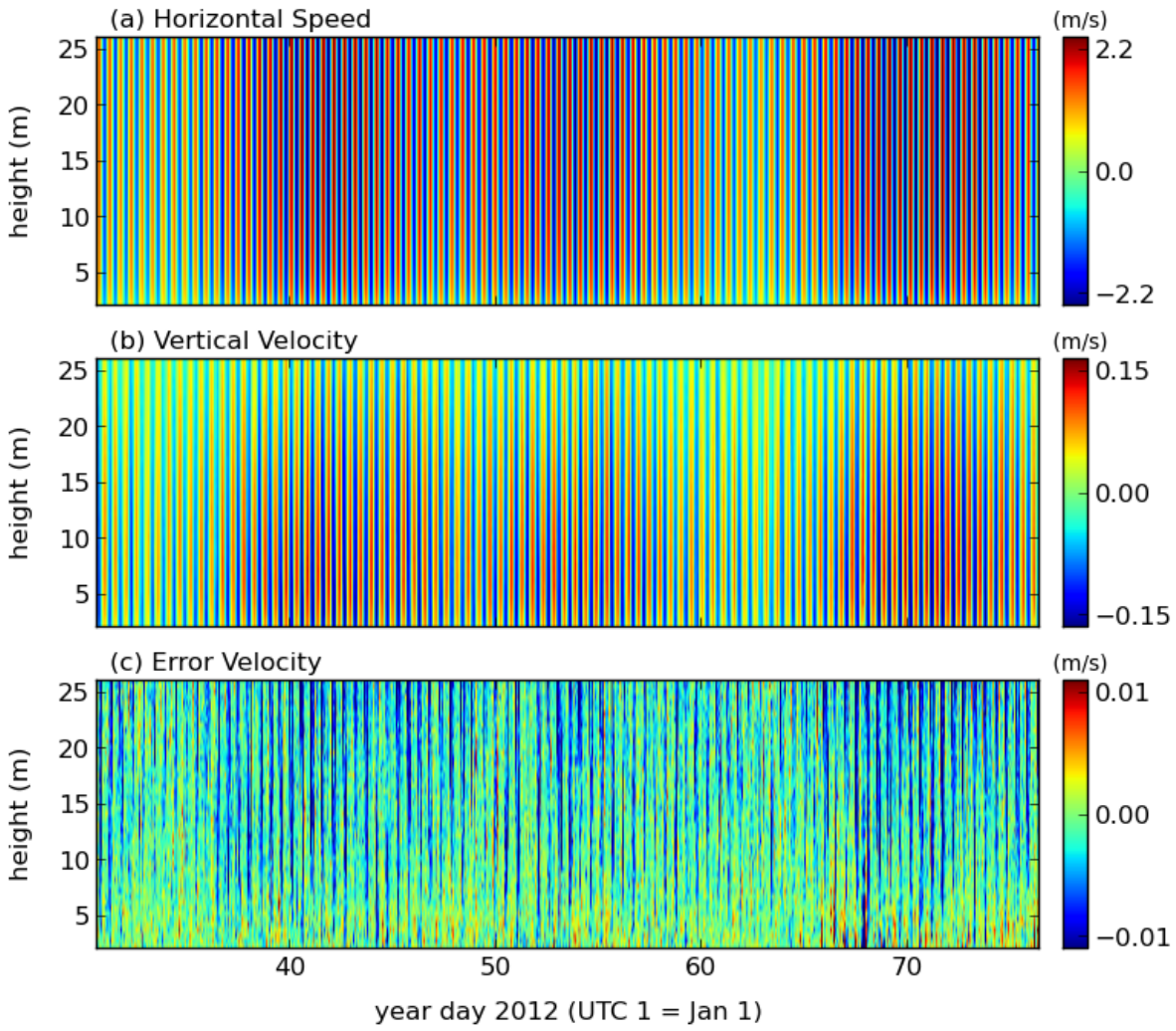

Figure A.4.3: Ten minute ensemble averaged horizontal current speeds, vertical velocities and error velocities for DG4. In panel (a), positive velocities correspond to the flood direction and negative velocities correspond to the ebb direction. The maximum depth is equivalent to 95% of the lowest low water.

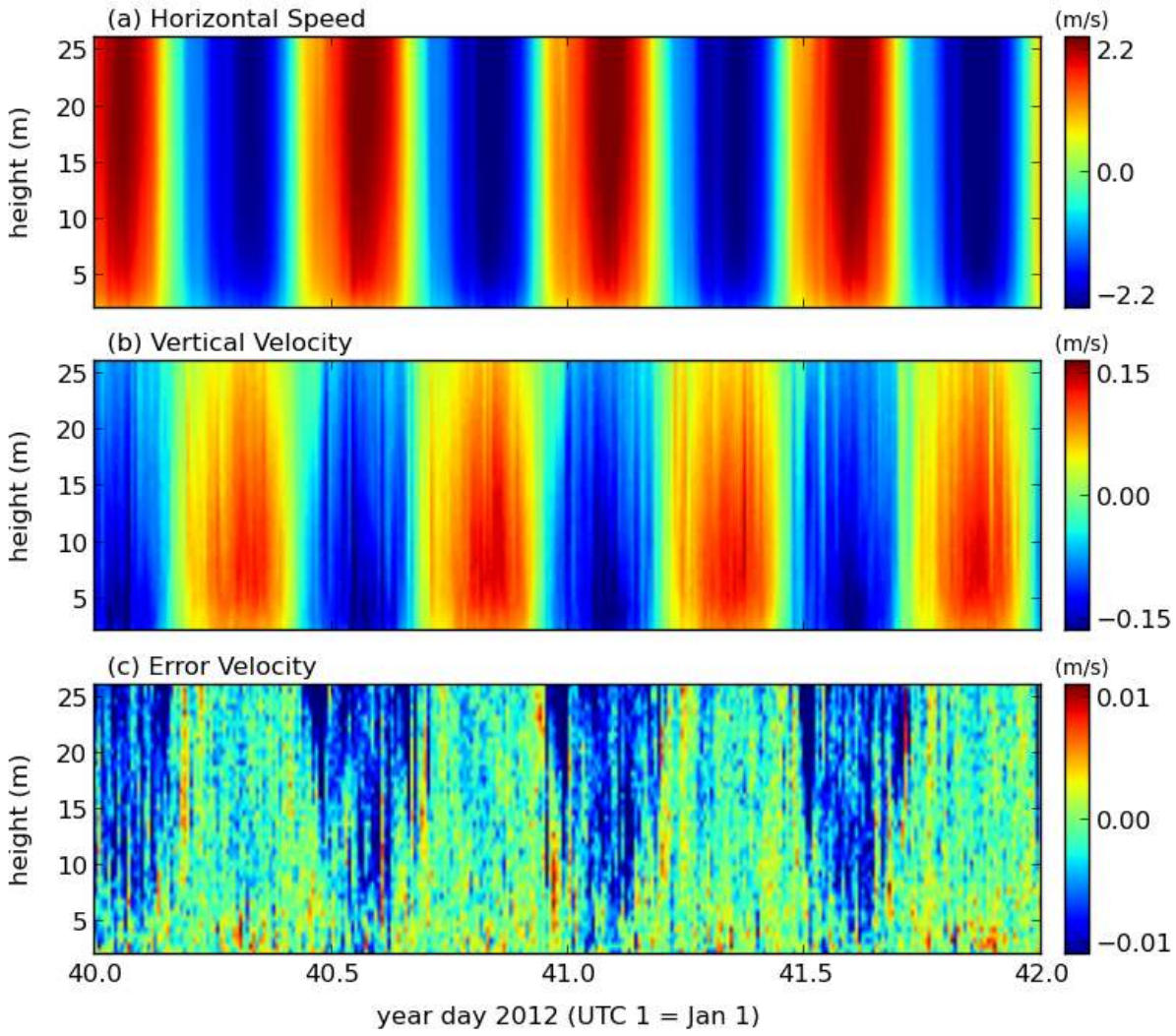

Figure A.4.4: As above, but during a 2-day period.

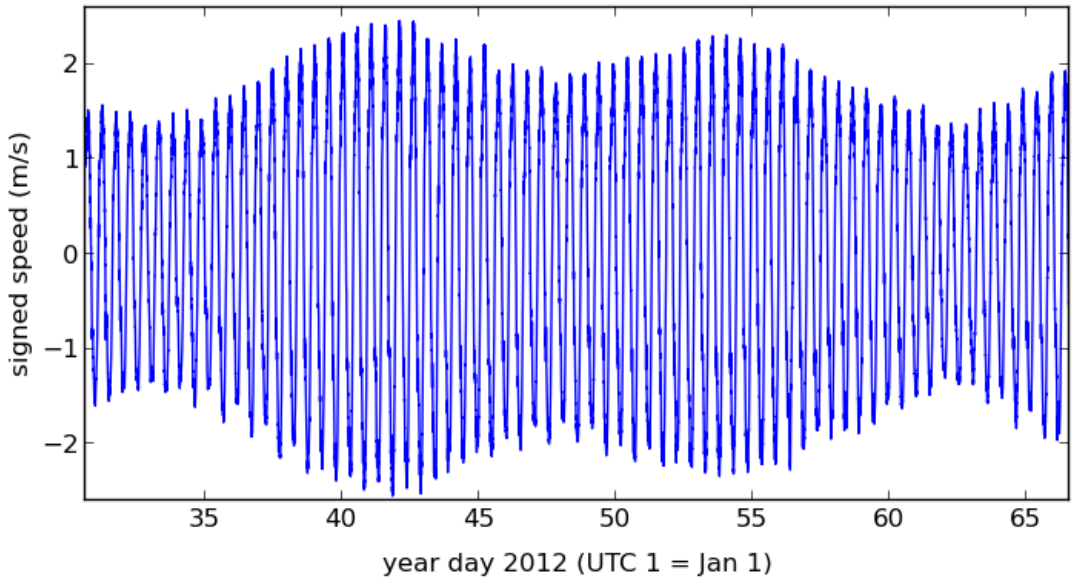

Figure A.4.5: Time series of the depth averaged velocity at DG4. The averages were computed to 95% of the surface signal. Positive velocities correspond to the flood direction and negative velocities correspond to the ebb direction.

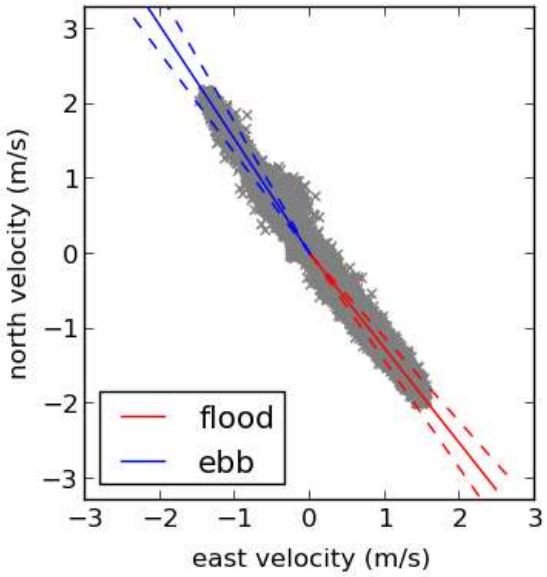

Figure A.4.6: The principal flow directions at DG4 are shown by the solid red and blue lines for the flood and ebb tides, respectively. The dashed lines indicate ±1 standard deviation from the mean. Individual values are plotted as grey x markers.

Constituent	Period (hr)	Elevation		Velocity			
		Amplitude (m)	Phase (°)	Major (m/s)	Minor (m/s)	Inclination (°)	Phase (°)
M2	12.42	3.05	88	1.89	0.01	126	179
S2	12.00	0.59	138	0.37	0.01	126	226
N2	12.66	0.52	74	0.33	0.00	127	165
K1	23.93	0.15	215	0.04	0.00	125	301
O1	25.82	0.09	168	0.03	0.00	123	265
M6	4.14	0.05	208	0.15	-0.00	127	288

Table A.4.1: Harmonic Analysis at DG4. The elevation fits were done over a period of 36 days and the velocity fits were done over a period of 46 days. The RMS amplitude of the residual elevation was NaN cm and the RMS amplitude of the residual current speed was 16 cm/s.

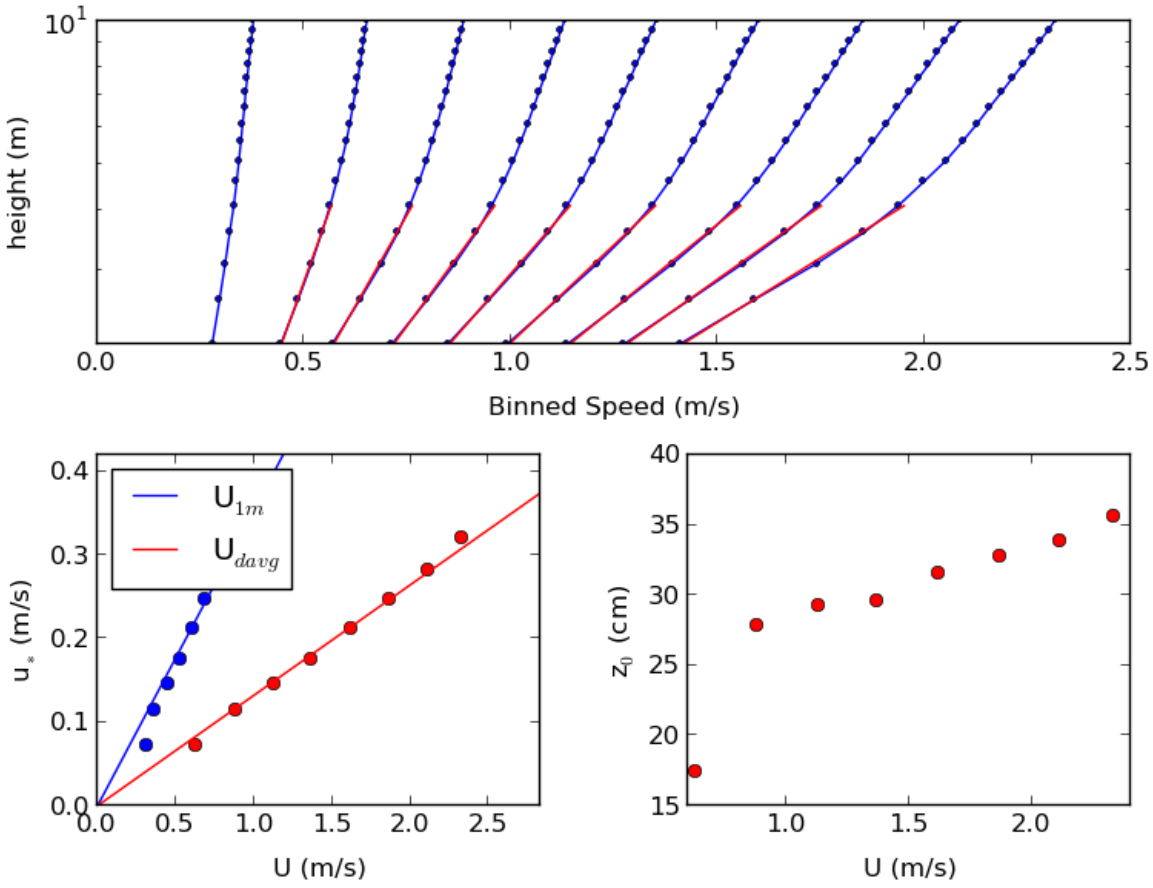

Figure A.4.7: The top panel shows the binned speed profiles during the flood tide at DG4. The red lines correspond to the law of the wall fits. The lower left panel plots u_* as determined from the law of the wall versus a reference speed. Since $u_*^2 = C_d U^2$, C_d is the is the square of the slope of the fitted line. These values are given in the table below. The lower right panel shows the estimates of z_0 from the law of the wall fits.

	Flood	**Ebb**
C_d $(U = V_{1m})$	0.1255	0.0424
C_d $(U = V_{davg})$	0.0175	0.0109
Mean z_0 (cm)	29.7	13.4

Table A.4.2: Drag coefficient, C_d, values at DG4. The values are separated into flood and ebb phases of the tide. Two different reference speeds were used – a theoretical estimate at $z = 1$ m (V_{1m}) and a depth averaged speed which was computed to 95 percent of the surface signal.

	A	**B**	**C**	**D**	**E**	**F**
Diameter (m)	8.0	10.0	12.0	8.0	10.0	12.0
Cut-in Speed (m/s)	1.0	1.0	1.0	1.0	1.0	1.0
Rated Power (kW)	-	-	-	500	500	500
Max Power Output (kW)	189	296	426	189	296	426
Avg. Energy Production (kWh/day)	867	1355	1951	867	1355	1951
Operating Time (%)	68.6	68.6	68.6	68.6	68.6	68.6

Table A.4.3: Turbine statistics for six configurations at DG4. All turbines are assumed to have a hub height of 10 m and a water-wire efficiency of 0.4.

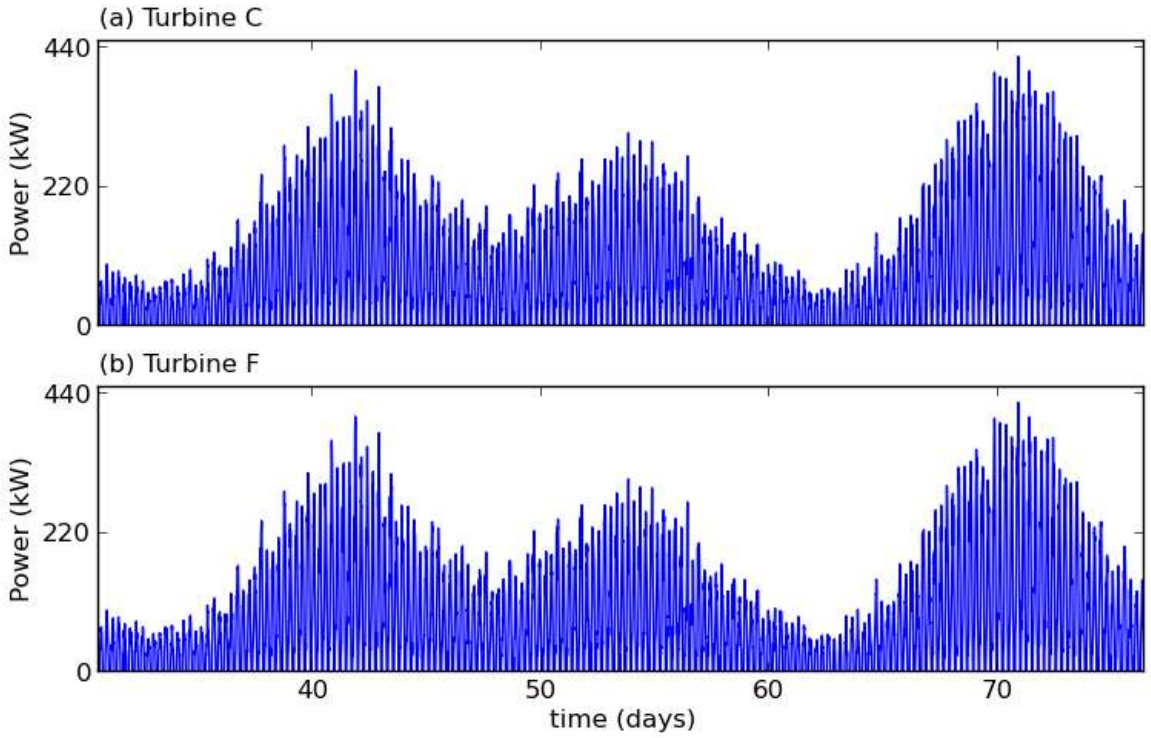

Figure A.4.8: A time series of the power output DG4 for the six turbine configuations listed in Table A.4.3. The power output was computed at a hub height of 10 m using the ten minute ensembled data.

A.5 DG5

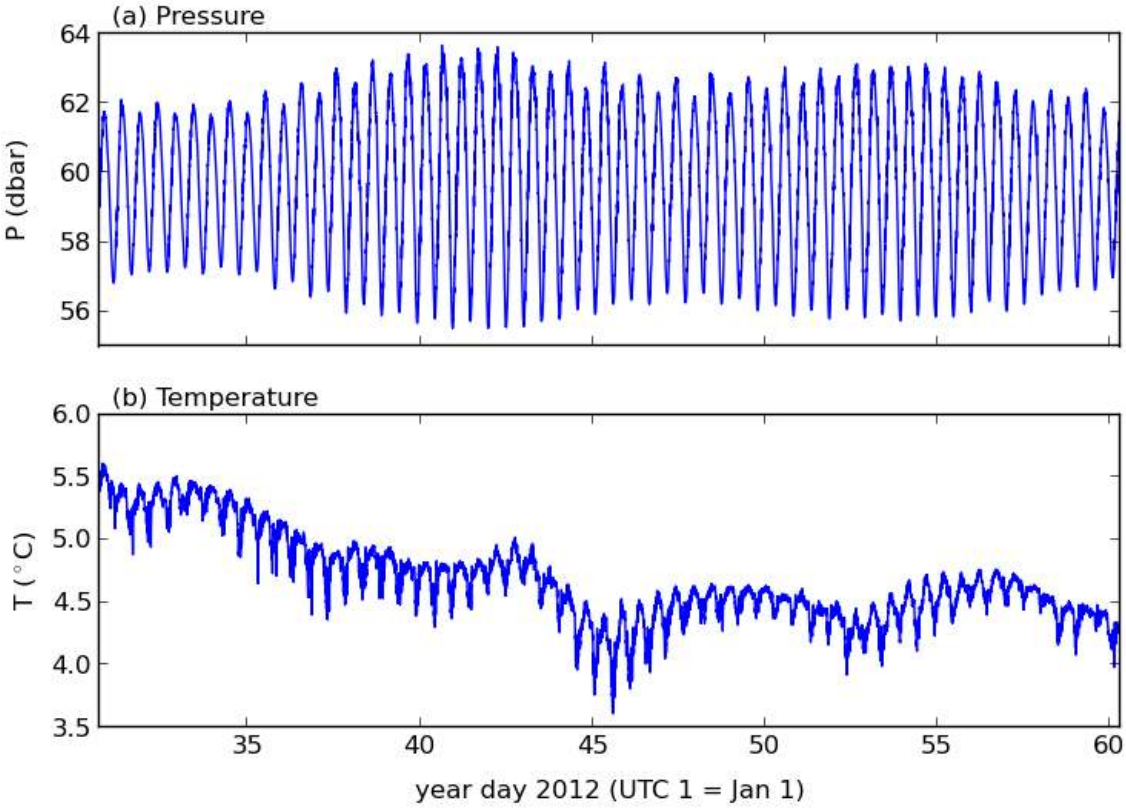

Figure A.5.1: Measurements of pressure and temperature at DG5.

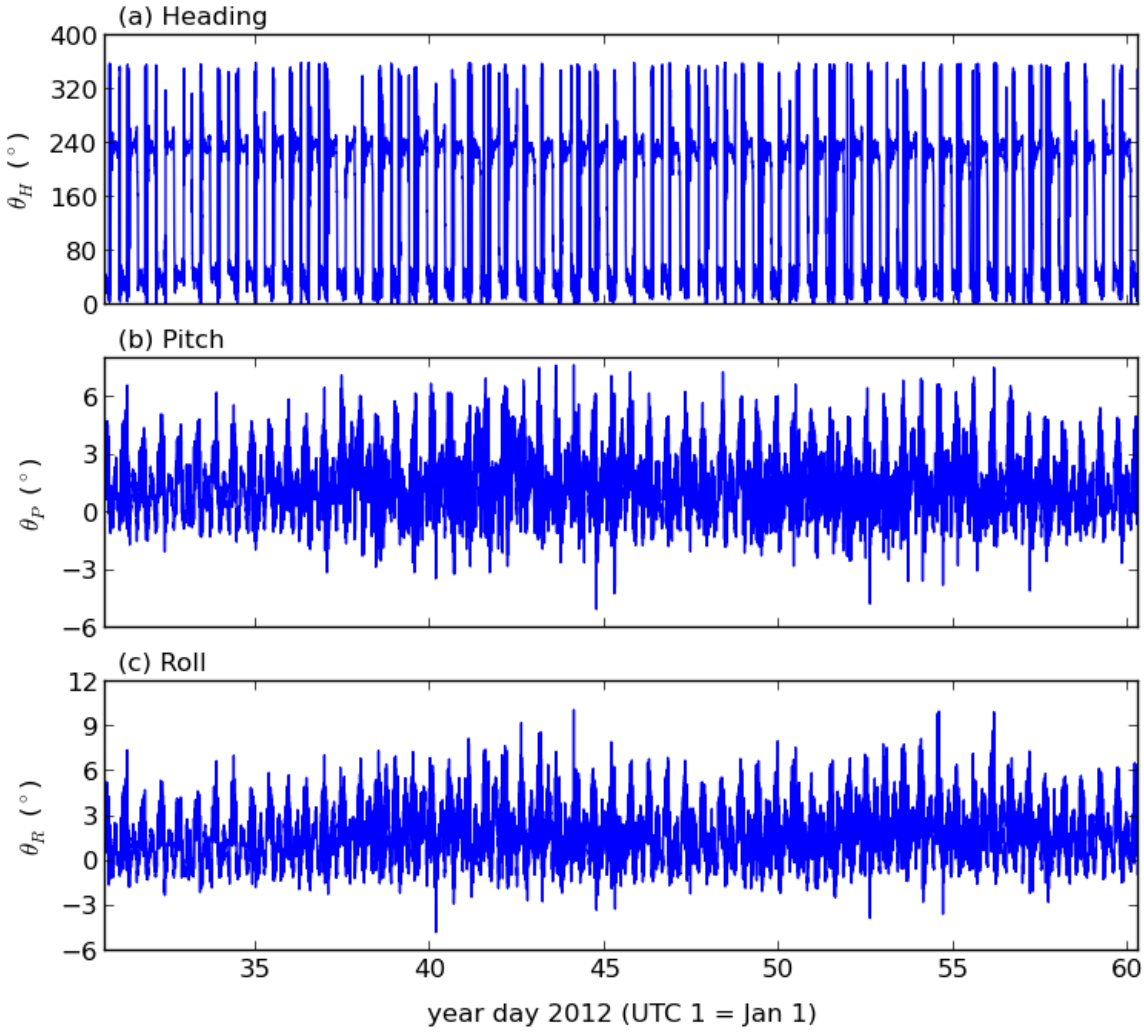

Figure A.5.2: Measurements of heading, pitch and roll at DG5.

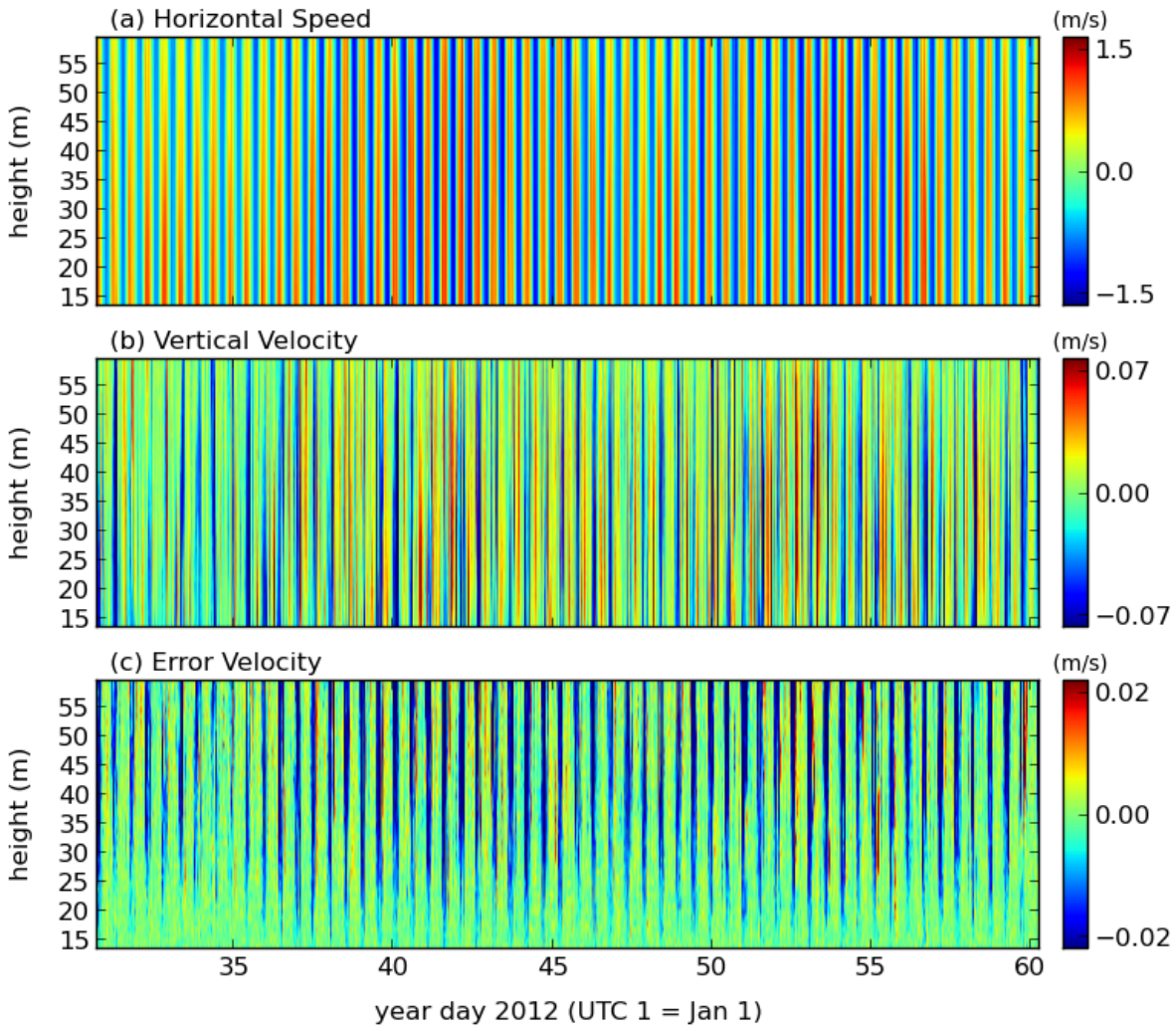

Figure A.5.3: Ten minute ensemble averaged horizontal current speeds, vertical velocities and error velocities for DG5. In panel (a), positive velocities correspond to the flood direction and negative velocities correspond to the ebb direction. The maximum depth is equivalent to 95% of the lowest low water.

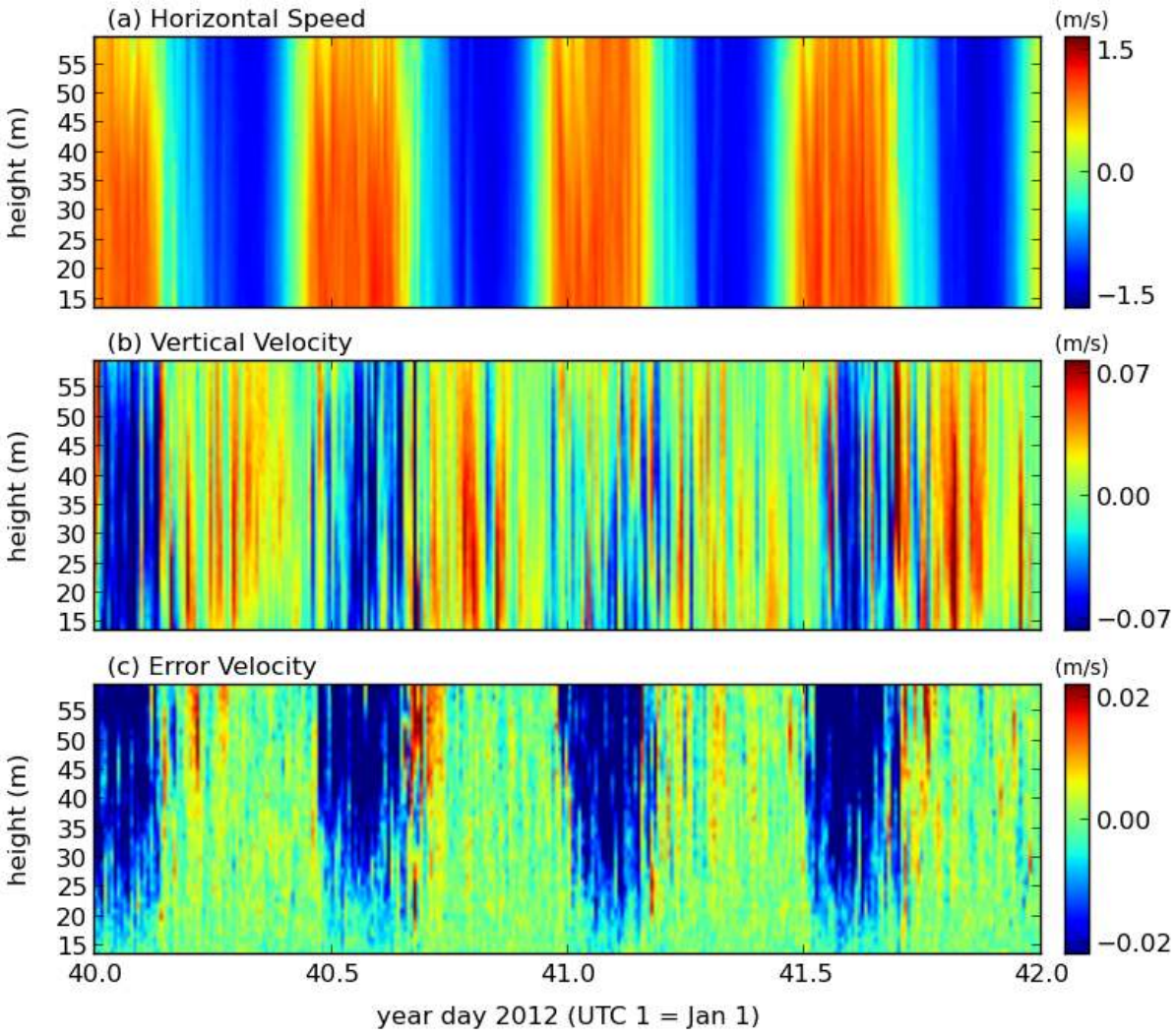

Figure A.5.4: As above, but during a 2-day period.

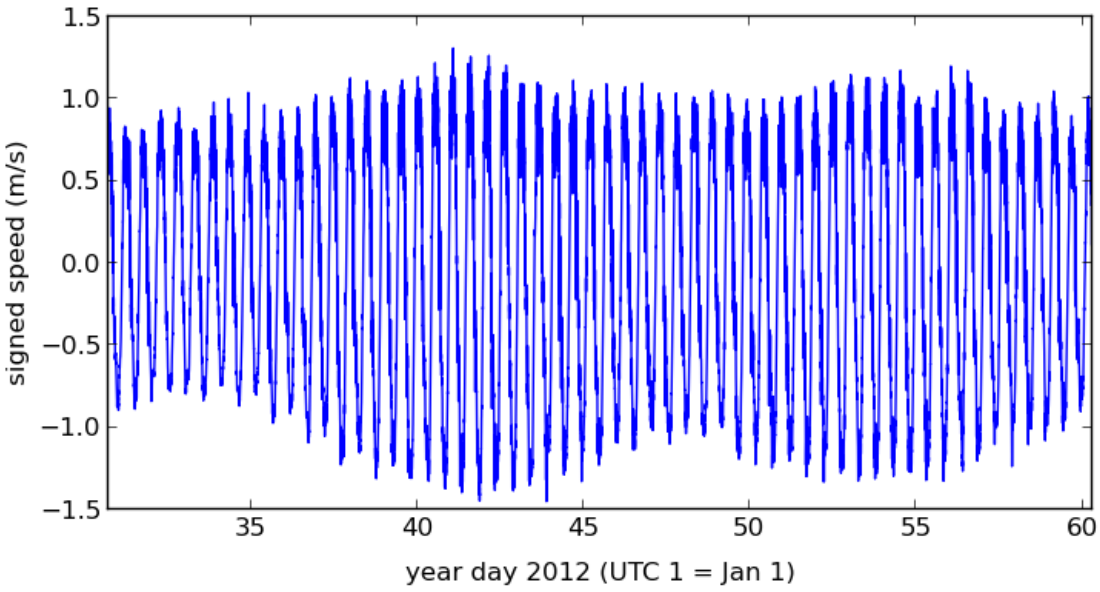

Figure A.5.5: Time series of the depth averaged velocity at DG5. The averages were computed to 95% of the surface signal. Positive velocities correspond to the flood direction and negative velocities correspond to the ebb direction.

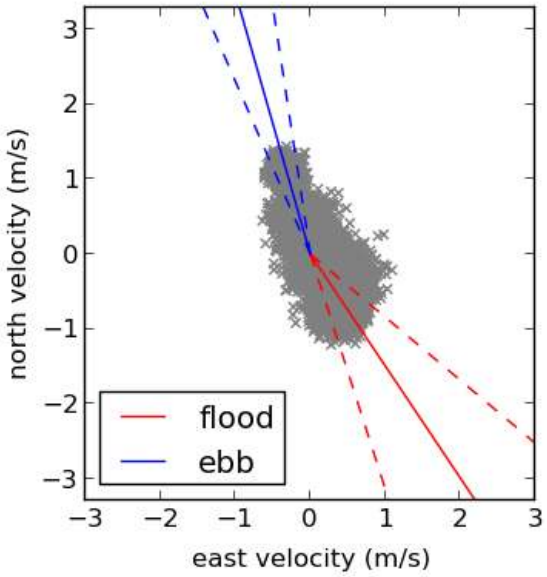

Figure A.5.6: The principal flow directions at DG5 are shown by the solid red and blue lines for the flood and ebb tides, respectively. The dashed lines indicate ±1 standard deviation from the mean. Individual values are plotted as grey x markers.

	A	B	C	D	E	F
Diameter (m)	8.0	10.0	12.0	8.0	10.0	12.0
Cut-in Speed (m/s)	1.0	1.0	1.0	1.0	1.0	1.0
Rated Power (kW)	-	-	-	500	500	500
Max Power Output (kW)	27	43	62	27	43	62
Avg. Energy Production (kWh/day)	88	138	199	88	138	199
Operating Time (%)	21.8	21.8	21.8	21.8	21.8	21.8

Table A.5.1: Turbine statistics for six configurations at DG5. All turbines are assumed to have a hub height of 10 m and a water-wire efficiency of 0.4.

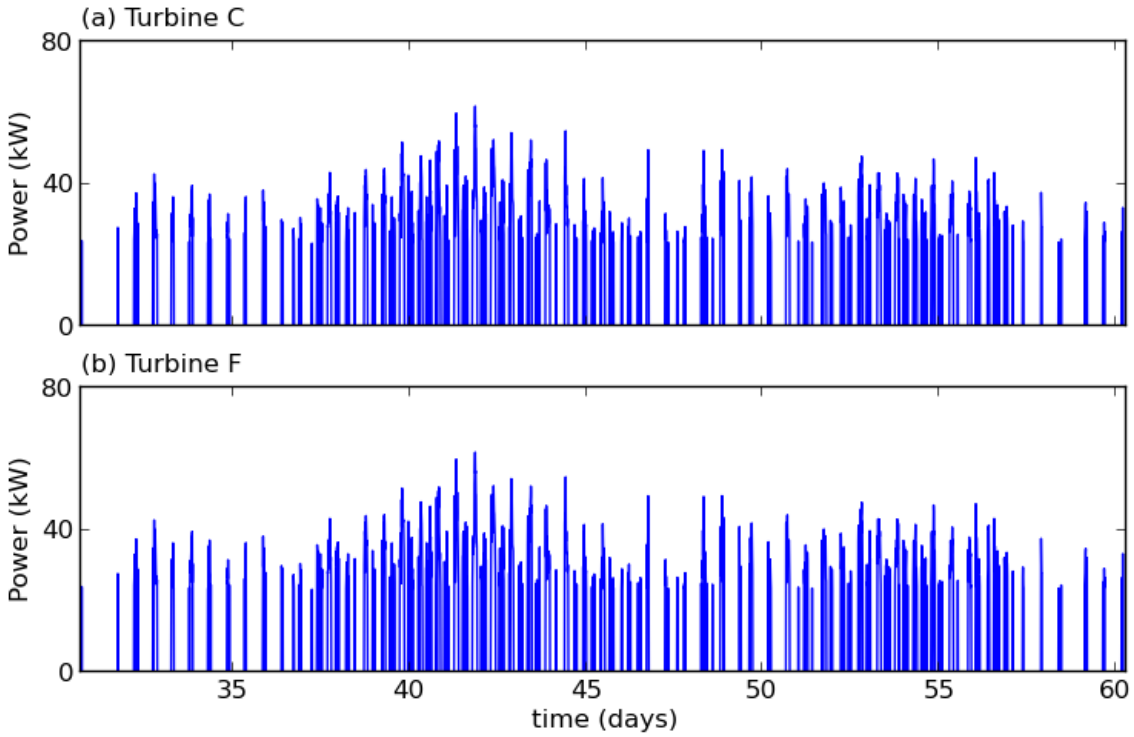

Figure A.5.7: A time series of the power output DG5 for the six turbine configuations listed in Table A.5.1. The power output was computed at a hub height of 10 m using the ten minute ensembled data.

A.6 GP1

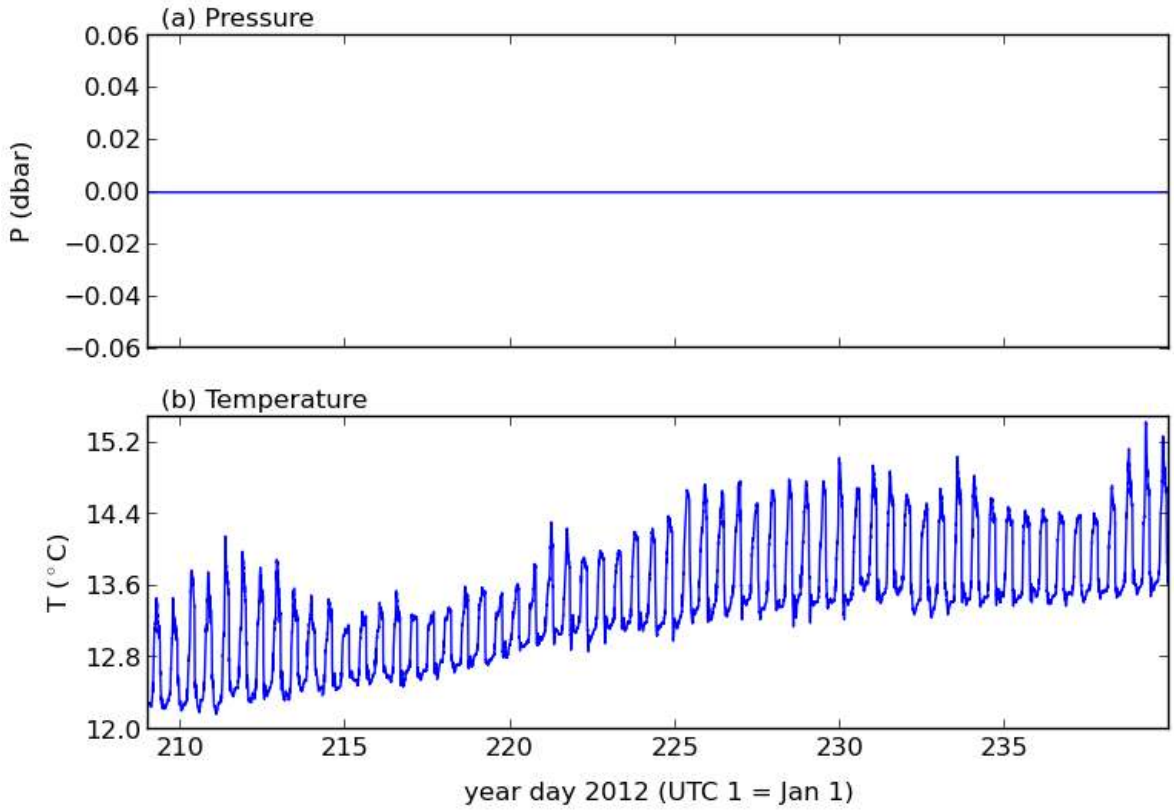

Figure A.6.1: Measurements of pressure and temperature at GP1. NOTE: This ADCP did not have a pressure sensor.

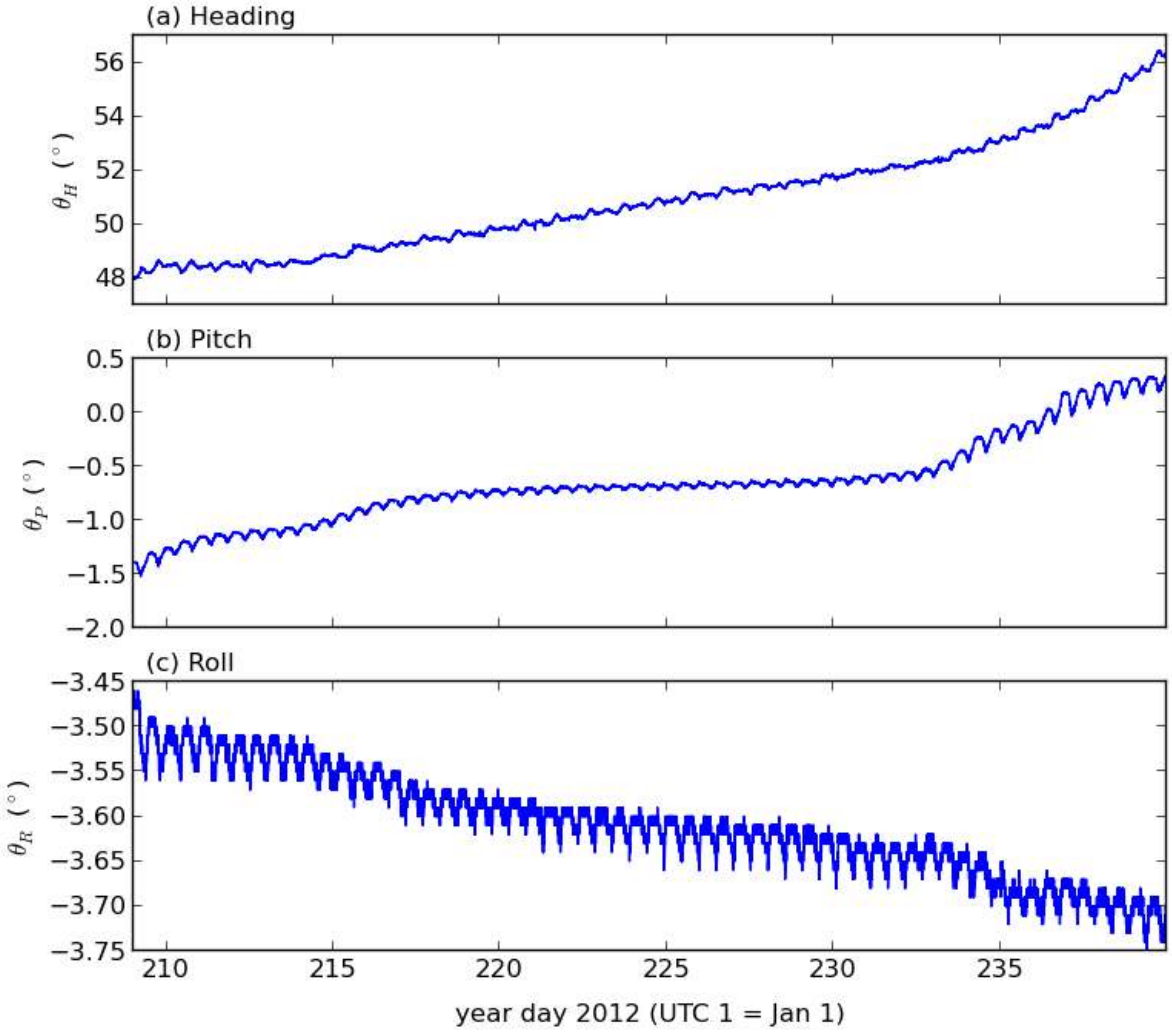

Figure A.6.2: Measurements of heading, pitch and roll at GP1.

A.7 GP2

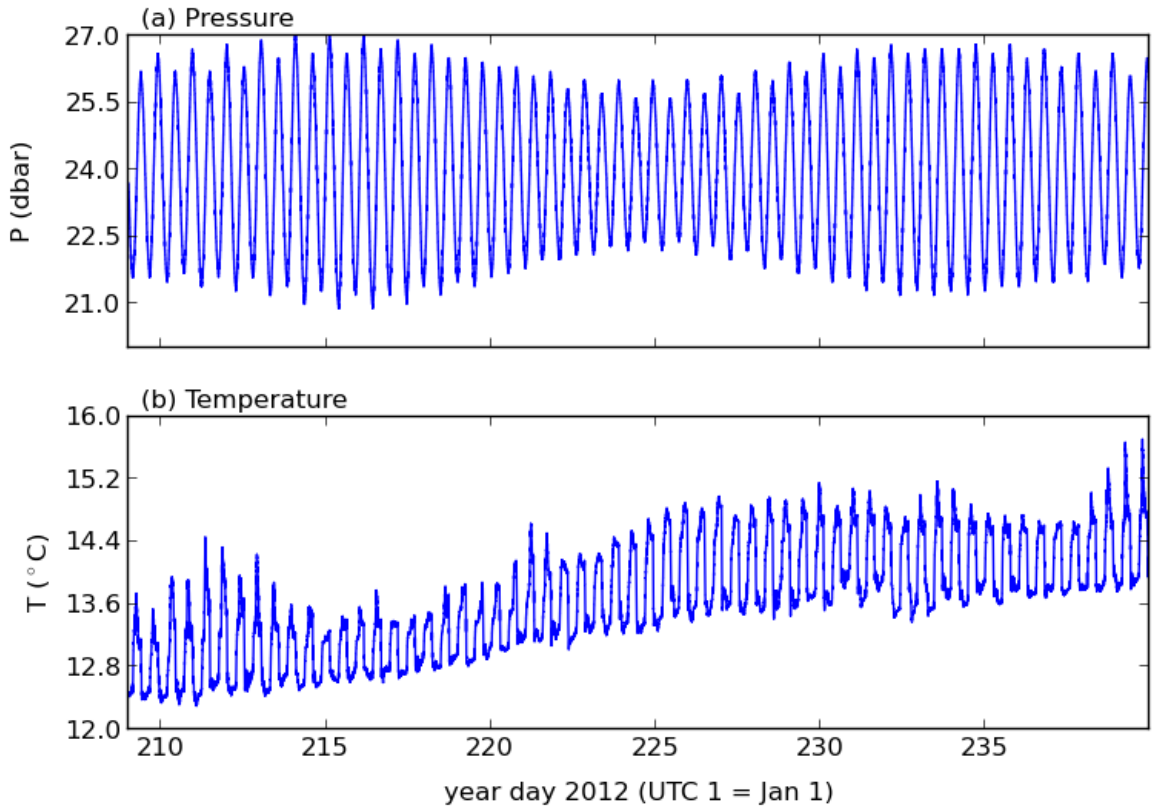

Figure A.7.1: Measurements of pressure and temperature at GP2.

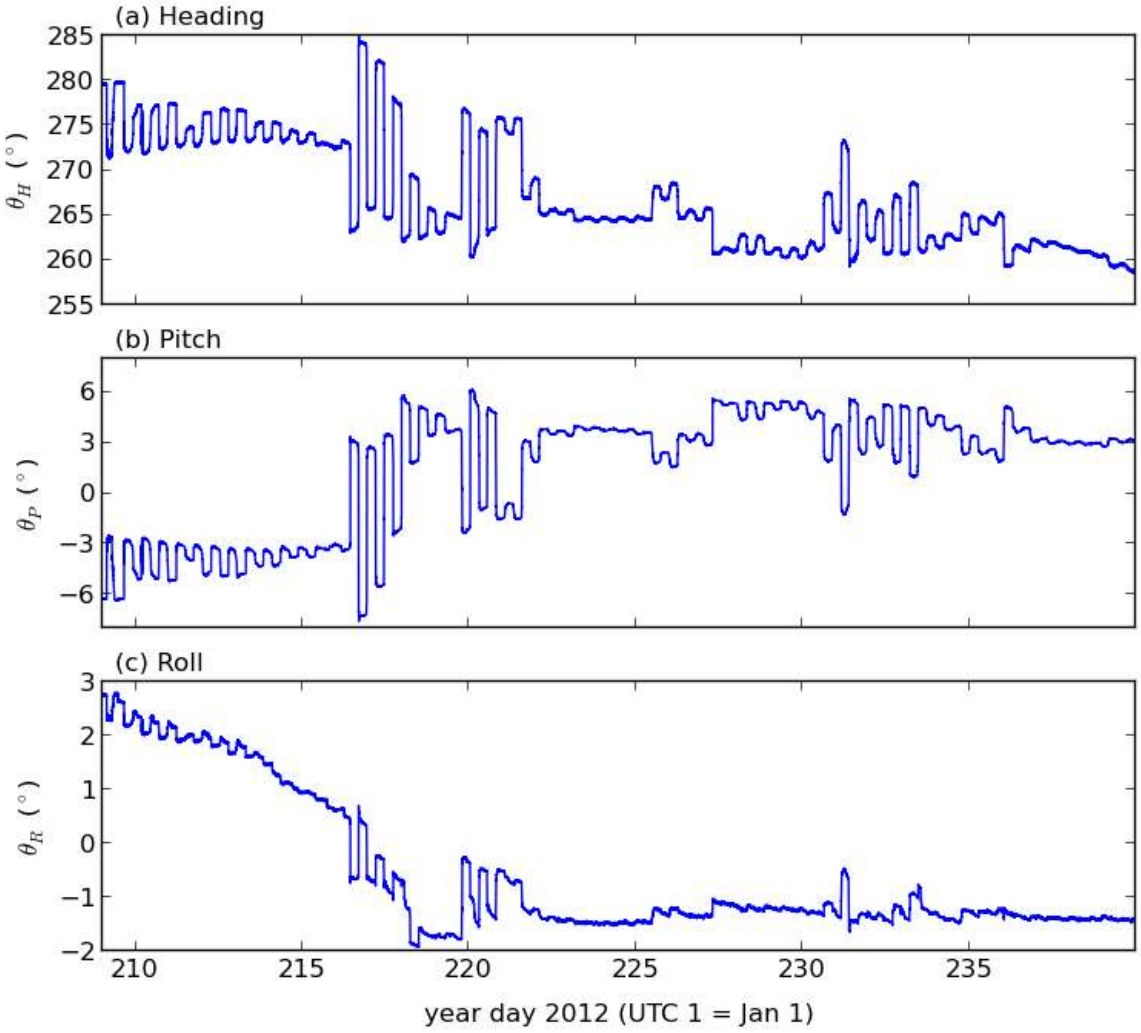

Figure A.7.2: Measurements of heading, pitch and roll at GP2.

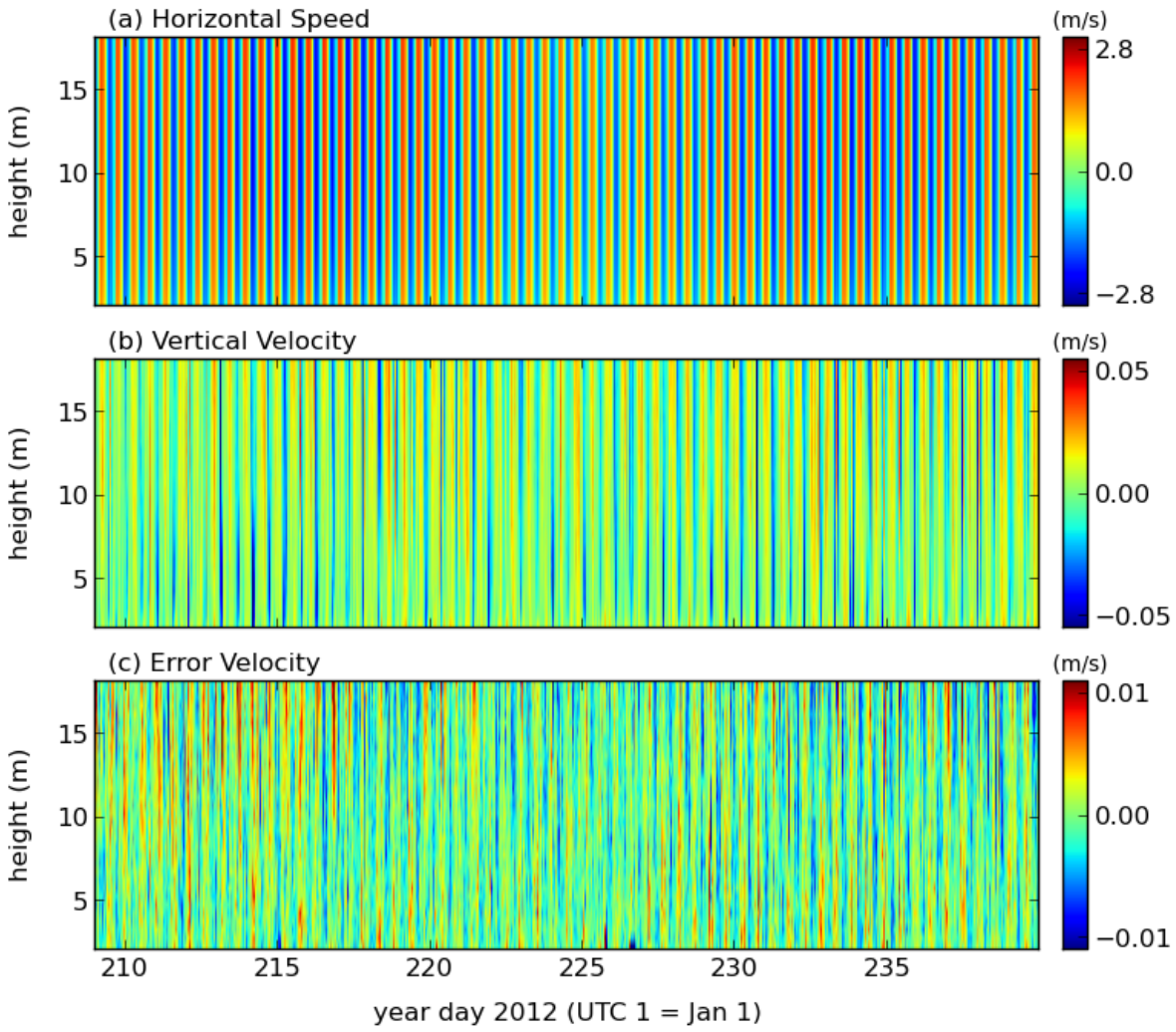

Figure A.7.3: Ten minute ensemble averaged horizontal current speeds, vertical velocities and error velocities for GP2. In panel (a), positive velocities correspond to the flood direction and negative velocities correspond to the ebb direction. The maximum depth is equivalent to 95% of the lowest low water. NOTE: This ADCP was not calibrated, so the pressure signal was used to estimate ebb/flood directions (as opposed to using the principal flow direction).

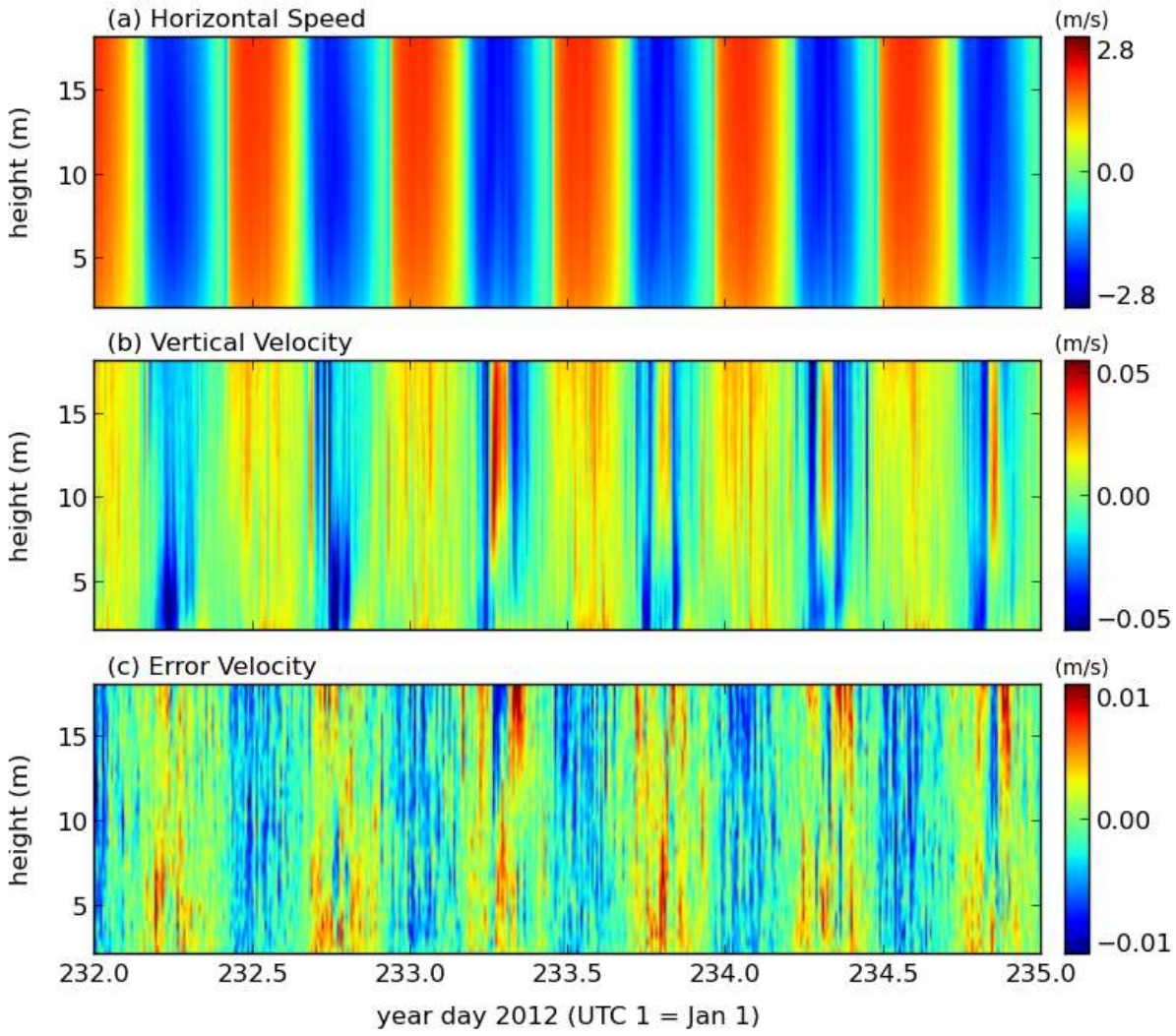

Figure A.7.4: As above, but during a 2-day period.

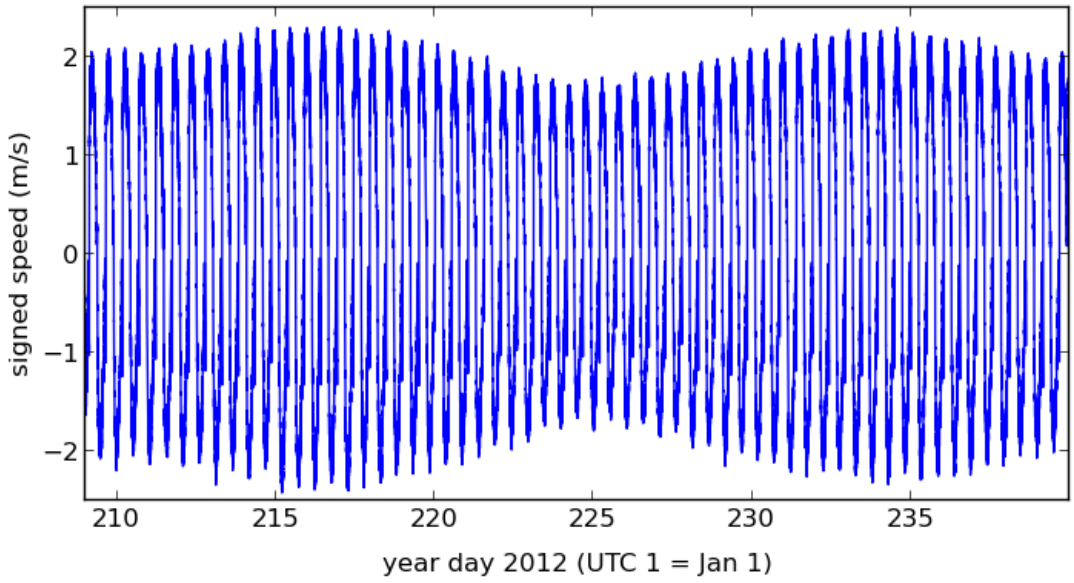

Figure A.7.5: Time series of the depth averaged velocity at GP2. The averages were computed to 95% of the surface signal. Positive velocities correspond to the flood direction and negative velocities correspond to the ebb direction.

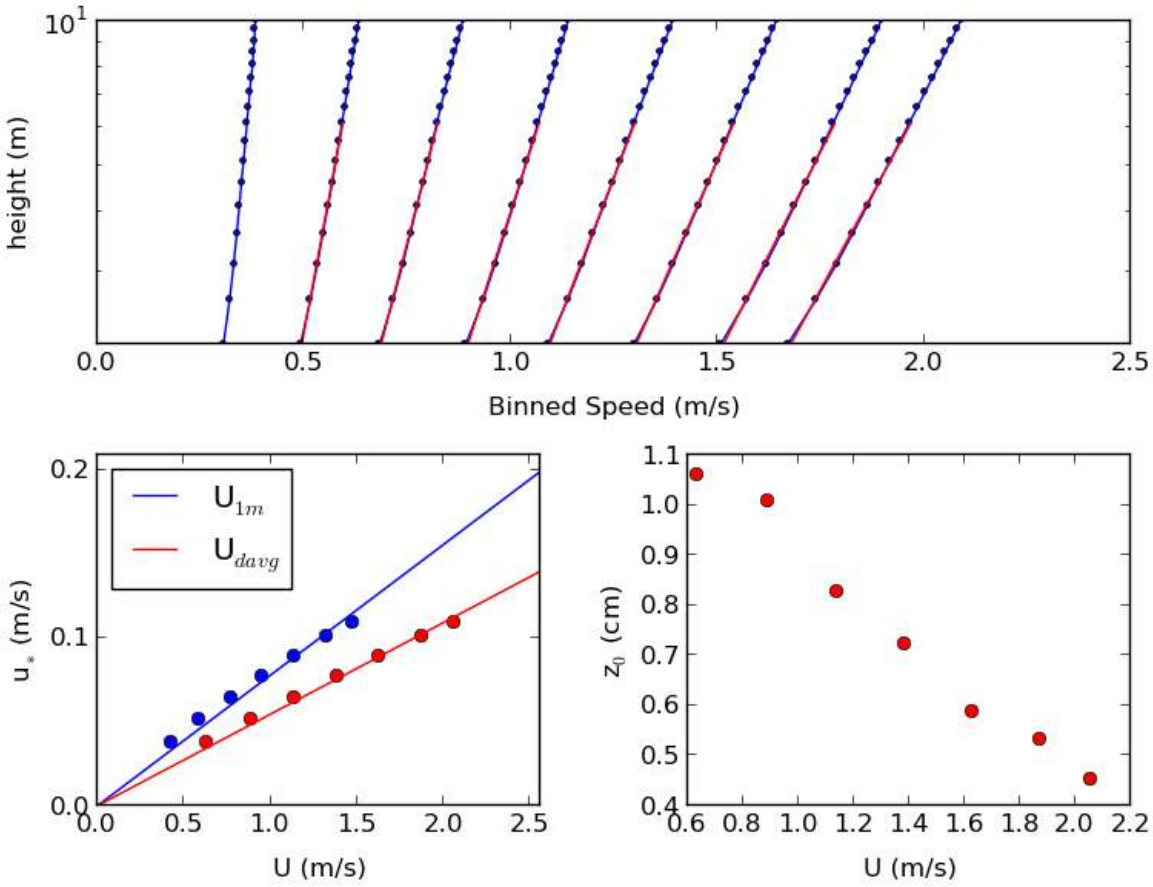

Figure A.7.6: The top panel shows the binned speed profiles during the flood tide at GP2. The red lines correspond to the law of the wall fits. The lower left panel plots u_* as determined from the law of the wall versus a reference speed. Since $u_*^2 = C_d U^2$, C_d is the is the square of the slope of the fitted line. These values are given in the table below. The lower right panel shows the estimates of z_0 from the law of the wall fits.

	Flood	**Ebb**
C_d $(U = V_{1m})$	0.0061	0.0163
C_d $(U = V_{davg})$	0.0030	0.0063
Mean z_0 (cm)	0.7	3.7

Table A.7.1: Drag coefficient, C_d, values at GP2. The values are separated into flood and ebb phases of the tide. Two different reference speeds were used – a theoretical estimate at $z = 1$ m (V_{1m}) and a depth averaged speed which was computed to 95 percent of the surface signal.

	A	B	C	D	E	F
Diameter (m)	8.0	10.0	12.0	8.0	10.0	12.0
Cut-in Speed (m/s)	1.0	1.0	1.0	1.0	1.0	1.0
Rated Power (kW)	-	-	-	500	500	500
Max Power Output (kW)	142	223	320	142	223	320
Avg. Energy Production (kWh/day)	992	1550	2232	992	1550	2232
Operating Time (%)	74.3	74.3	74.3	74.3	74.3	74.3

Table A.7.2: Turbine statistics for six configurations at GP2. All turbines are assumed to have a hub height of 10 m and a water-wire efficiency of 0.4.

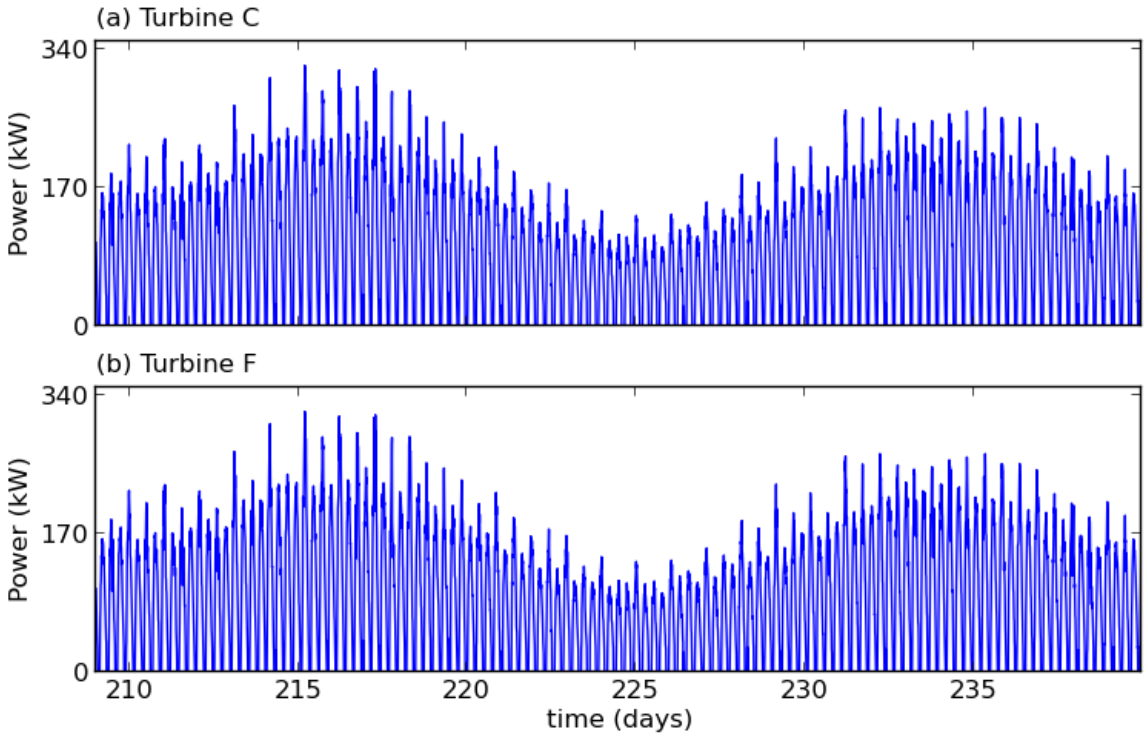

Figure A.7.7: A time series of the power output GP2 for the six turbine configuations listed in Table A.7.2. The power output was computed at a hub height of 10 m using the ten minute ensembled data.

A.8 GP3

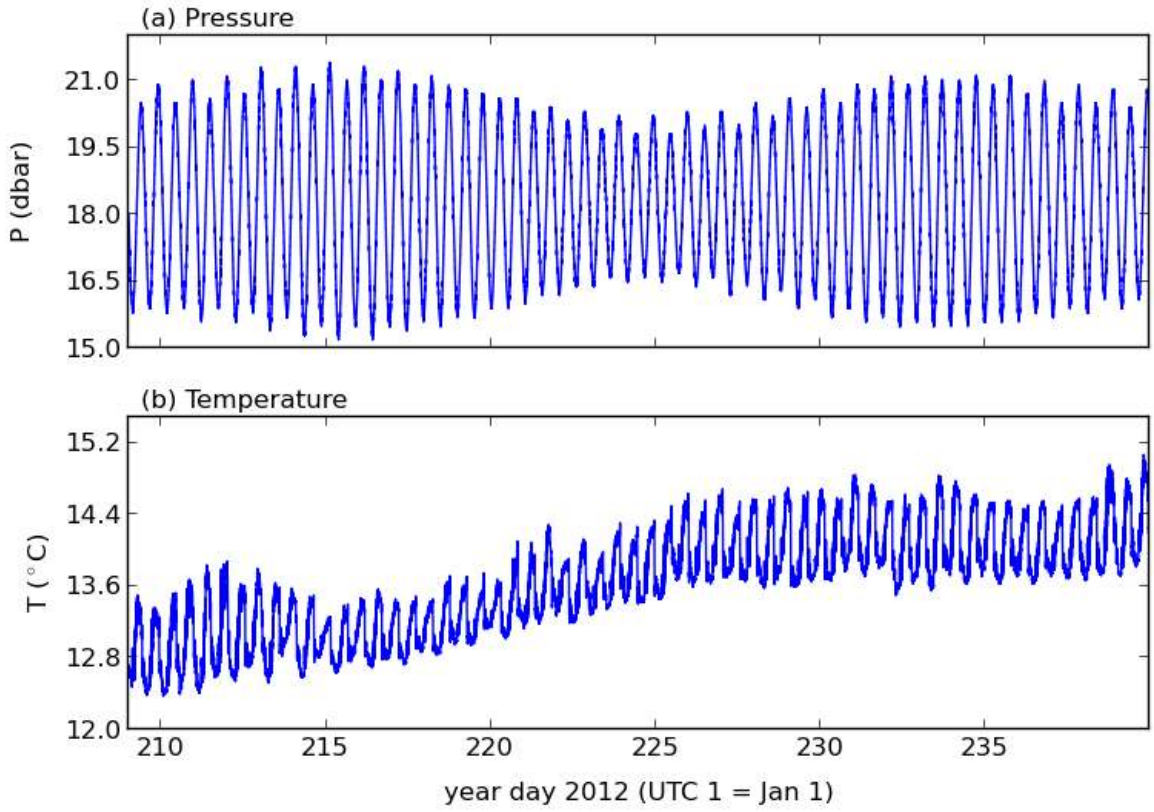

Figure A.8.1: Measurements of pressure and temperature at GP3.

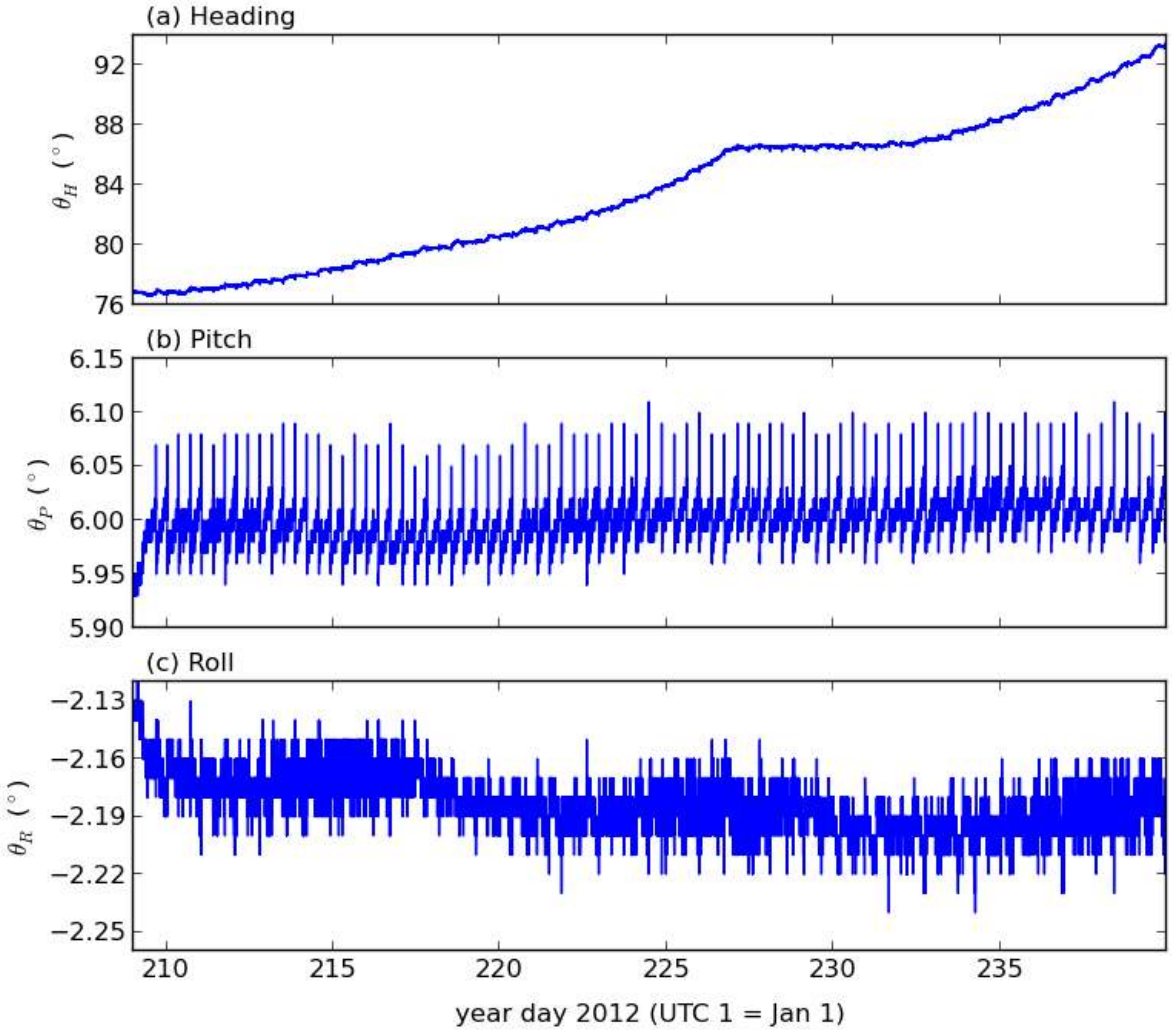

Figure A.8.2: Measurements of heading, pitch and roll at GP3.

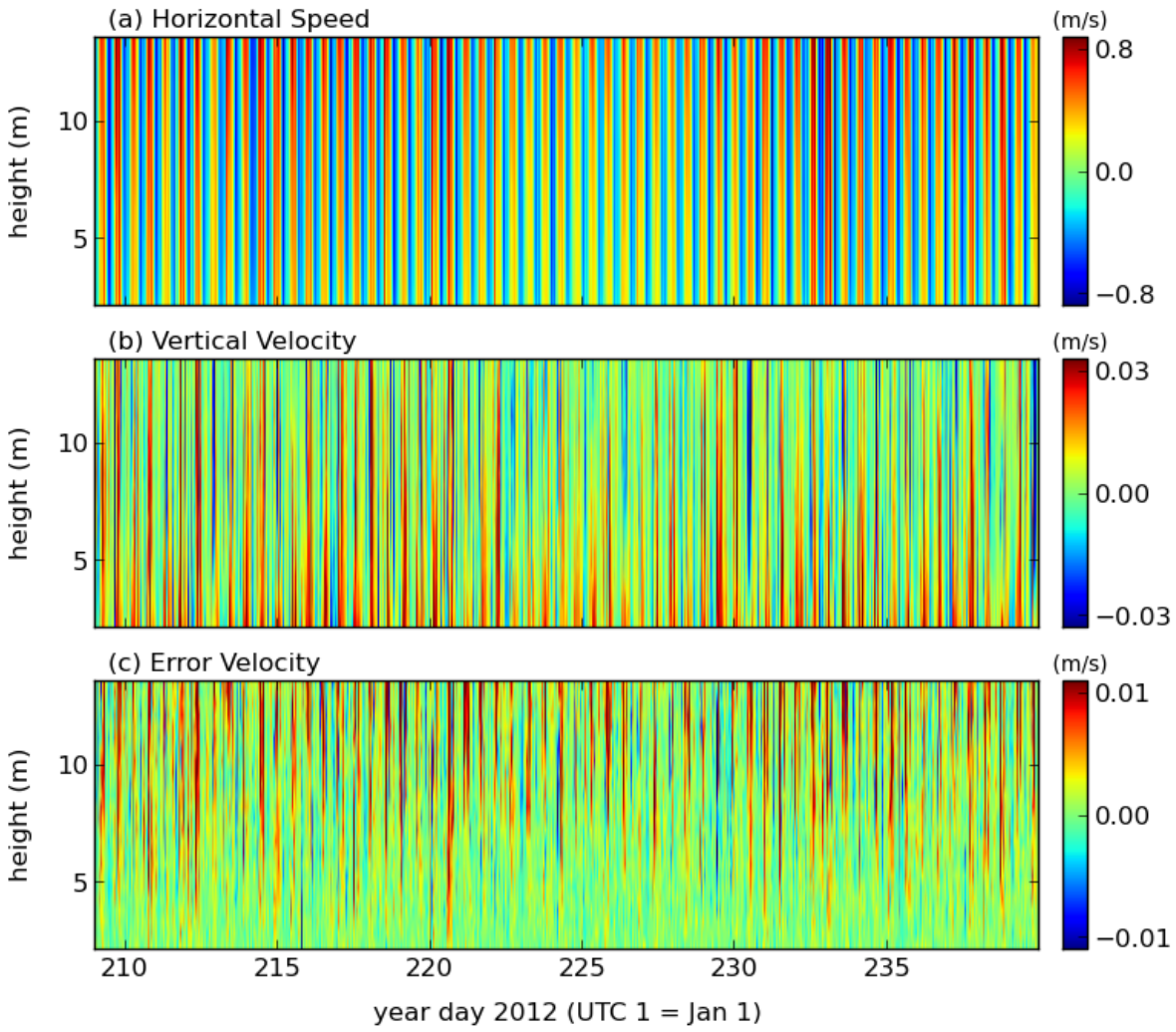

Figure A.8.3: Ten minute ensemble averaged horizontal current speeds, vertical velocities and error velocities for GP3. In panel (a), positive velocities correspond to the flood direction and negative velocities correspond to the ebb direction. The maximum depth is equivalent to 95% of the lowest low water.

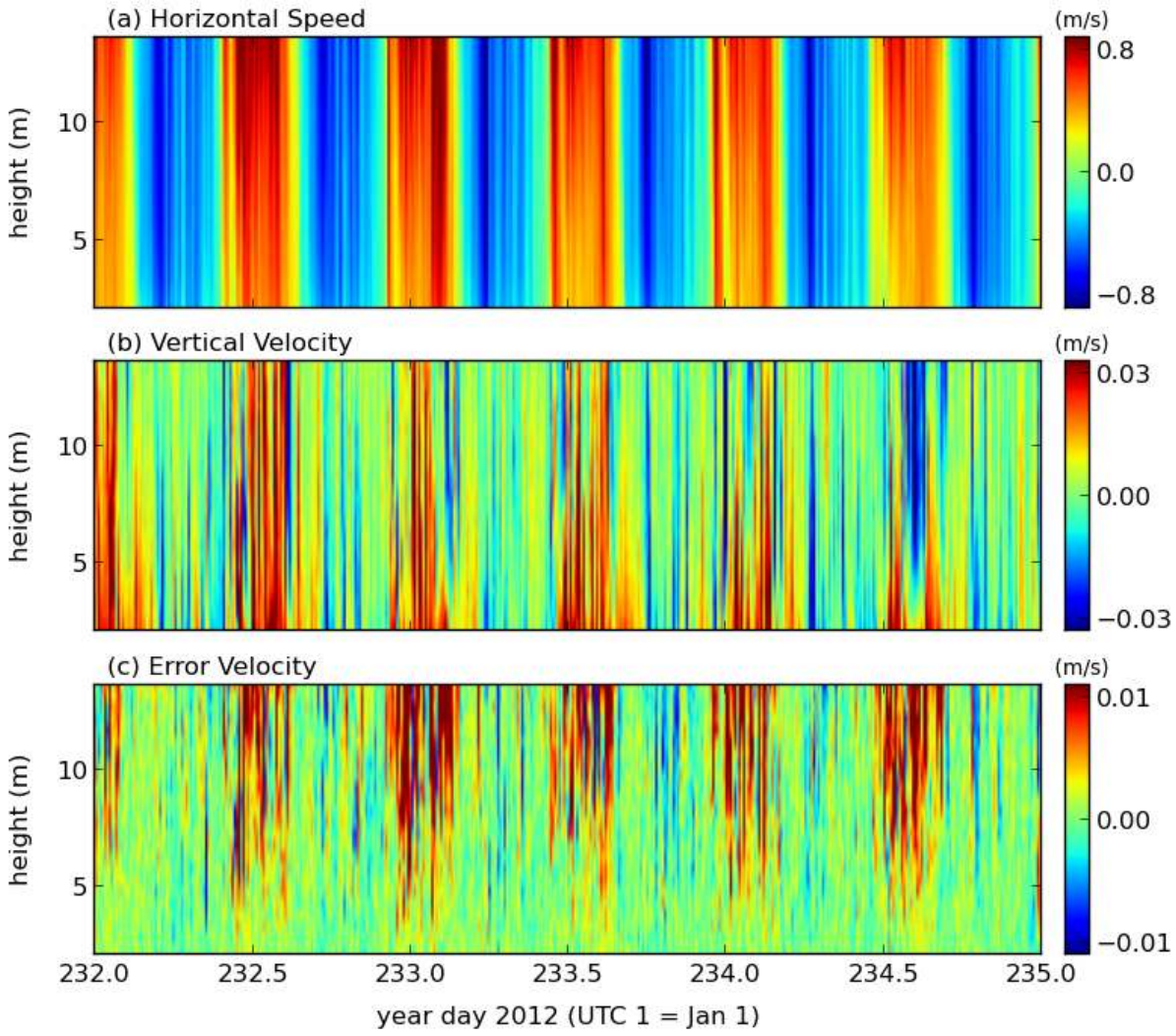

Figure A.8.4: As above, but during a 2-day period.

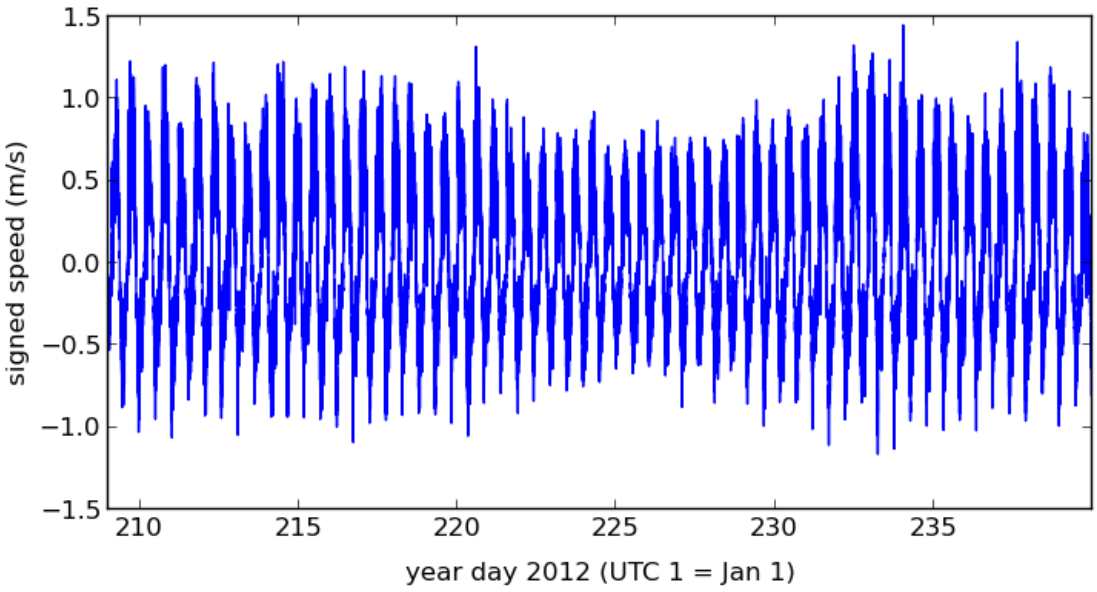

Figure A.8.5: Time series of the depth averaged velocity at GP3. The averages were computed to 95% of the surface signal. Positive velocities correspond to the flood direction and negative velocities correspond to the ebb direction.

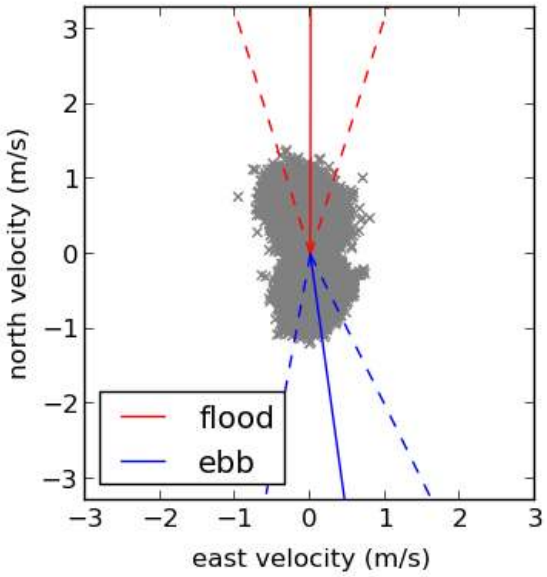

Figure A.8.6: The principal flow directions at GP3 are shown by the solid red and blue lines for the flood and ebb tides, respectively. The dashed lines indicate ±1 standard deviation from the mean. Individual values are plotted as grey x markers.

Constituent	Period (hr)	Elevation		Velocity			
		Amplitude (m)	Phase (°)	Major (m/s)	Minor (m/s)	Inclination (°)	Phase (°)
M2	12.42	2.25	81	0.46	-0.06	92	328
N2	12.66	0.39	46	0.06	-0.02	100	287
S2	12.00	0.34	126	0.06	-0.01	87	24
K1	23.93	0.15	208	0.01	-0.00	100	88
O1	25.82	0.12	164	0.00	-0.00	45	104
M6	4.14	0.02	246	0.08	-0.03	103	113

Table A.8.1: Harmonic Analysis at GP3. The elevation fits were done over a period of 31 days and the velocity fits were done over a period of 31 days. The RMS amplitude of the residual elevation was 9.1 cm and the RMS amplitude of the residual current speed was 10 cm/s.

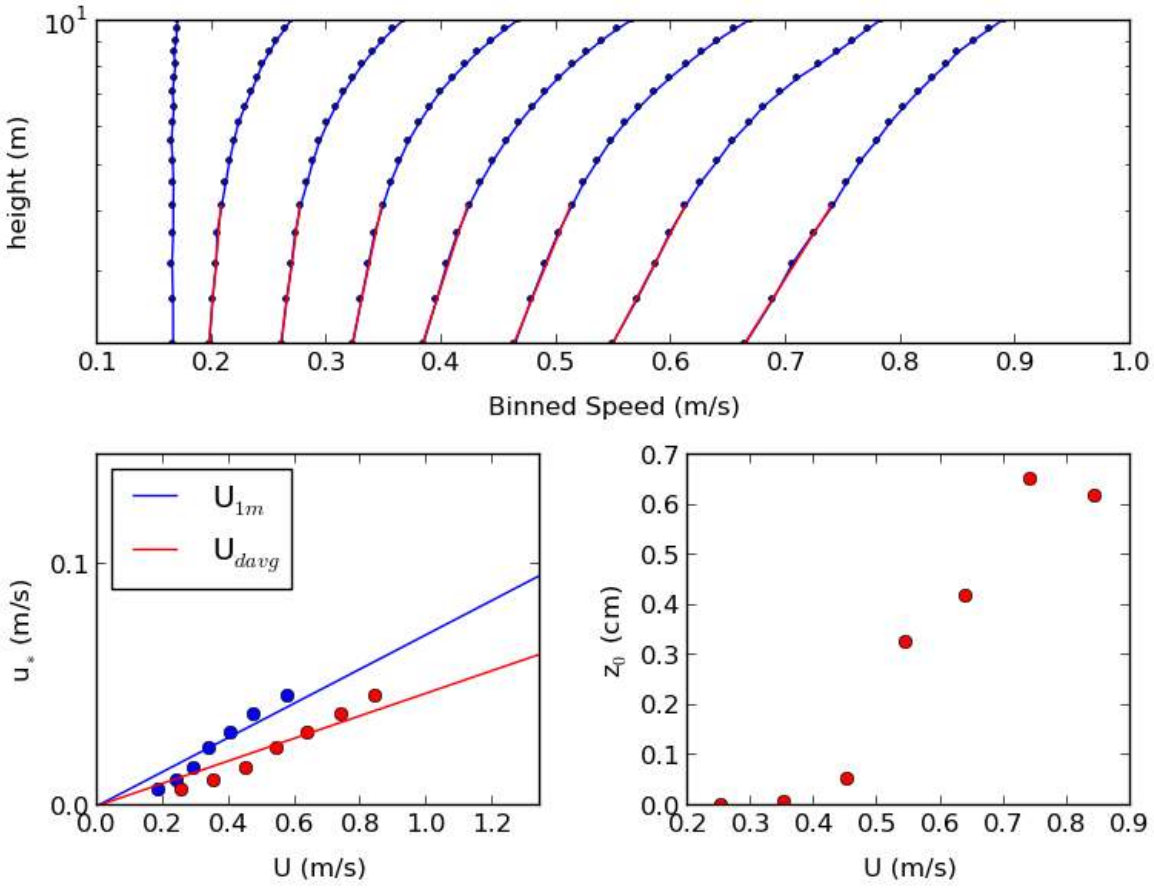

Figure A.8.7: The top panel shows the binned speed profiles during the flood tide at GP3. The red lines correspond to the law of the wall fits. The lower left panel plots u_* as determined from the law of the wall versus a reference speed. Since $u_*^2 = C_d U^2$, C_d is the is the square of the slope of the fitted line. These values are given in the table below. The lower right panel shows the estimates of z_0 from the law of the wall fits.

	Flood	**Ebb**
C_d $(U = V_{1m})$	0.0051	0.0136
C_d $(U = V_{davg})$	0.0022	0.0056
Mean z_0 (cm)	0.3	3.2

Table A.8.2: Drag coefficient, C_d, values at GP3. The values are separated into flood and ebb phases of the tide. Two different reference speeds were used – a theoretical estimate at $z = 1$ m (V_{1m}) and a depth averaged speed which was computed to 95 percent of the surface signal.

	A	**B**	**C**	**D**	**E**	**F**
Diameter (m)	8.0	10.0	12.0	8.0	10.0	12.0
Cut-in Speed (m/s)	1.0	1.0	1.0	1.0	1.0	1.0
Rated Power (kW)	-	-	-	500	500	500
Max Power Output (kW)	11	18	25	11	18	25
Avg. Energy Production (kWh/day)	0	0	1	0	0	1
Operating Time (%)	0.0	0.0	0.0	0.0	0.0	0.0

Table A.8.3: Turbine statistics for six configurations at GP3. All turbines are assumed to have a hub height of 10 m and a water-wire efficiency of 0.4.

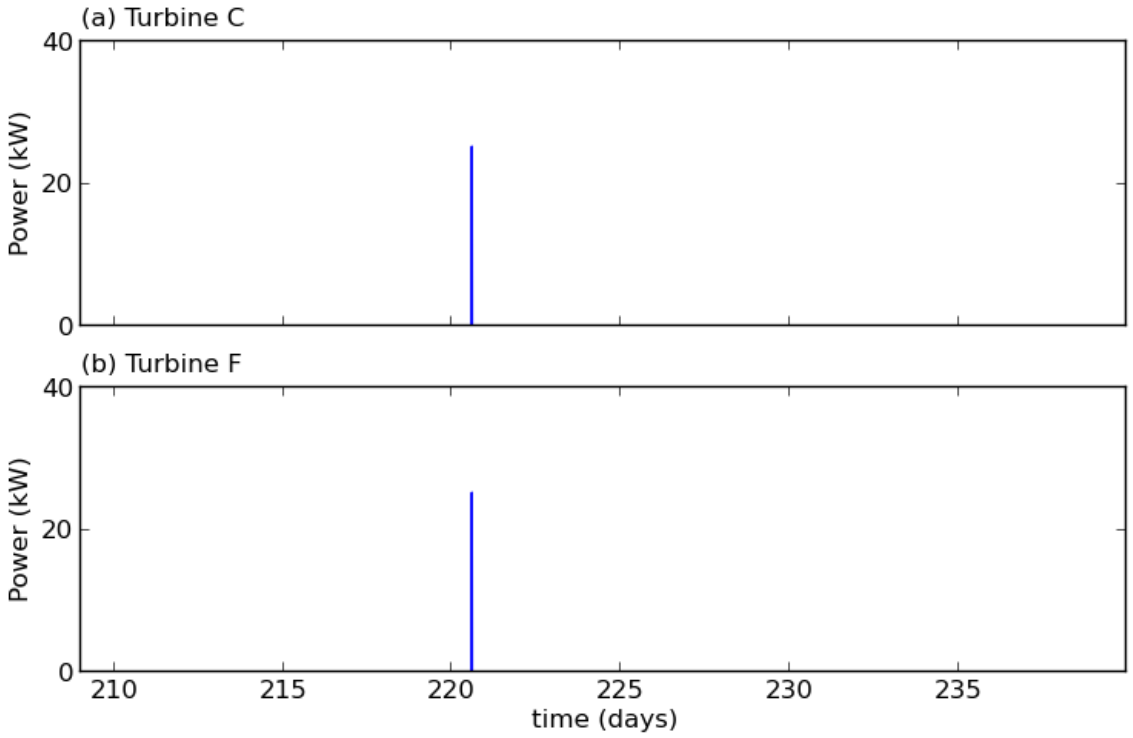

Figure A.8.8: A time series of the power output GP3 for the six turbine configuations listed in Table A.8.3. The power output was computed at a hub height of 10 m using the ten minute ensembled data.

A.9 GP4

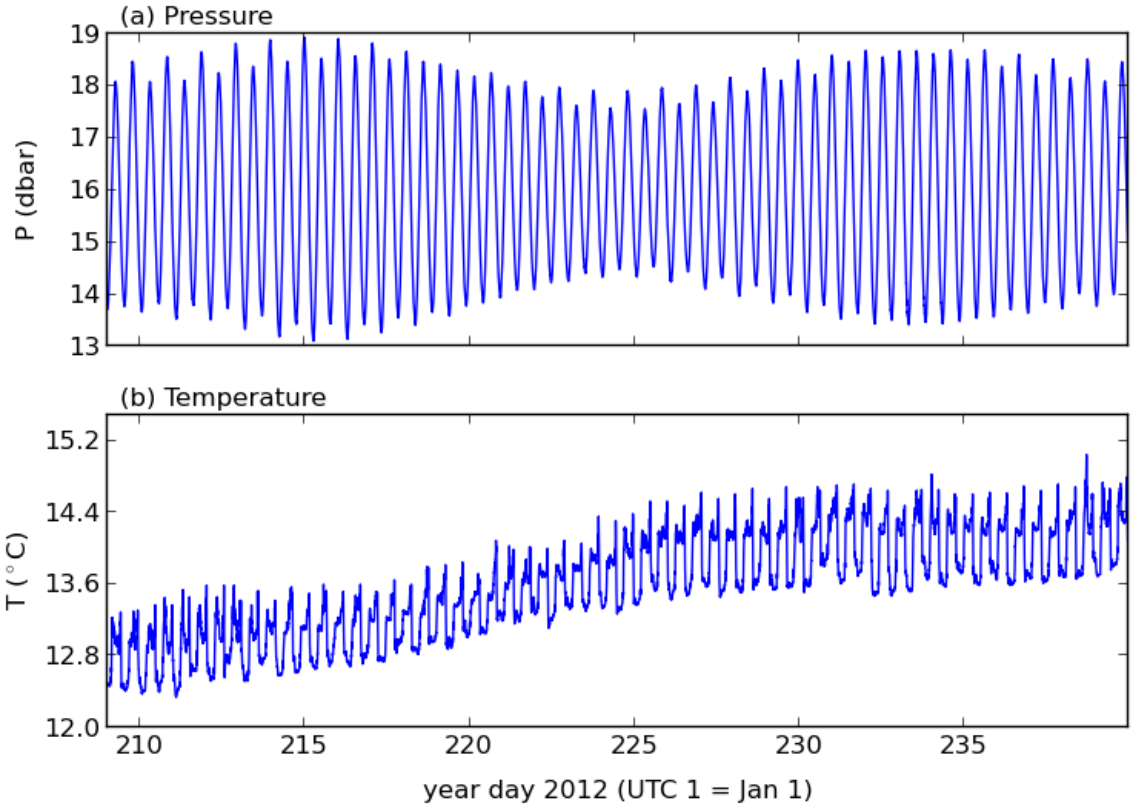

Figure A.9.1: Measurements of pressure and temperature at GP4.

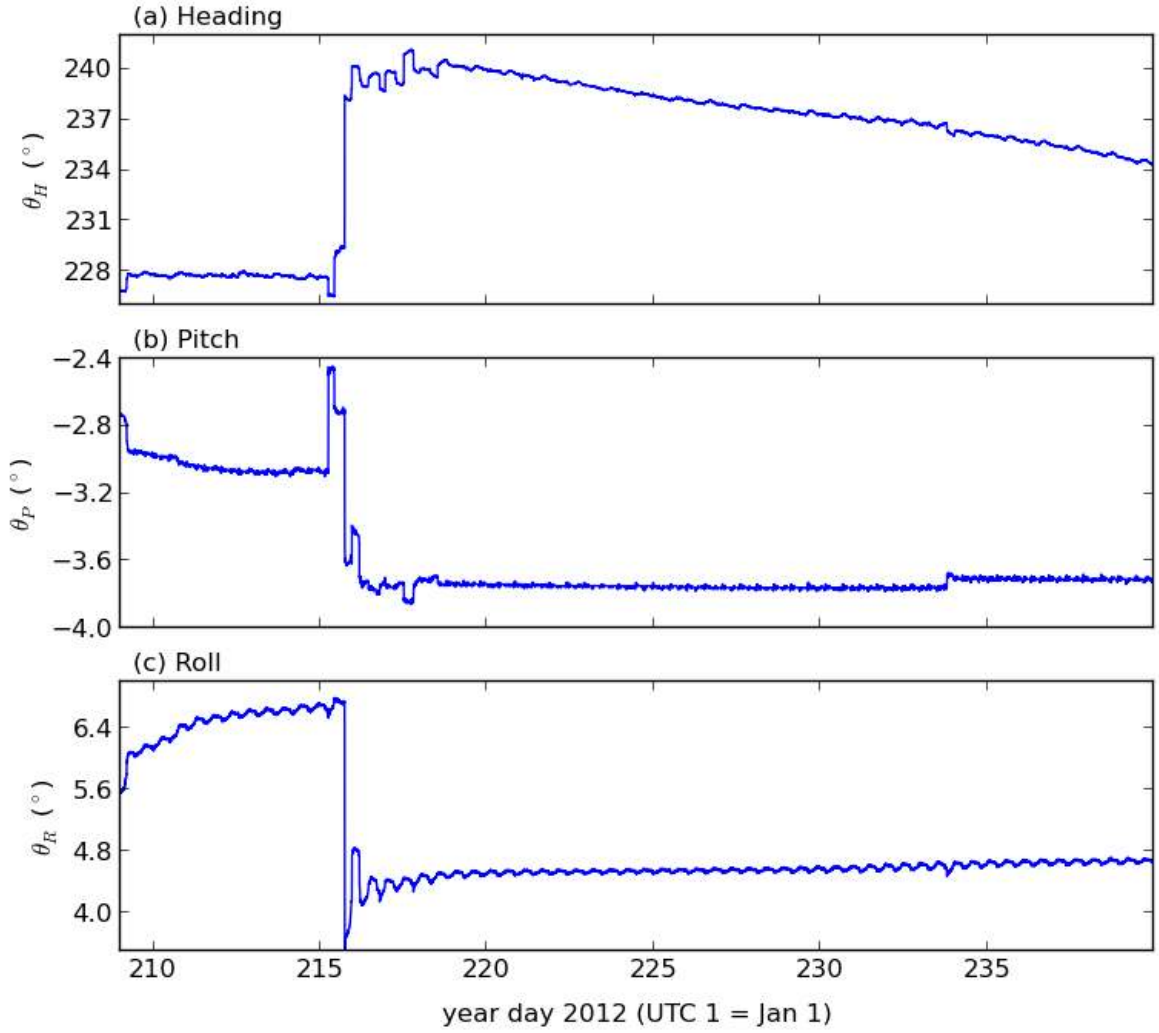

Figure A.9.2: Measurements of heading, pitch and roll at GP4.

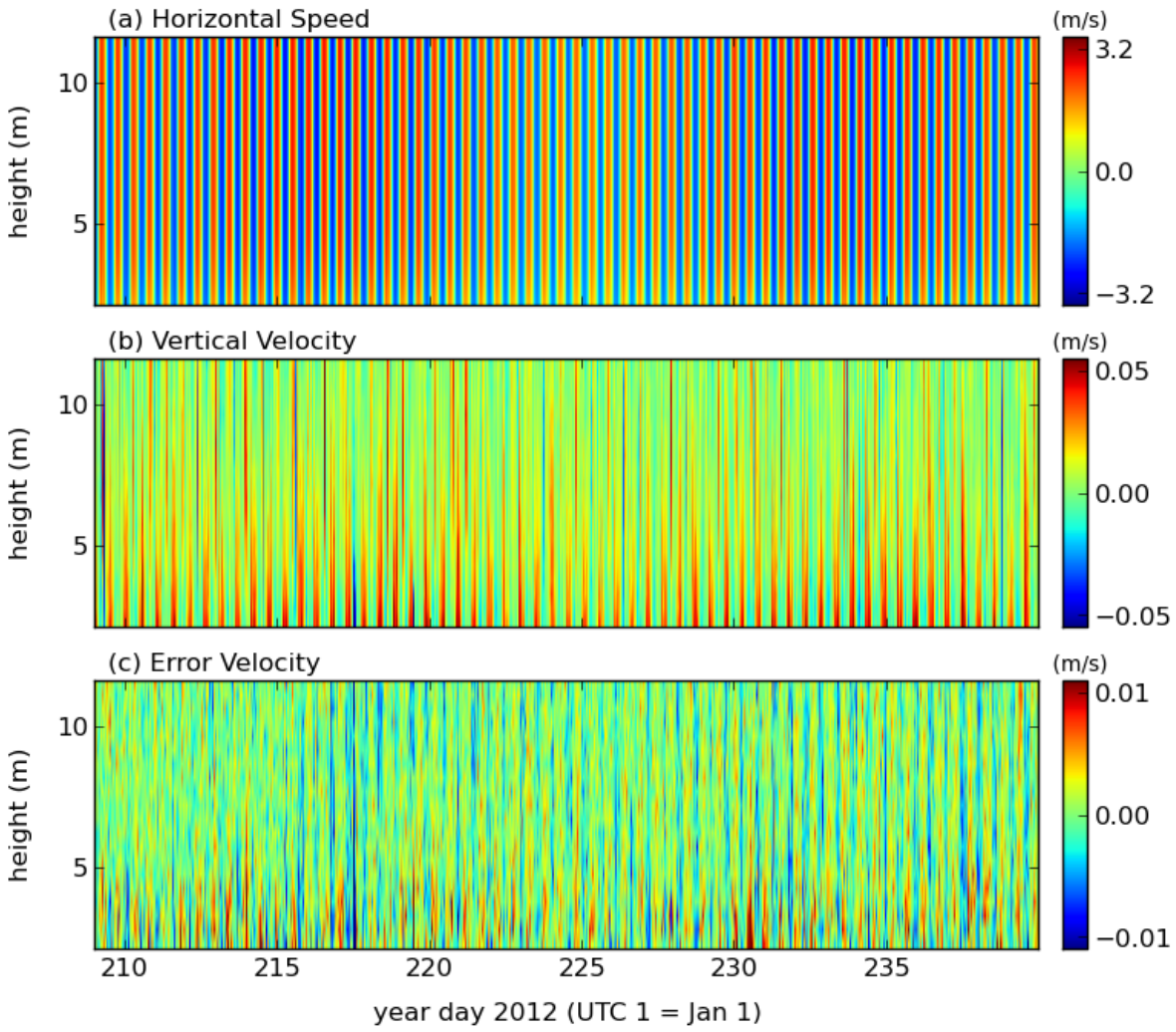

Figure A.9.3: Ten minute ensemble averaged horizontal current speeds, vertical velocities and error velocities for GP4. In panel (a), positive velocities correspond to the flood direction and negative velocities correspond to the ebb direction. The maximum depth is equivalent to 95% of the lowest low water.

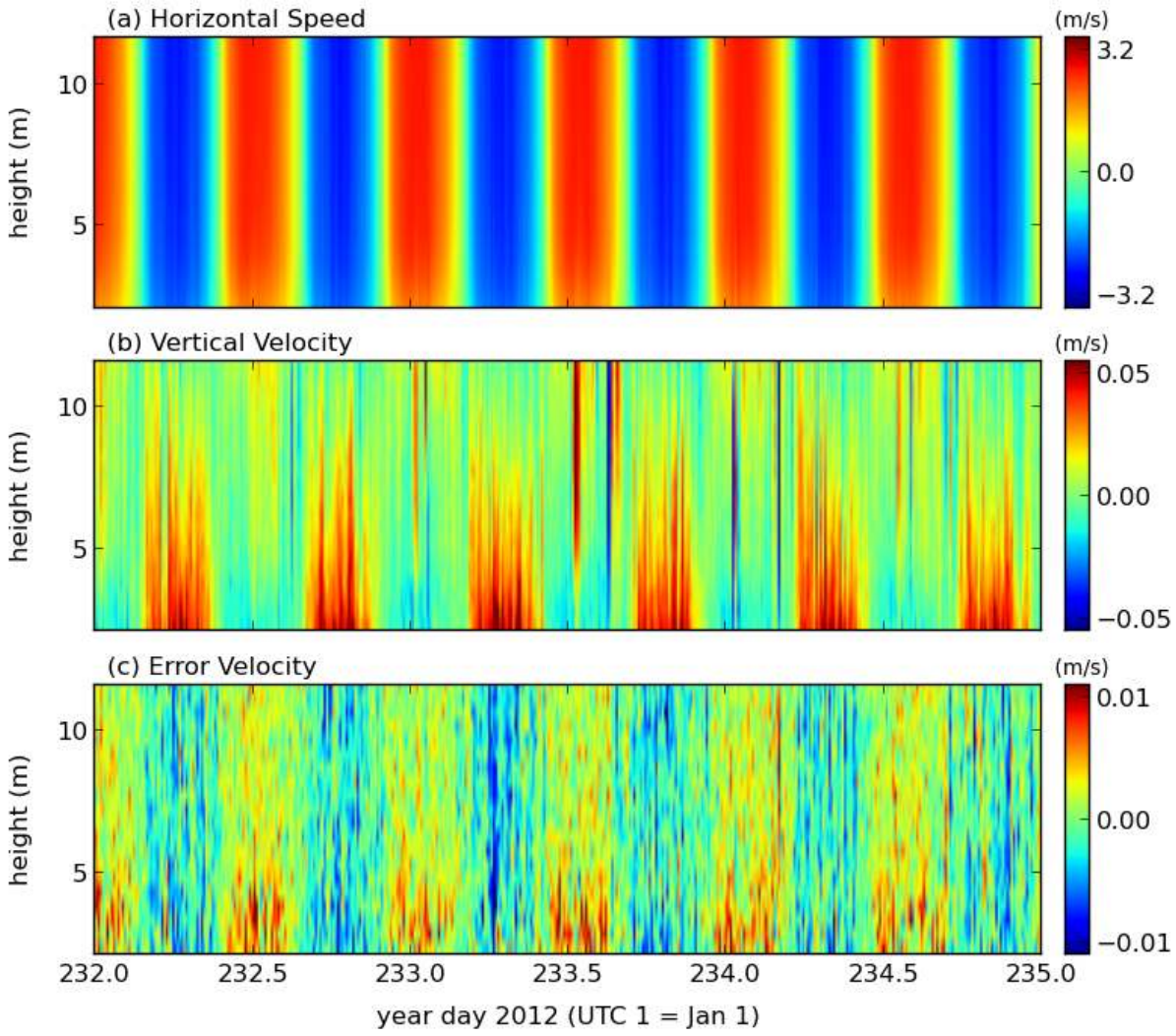

Figure A.9.4: As above, but during a 2-day period.

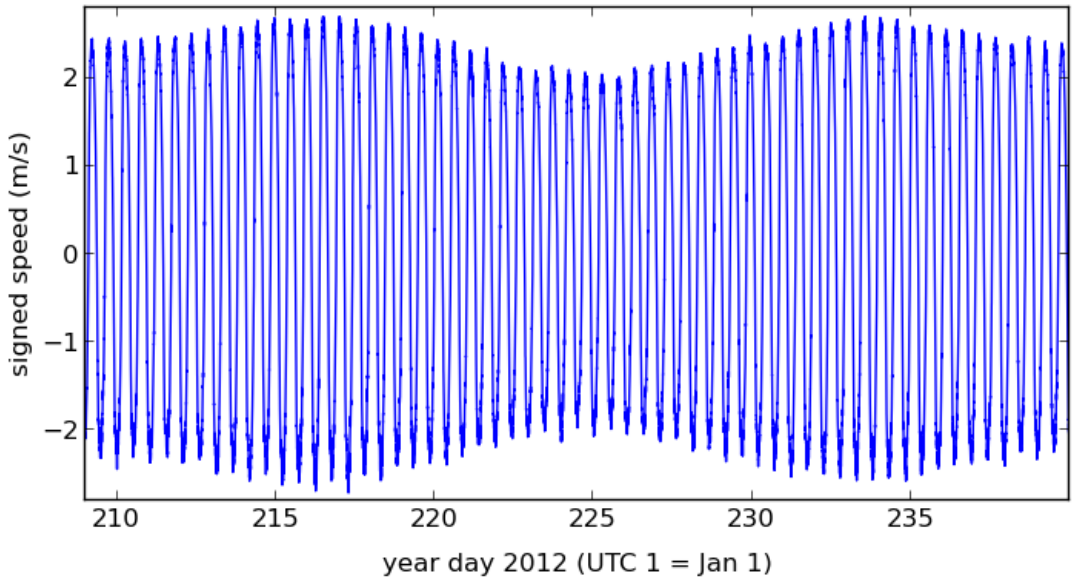

Figure A.9.5: Time series of the depth averaged velocity at GP4. The averages were computed to 95% of the surface signal. Positive velocities correspond to the flood direction and negative velocities correspond to the ebb direction.

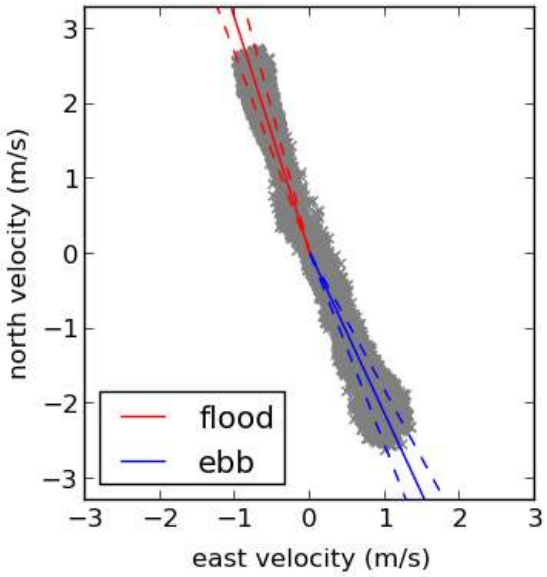

Figure A.9.6: The principal flow directions at GP4 are shown by the solid red and blue lines for the flood and ebb tides, respectively. The dashed lines indicate ±1 standard deviation from the mean. Individual values are plotted as grey x markers.

Constituent	Period (hr)	Elevation		Velocity			
		Amplitude (m)	Phase (°)	Major (m/s)	Minor (m/s)	Inclination (°)	Phase (°)
M2	12.42	2.14	77	2.41	-0.00	111	331
N2	12.66	0.36	44	0.29	0.04	109	293
S2	12.00	0.32	123	0.30	0.02	112	25
K1	23.93	0.14	206	0.03	0.00	109	95
O1	25.82	0.12	163	0.02	-0.00	112	64
M4	6.21	0.07	112	0.07	-0.05	118	199

Table A.9.1: Harmonic Analysis at GP4. The elevation fits were done over a period of 31 days and the velocity fits were done over a period of 31 days. The RMS amplitude of the residual elevation was 9.5 cm and the RMS amplitude of the residual current speed was 20 cm/s.

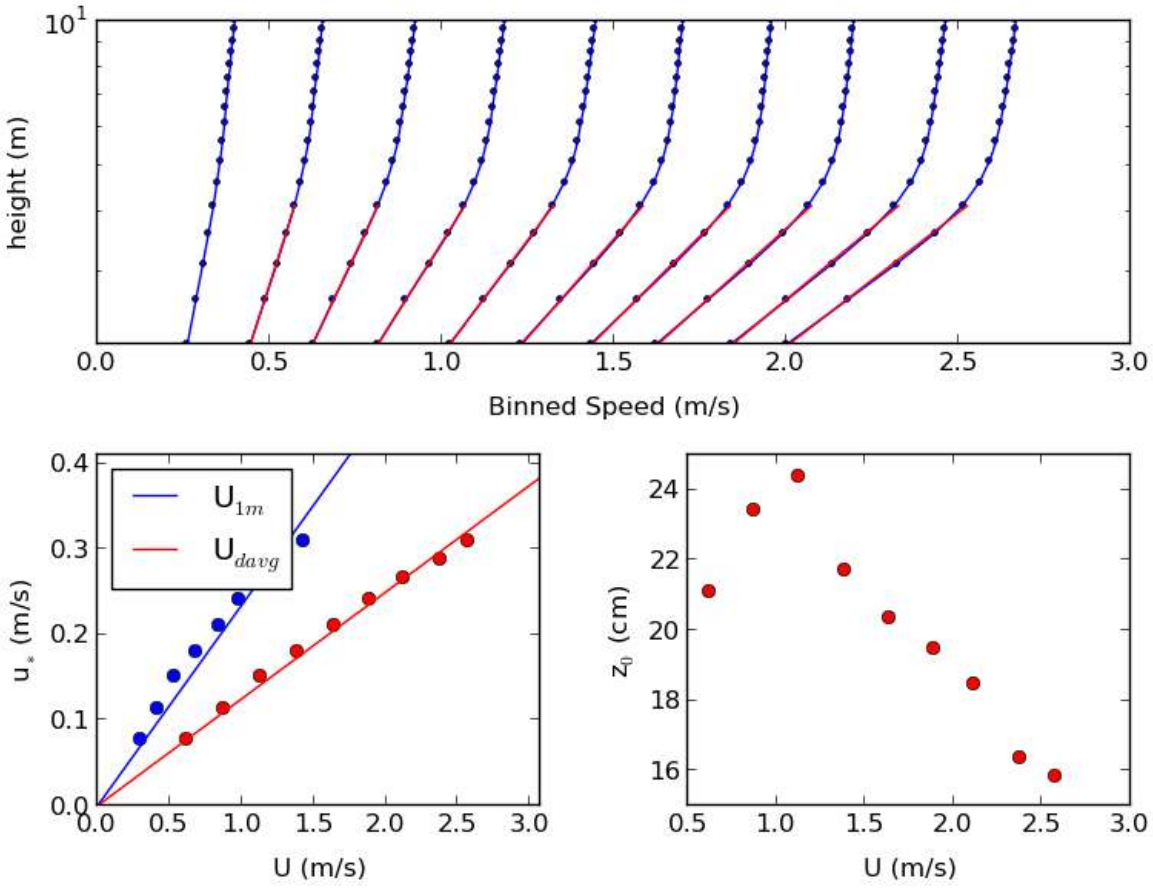

Figure A.9.7: The top panel shows the binned speed profiles during the flood tide at GP4. The red lines correspond to the law of the wall fits. The lower left panel plots u_* as determined from the law of the wall versus a reference speed. Since $u_*^2 = C_d U^2$, C_d is the is the square of the slope of the fitted line. These values are given in the table below. The lower right panel shows the estimates of z_0 from the law of the wall fits.

	Flood	**Ebb**
C_d $(U = V_{1m})$	0.0551	0.0092
C_d $(U = V_{davg})$	0.0156	0.0048
Mean z_0 (cm)	20.1	2.3

Table A.9.2: Drag coefficient, C_d, values at GP4. The values are separated into flood and ebb phases of the tide. Two different reference speeds were used – a theoretical estimate at $z = 1$ m (V_{1m}) and a depth averaged speed which was computed to 95 percent of the surface signal.

	A	**B**	**C**	**D**	**E**	**F**
Diameter (m)	8.0	10.0	12.0	8.0	10.0	12.0
Cut-in Speed (m/s)	1.0	1.0	1.0	1.0	1.0	1.0
Rated Power (kW)	-	-	-	500	500	500
Max Power Output (kW)	221	345	496	221	345	496
Avg. Energy Production (kWh/day)	1852	2894	4168	1852	2894	4167
Operating Time (%)	82.4	82.4	82.4	82.4	82.4	82.4

Table A.9.3: Turbine statistics for six configurations at GP4. All turbines are assumed to have a hub height of 10 m and a water-wire efficiency of 0.4.

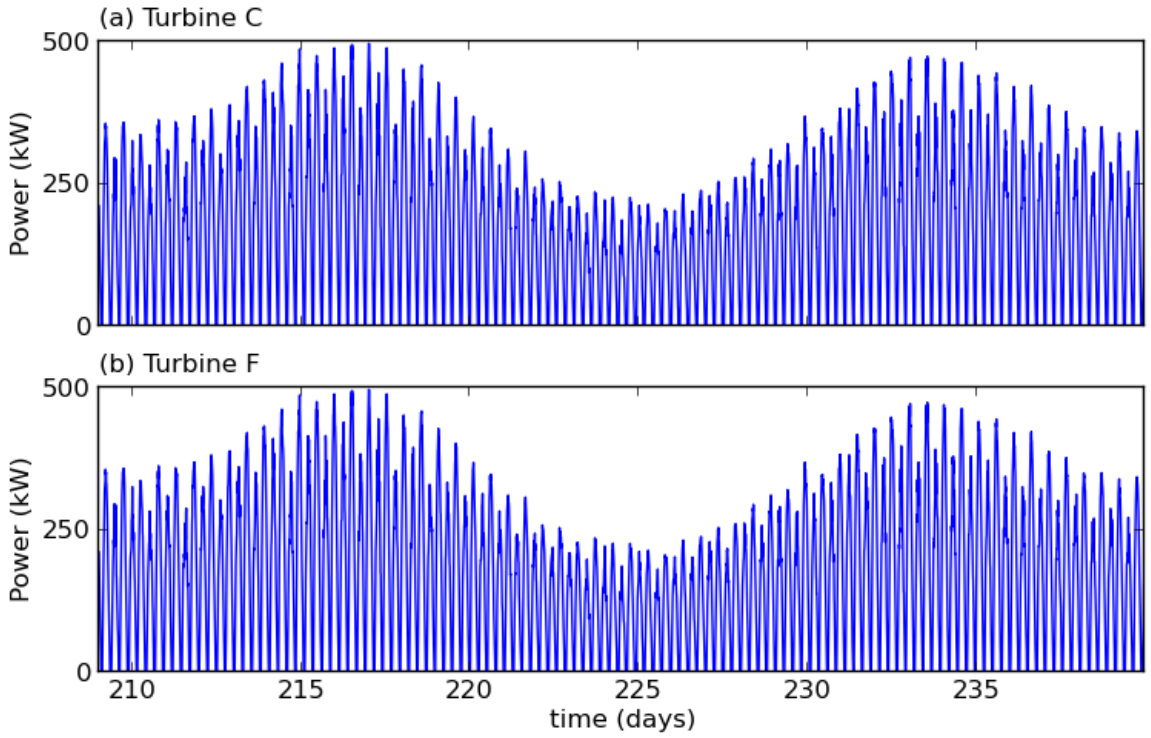

Figure A.9.8: A time series of the power output GP4 for the six turbine configuations listed in Table A.9.3. The power output was computed at a hub height of 10 m using the ten minute ensembled data.

A.10 GP5

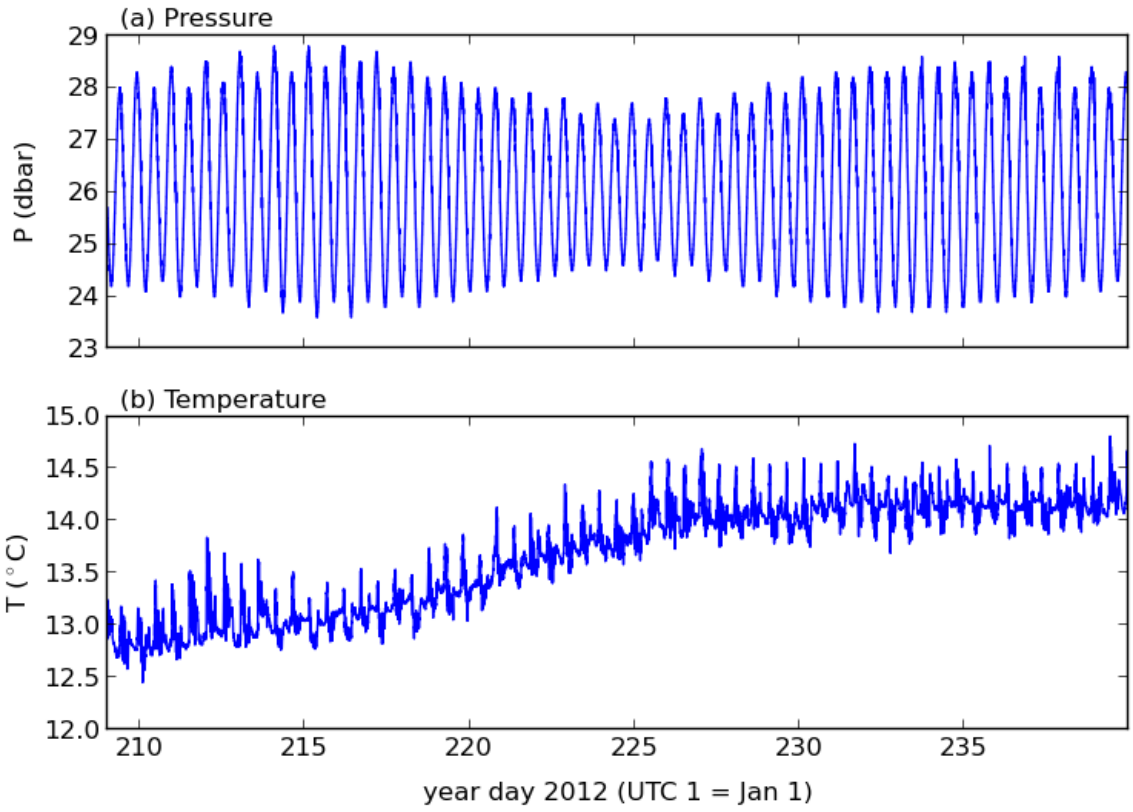

Figure A.10.1: Measurements of pressure and temperature at GP5.

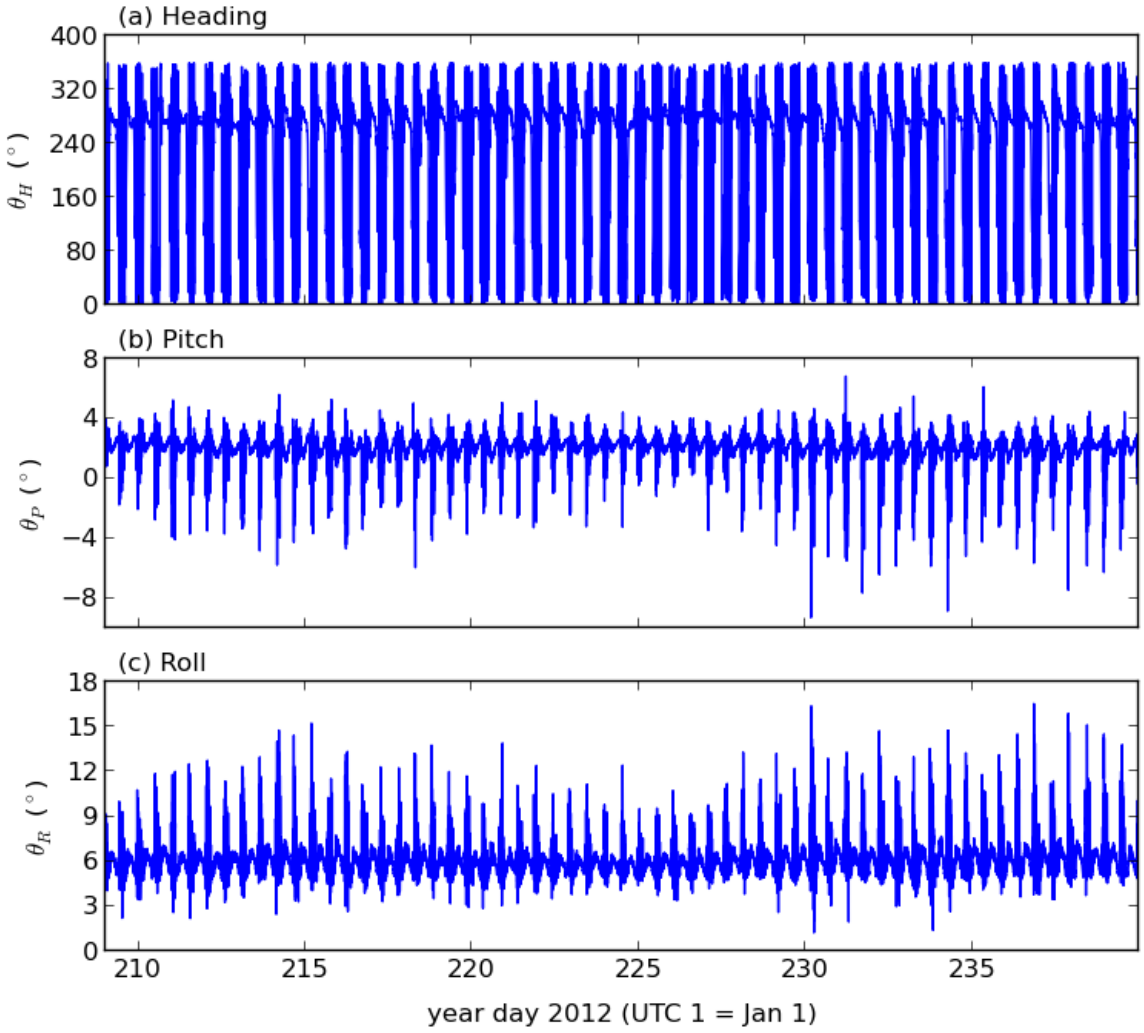

Figure A.10.2: Measurements of heading, pitch and roll at GP5.

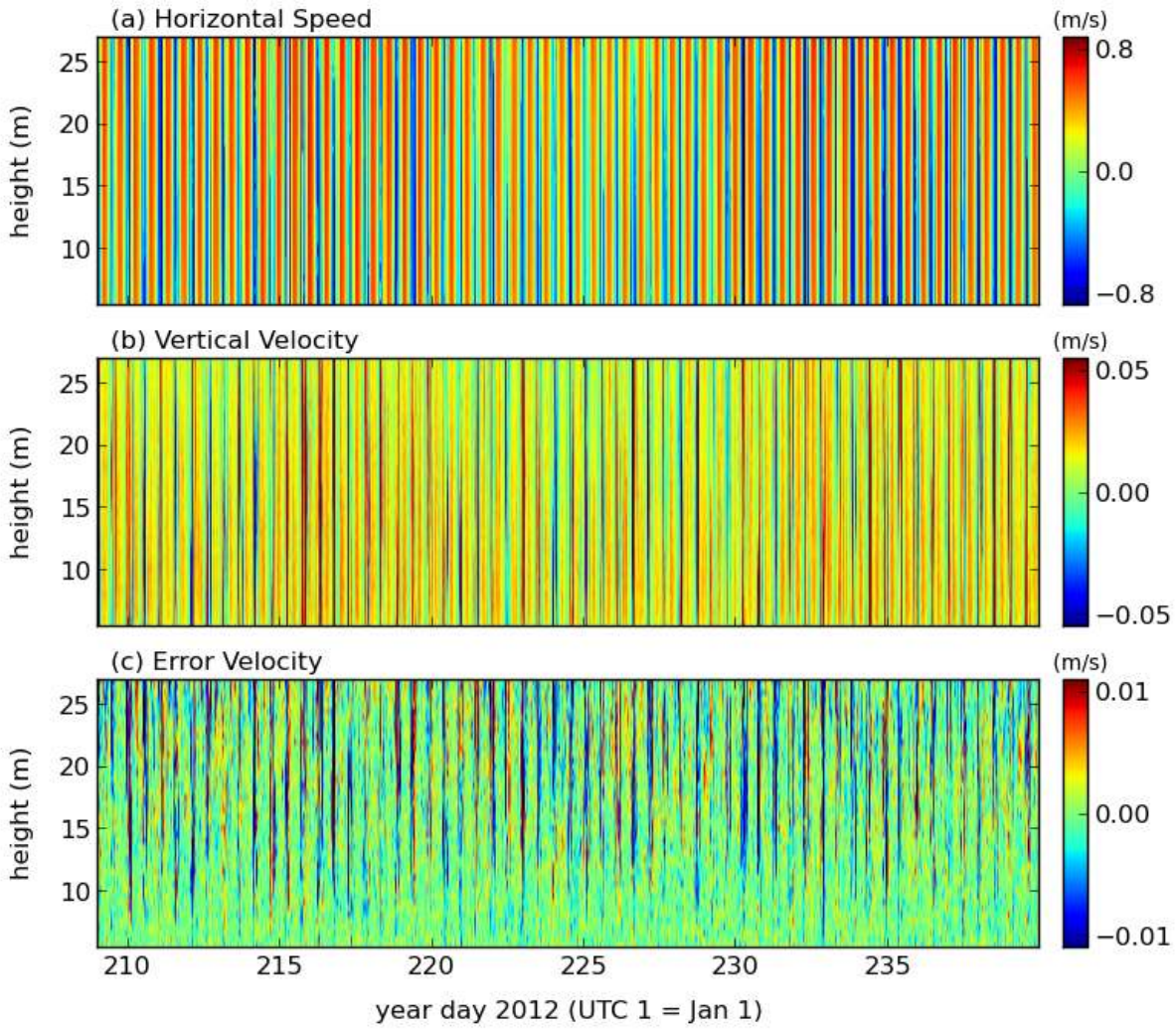

Figure A.10.3: Ten minute ensemble averaged horizontal current speeds, vertical velocities and error velocities for GP5. In panel (a), positive velocities correspond to the flood direction and negative velocities correspond to the ebb direction. The maximum depth is equivalent to 95% of the lowest low water.

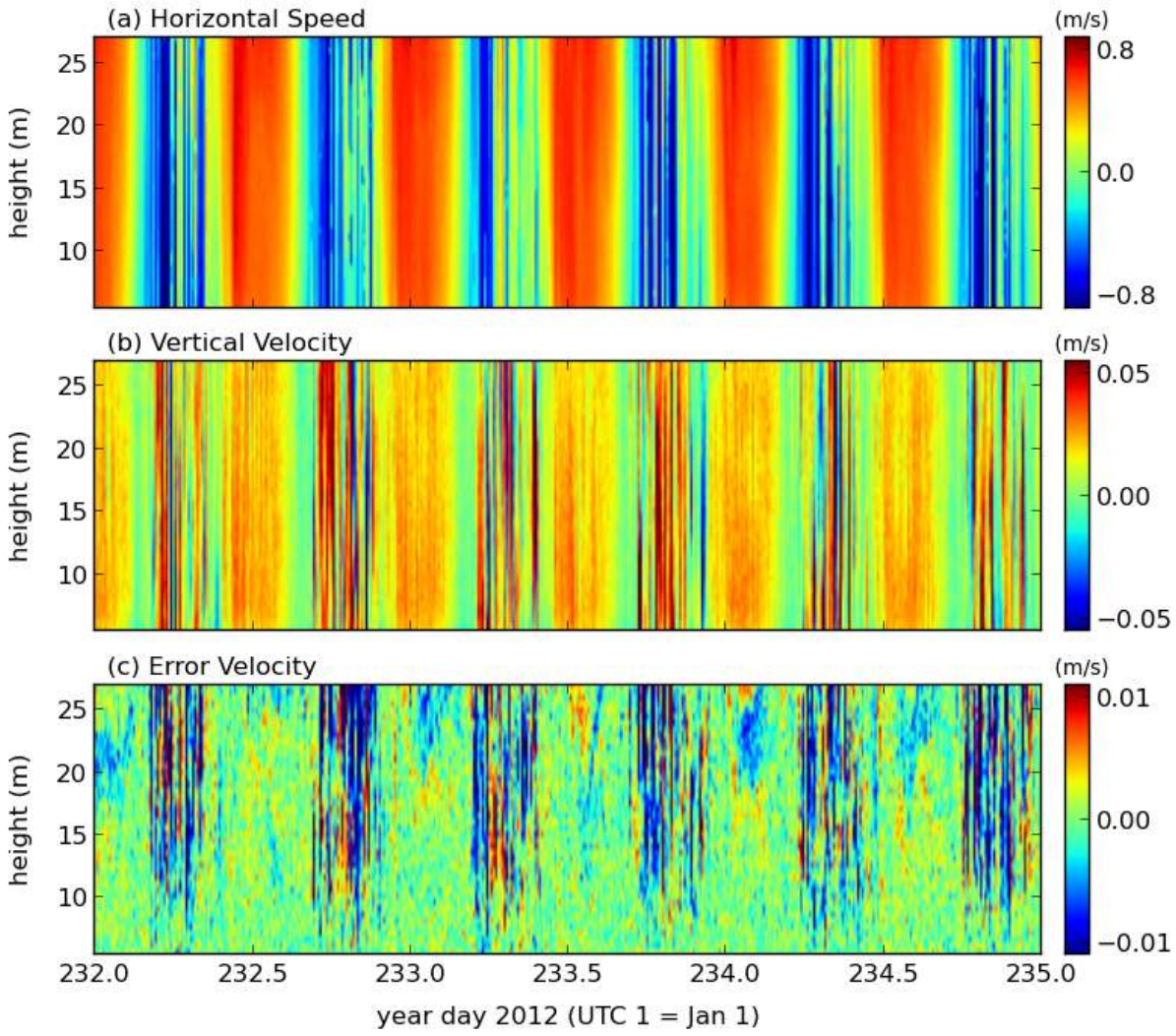

Figure A.10.4: As above, but during a 2-day period.

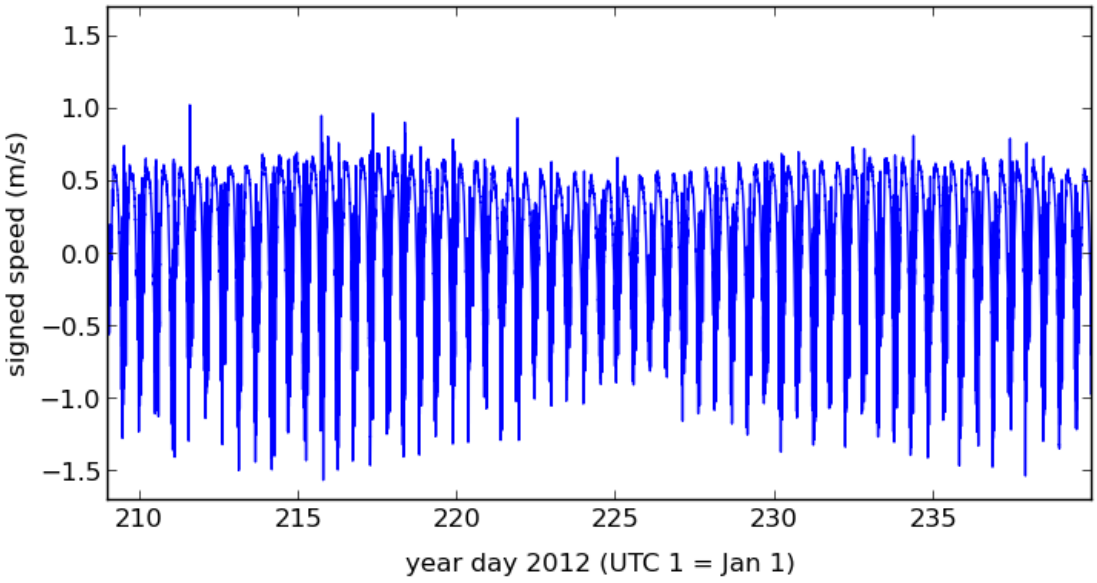

Figure A.10.5: Time series of the depth averaged velocity at GP5. The averages were computed to 95% of the surface signal. Positive velocities correspond to the flood direction and negative velocities correspond to the ebb direction.

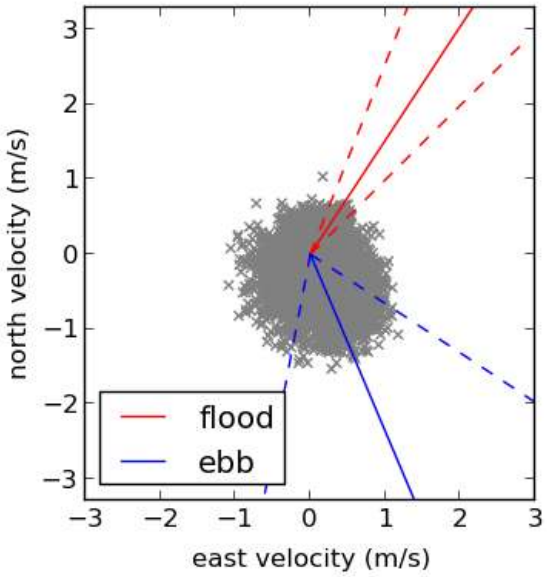

Figure A.10.6: The principal flow directions at GP5 are shown by the solid red and blue lines for the flood and ebb tides, respectively. The dashed lines indicate ±1 standard deviation from the mean. Individual values are plotted as grey x markers.

	A	B	C	D	E	F
Diameter (m)	8.0	10.0	12.0	8.0	10.0	12.0
Cut-in Speed (m/s)	1.0	1.0	1.0	1.0	1.0	1.0
Rated Power (kW)	-	-	-	500	500	500
Max Power Output (kW)	20	32	46	20	32	46
Avg. Energy Production (kWh/day)	4	6	9	4	6	9
Operating Time (%)	1.0	1.0	1.0	1.0	1.0	1.0

Table A.10.1: Turbine statistics for six configurations at GP5. All turbines are assumed to have a hub height of 10 m and a water-wire efficiency of 0.4.

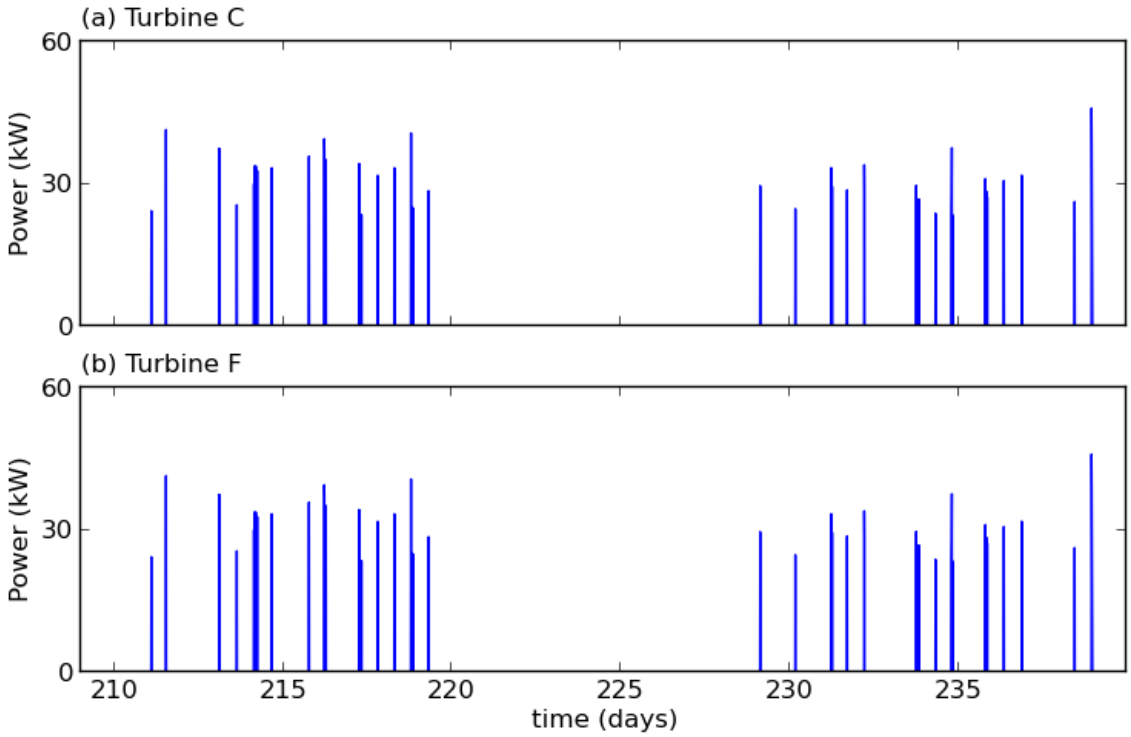

Figure A.10.7: A time series of the power output GP5 for the six turbine configuations listed in Table A.10.1. The power output was computed at a hub height of 10 m using the ten minute ensembled data.

A.11 PP1

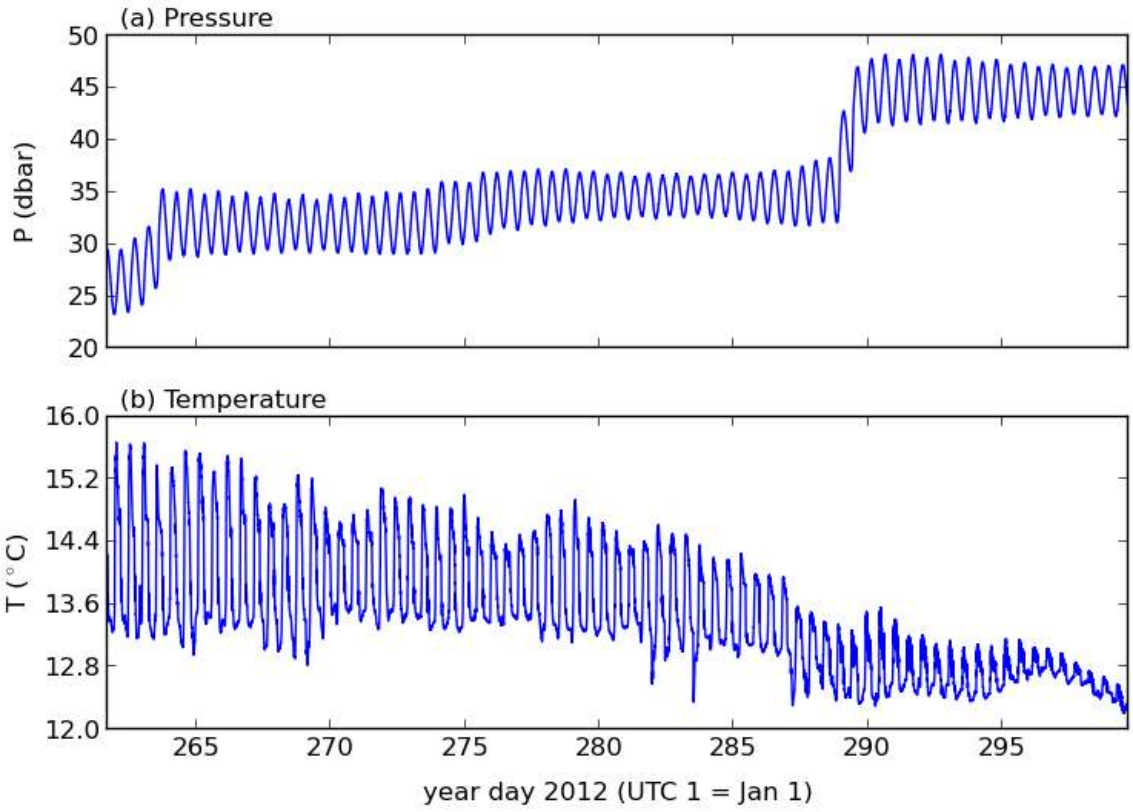

Figure A.11.1: Measurements of pressure and temperature at PP1.

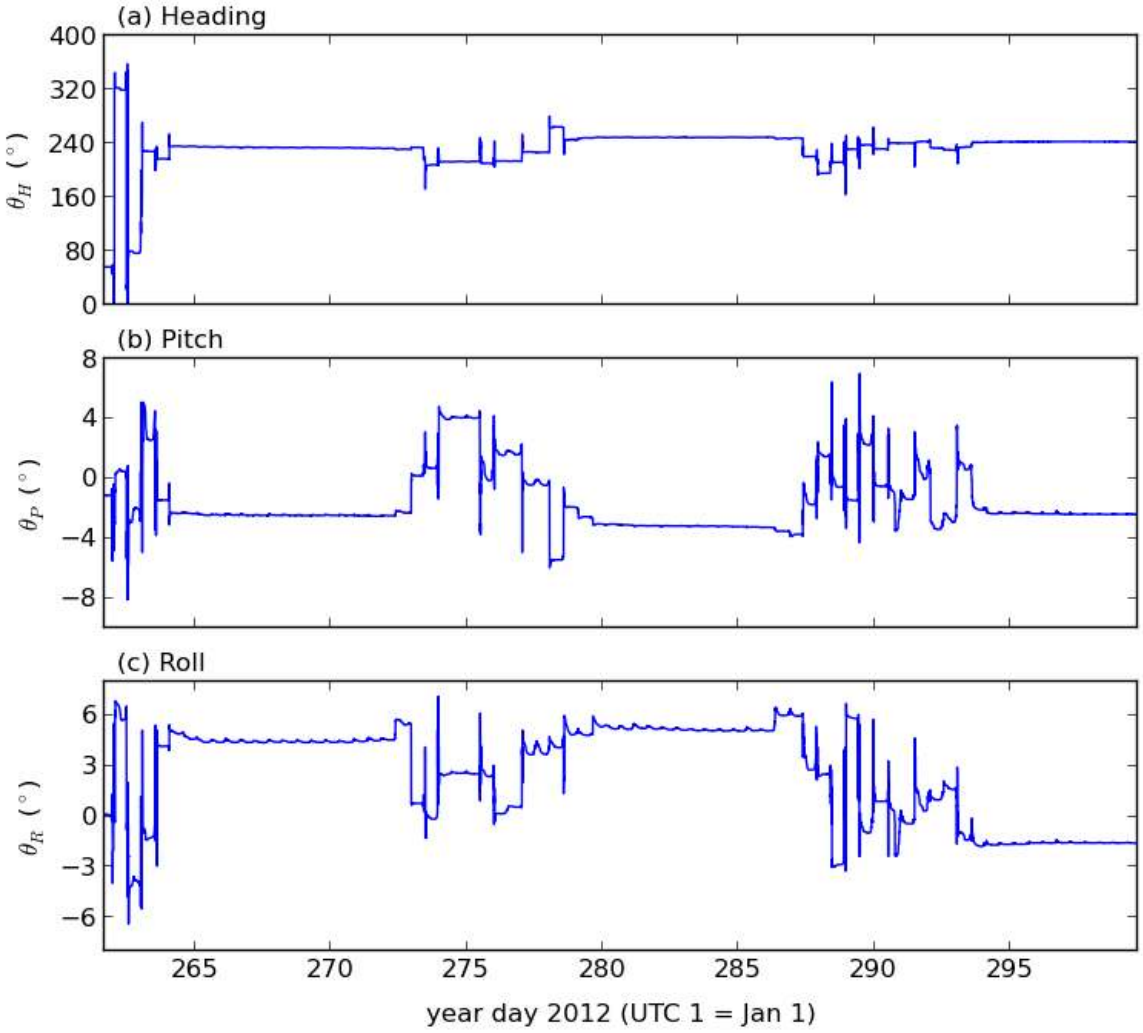

Figure A.11.2: Measurements of heading, pitch and roll at PP1.

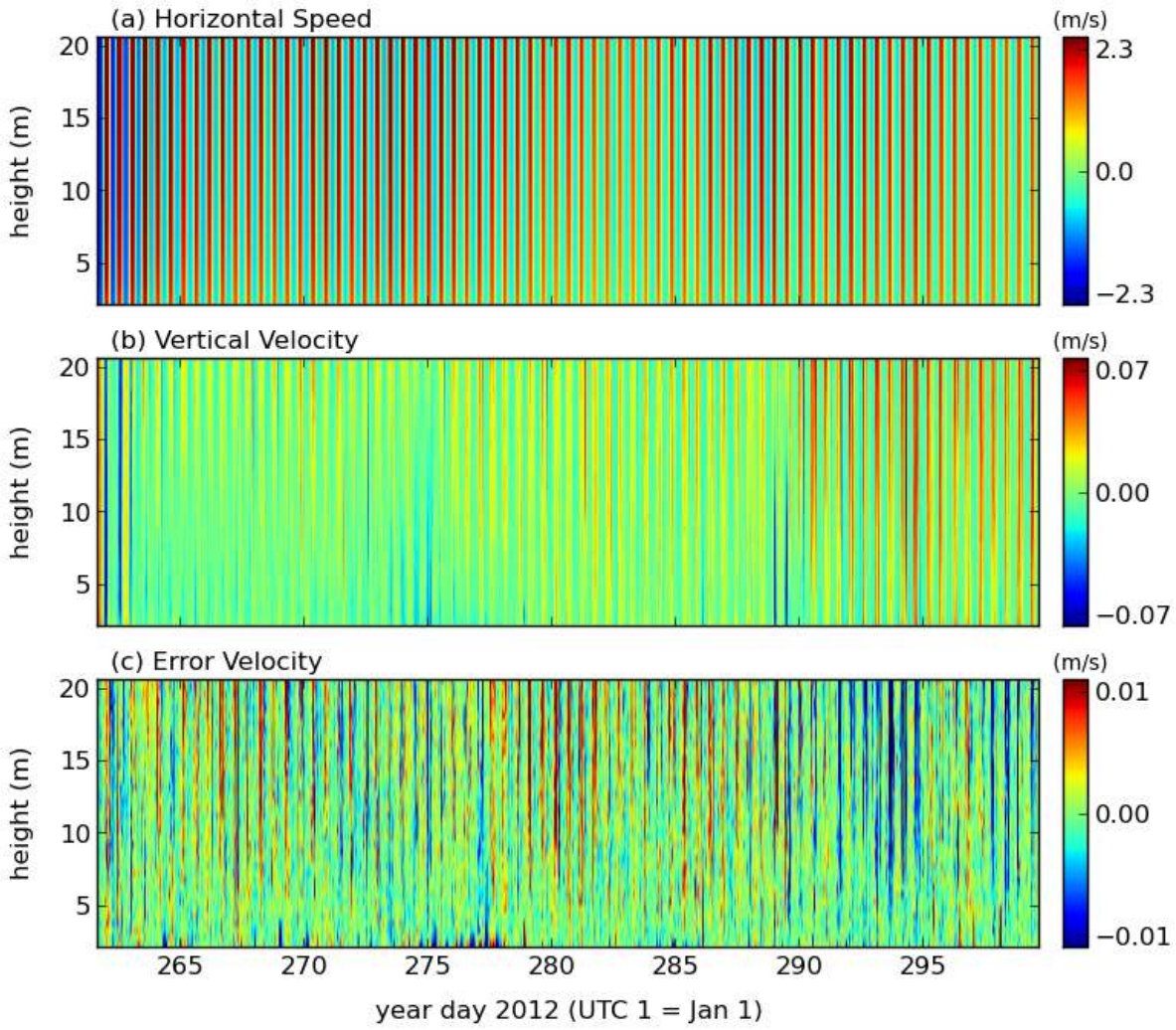

Figure A.11.3: Ten minute ensemble averaged horizontal current speeds, vertical velocities and error velocities for PP1. In panel (a), positive velocities correspond to the flood direction and negative velocities correspond to the ebb direction. The maximum depth is equivalent to 95% of the lowest low water.

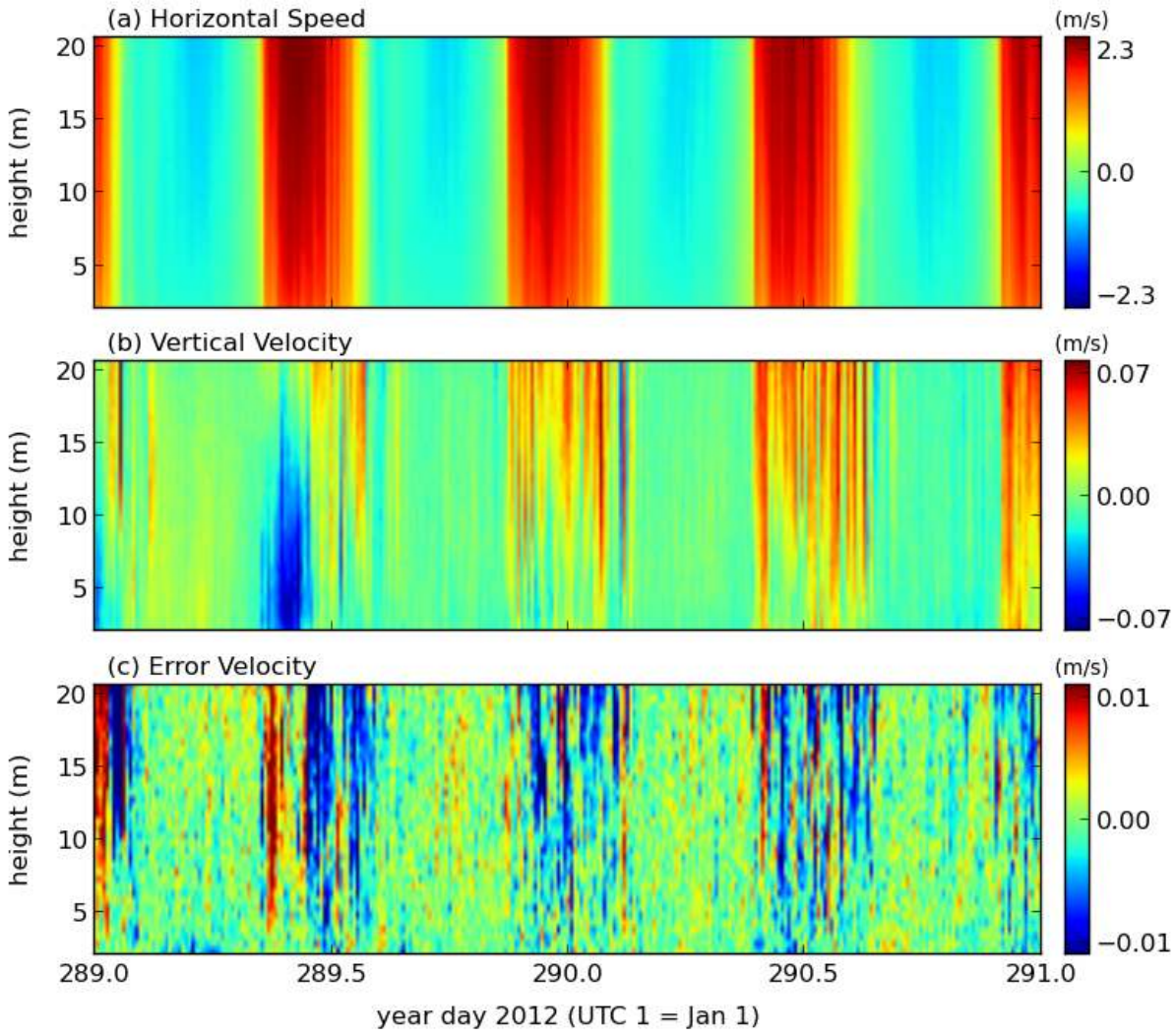

Figure A.11.4: As above, but during a 2-day period.

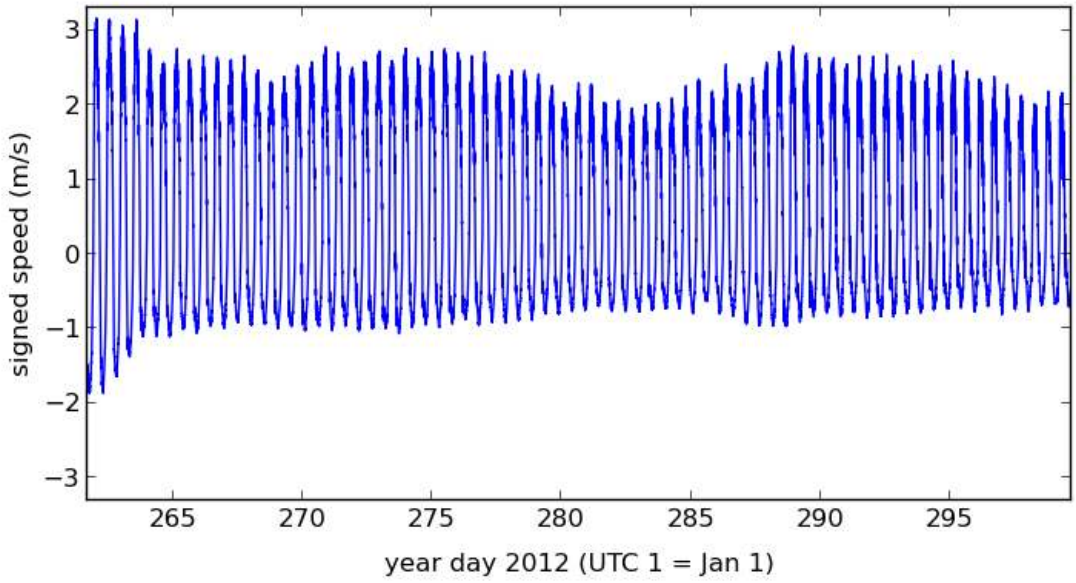

Figure A.11.5: Time series of the depth averaged velocity at PP1. The averages were computed to 95% of the surface signal. Positive velocities correspond to the flood direction and negative velocities correspond to the ebb direction.

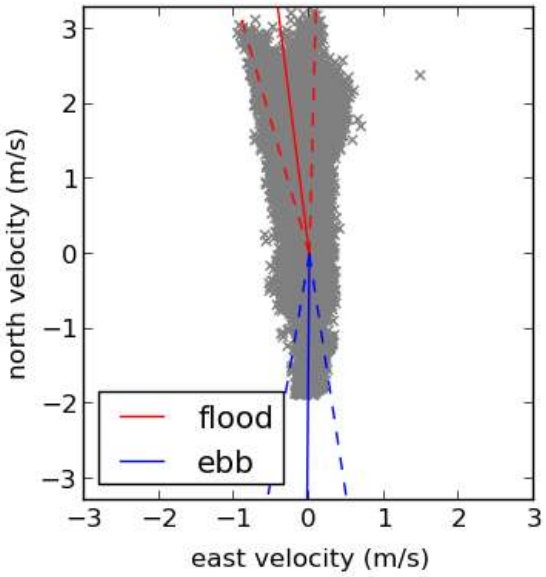

Figure A.11.6: The principal flow directions at PP1 are shown by the solid red and blue lines for the flood and ebb tides, respectively. The dashed lines indicate ±1 standard deviation from the mean. Individual values are plotted as grey x markers.

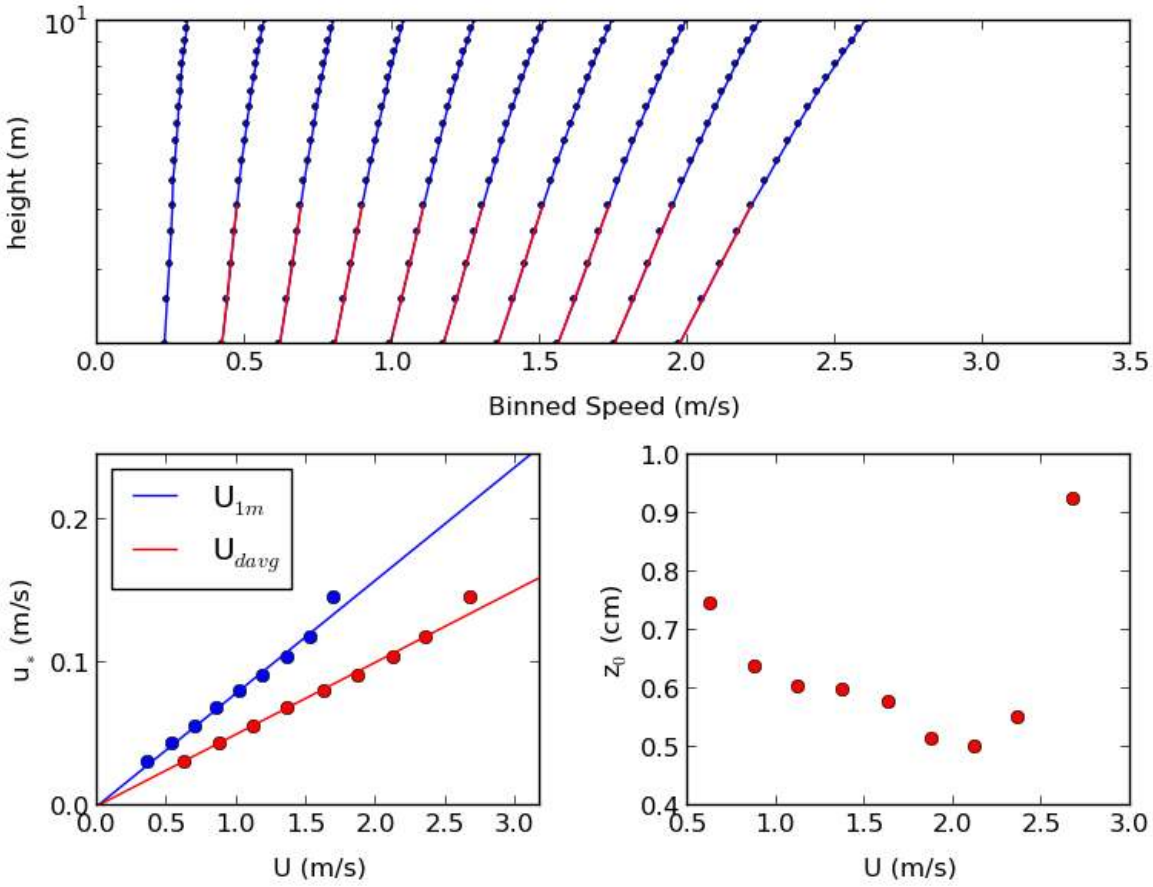

Figure A.11.7: The top panel shows the binned speed profiles during the flood tide at PP1. The red lines correspond to the law of the wall fits. The lower left panel plots u_* as determined from the law of the wall versus a reference speed. Since $u_*^2 = C_d U^2$, C_d is the is the square of the slope of the fitted line. These values are given in the table below. The lower right panel shows the estimates of z_0 from the law of the wall fits.

	Flood	**Ebb**
C_d $(U = V_{1m})$	0.0062	0.0058
C_d $(U = V_{davg})$	0.0025	0.0031
Mean z_0 (cm)	0.6	1.0

Table A.11.1: Drag coefficient, C_d, values at PP1. The values are separated into flood and ebb phases of the tide. Two different reference speeds were used – a theoretical estimate at $z = 1$ m (V_{1m}) and a depth averaged speed which was computed to 95 percent of the surface signal.

	A	B	C	D	E	F
Diameter (m)	8.0	10.0	12.0	8.0	10.0	12.0
Cut-in Speed (m/s)	1.0	1.0	1.0	1.0	1.0	1.0
Rated Power (kW)	-	-	-	500	500	500
Max Power Output (kW)	274	427	615	274	427	500
Avg. Energy Production (kWh/day)	653	1020	1469	653	1020	1461
Operating Time (%)	39.6	39.6	39.6	39.6	39.6	39.6

Table A.11.2: Turbine statistics for six configurations at PP1. All turbines are assumed to have a hub height of 10 m and a water-wire efficiency of 0.4.

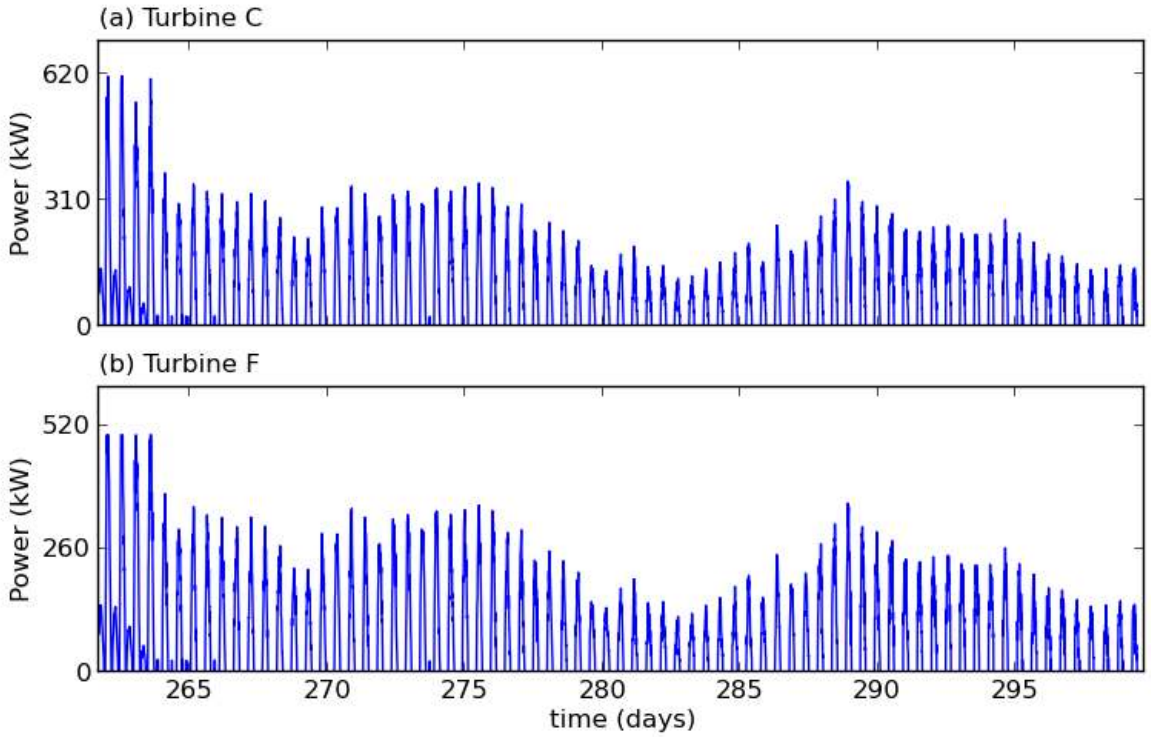

Figure A.11.8: A time series of the power output PP1 for the six turbine configuations listed in Table A.11.2. The power output was computed at a hub height of 10 m using the ten minute ensembled data.

A.12 PP2

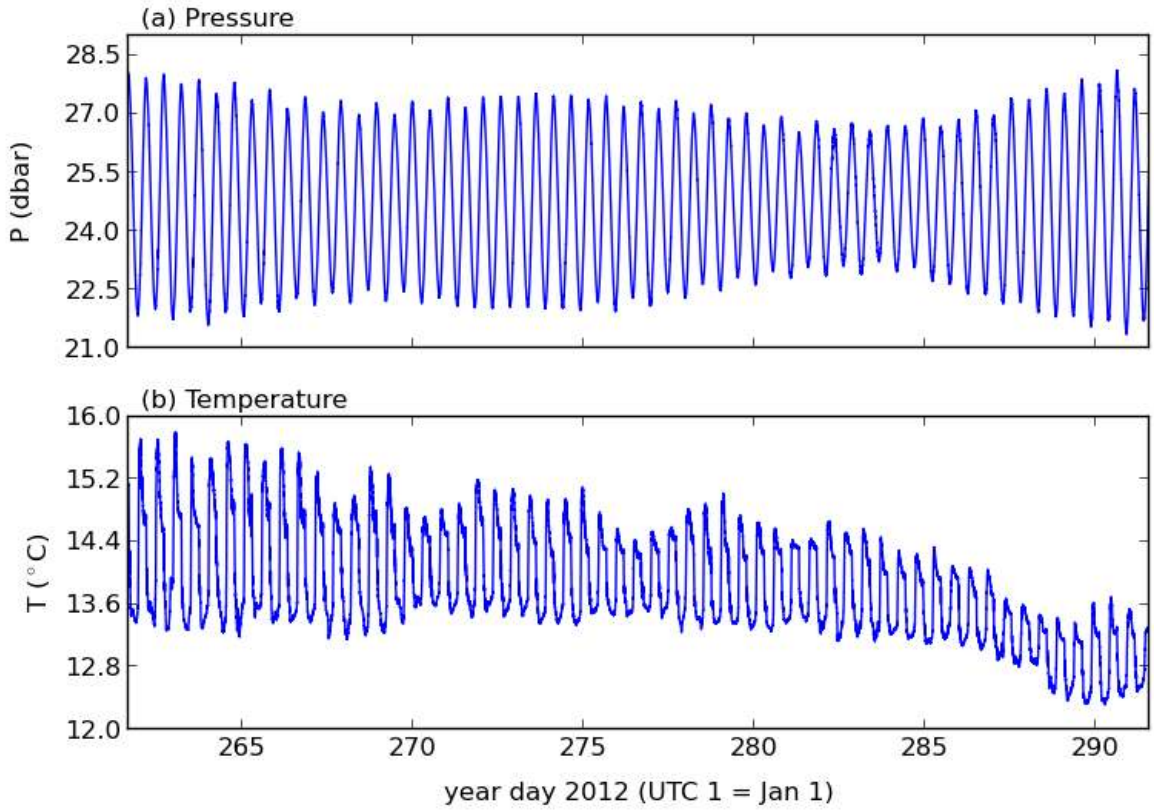

Figure A.12.1: Measurements of pressure and temperature at PP2.

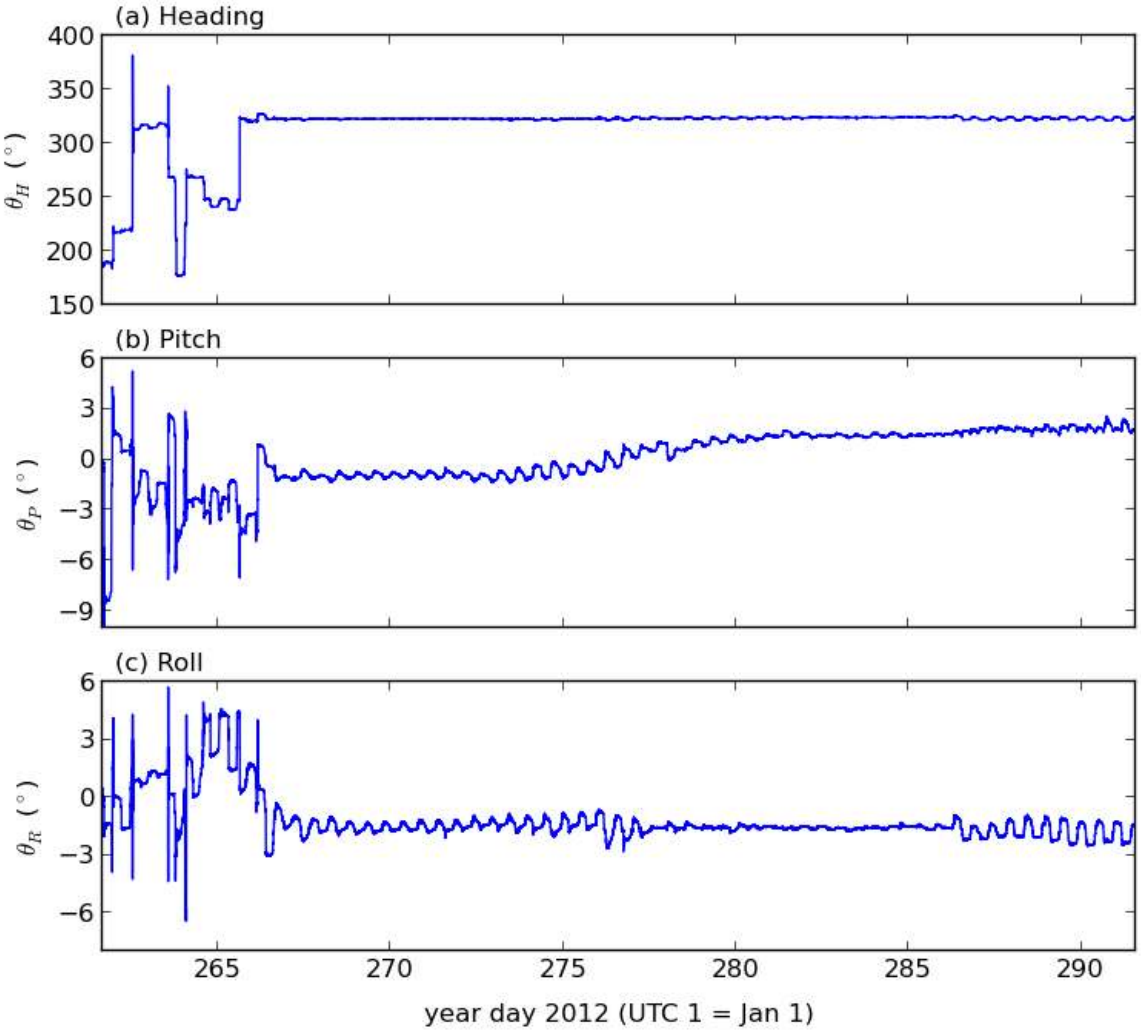

Figure A.12.2: Measurements of heading, pitch and roll at PP2.

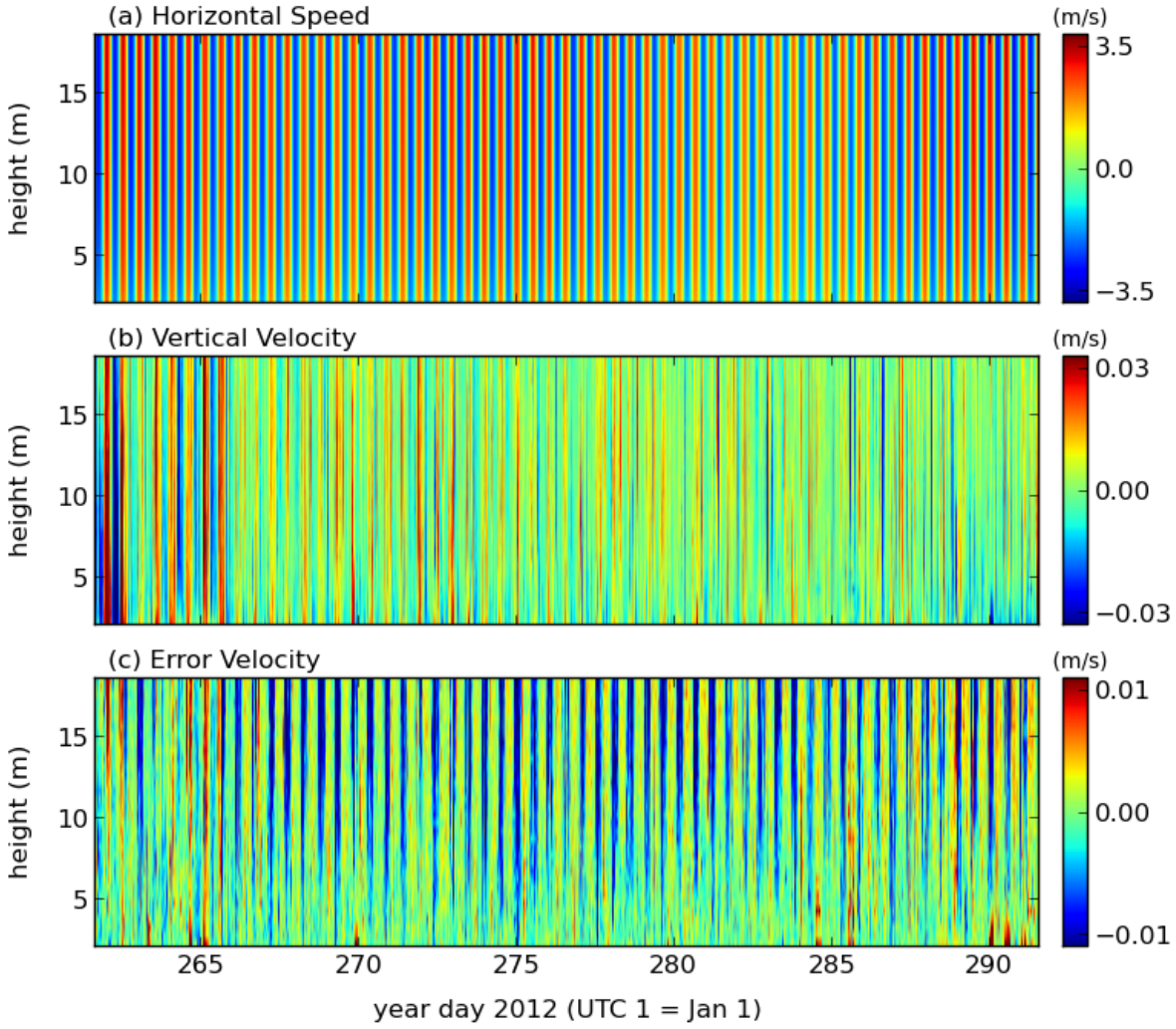

Figure A.12.3: Ten minute ensemble averaged horizontal current speeds, vertical velocities and error velocities for PP2. In panel (a), positive velocities correspond to the flood direction and negative velocities correspond to the ebb direction. The maximum depth is equivalent to 95% of the lowest low water.

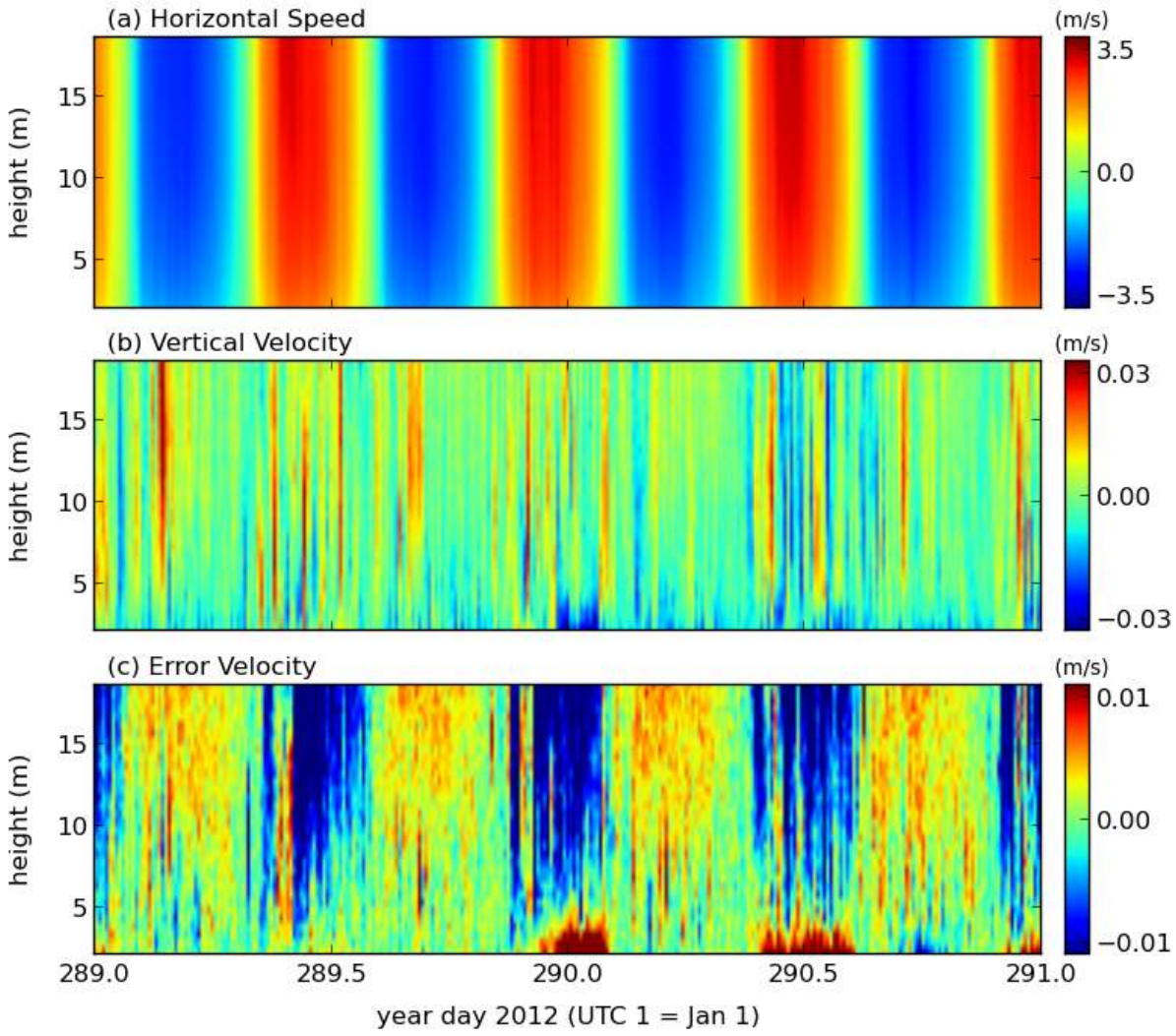

Figure A.12.4: As above, but during a 2-day period.

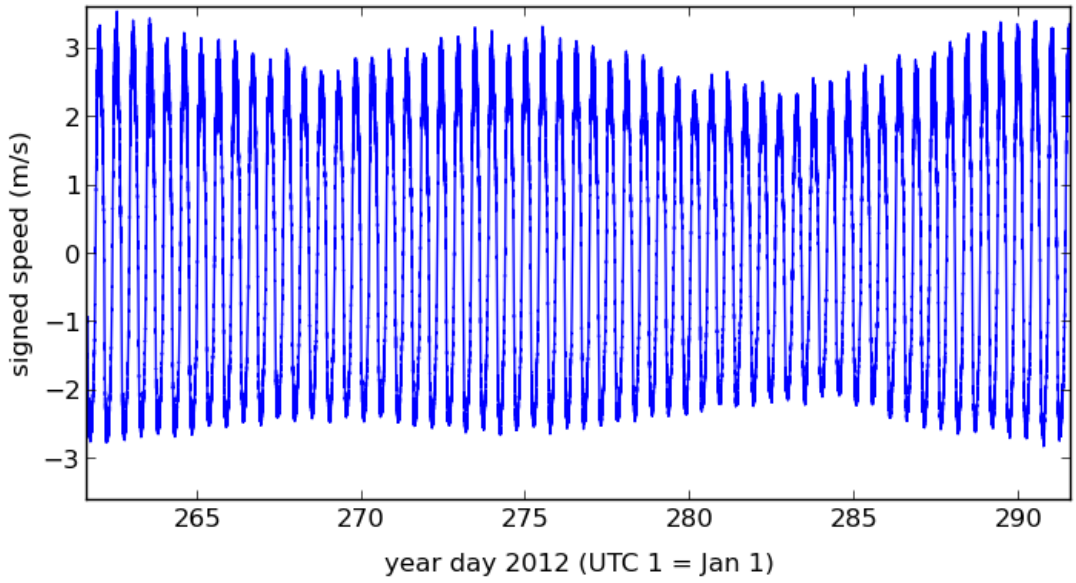

Figure A.12.5: Time series of the depth averaged velocity at PP2. The averages were computed to 95% of the surface signal. Positive velocities correspond to the flood direction and negative velocities correspond to the ebb direction.

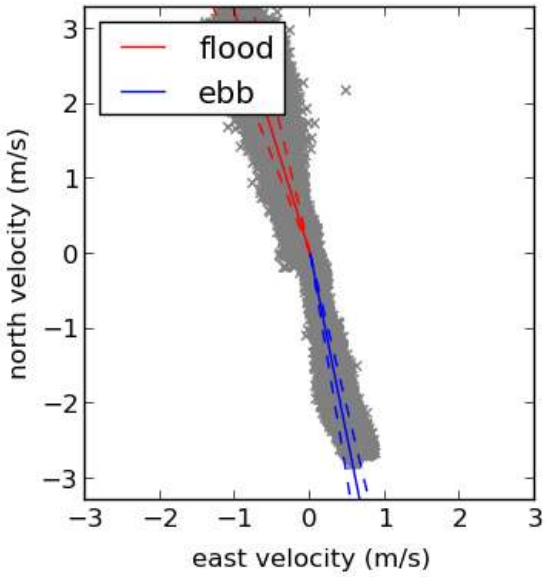

Figure A.12.6: The principal flow directions at PP2 are shown by the solid red and blue lines for the flood and ebb tides, respectively. The dashed lines indicate ±1 standard deviation from the mean. Individual values are plotted as grey x markers.

Constituent	Period (hr)	Elevation		Velocity			
		Amplitude (m)	Phase (°)	Major (m/s)	Minor (m/s)	Inclination (°)	Phase (°)
M2	12.42	2.30	81	2.49	0.03	105	330
N2	12.66	0.48	65	0.42	0.01	107	319
S2	12.00	0.41	111	0.38	0.02	107	5
K1	23.93	0.12	173	0.02	0.00	102	94
O1	25.82	0.11	173	0.01	-0.00	113	16
M4	6.21	0.08	101	0.06	0.01	126	348

Table A.12.1: Harmonic Analysis at PP2. The elevation fits were done over a period of 30 days and the velocity fits were done over a period of 30 days. The RMS amplitude of the residual elevation was 13 cm and the RMS amplitude of the residual current speed was 24 cm/s.

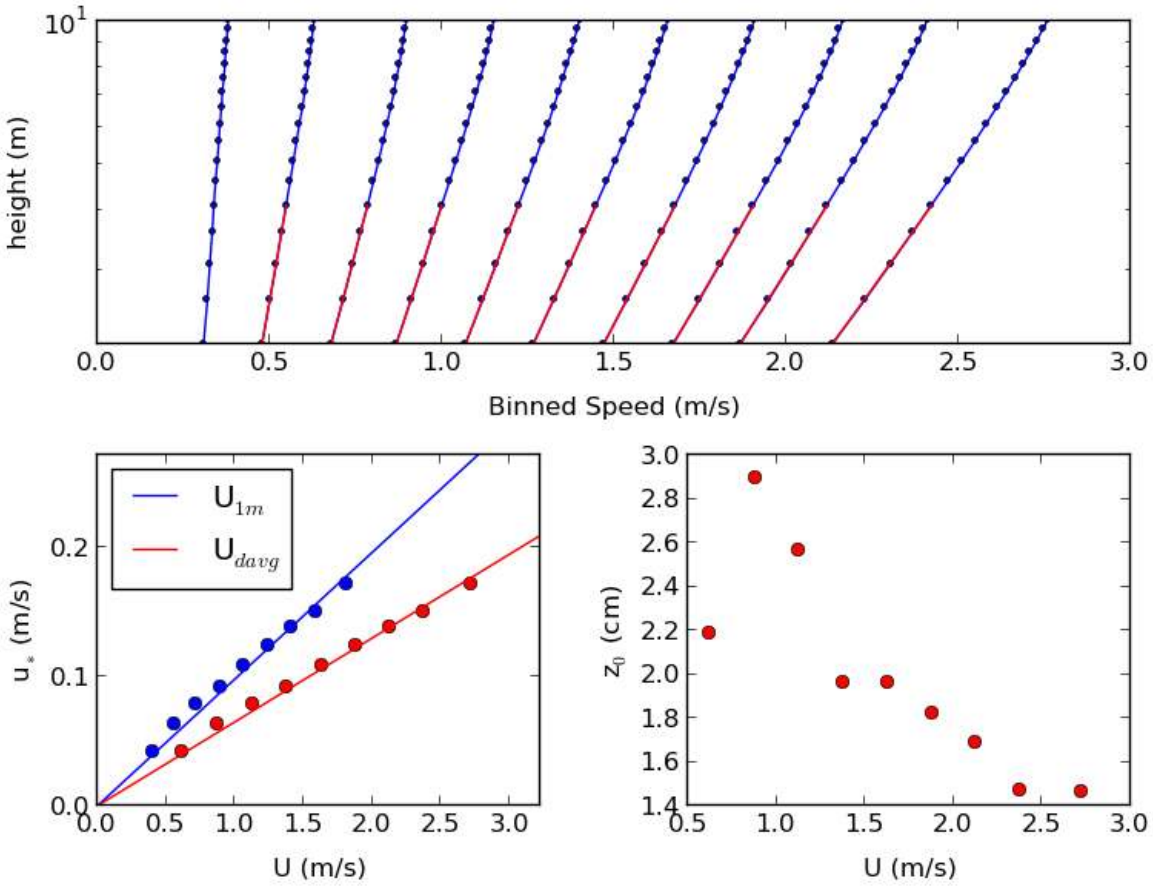

Figure A.12.7: The top panel shows the binned speed profiles during the flood tide at PP2. The red lines correspond to the law of the wall fits. The lower left panel plots u_* as determined from the law of the wall versus a reference speed. Since $u_*^2 = C_d U^2$, C_d is the is the square of the slope of the fitted line. These values are given in the table below. The lower right panel shows the estimates of z_0 from the law of the wall fits.

	Flood	**Ebb**
C_d $(U = V_{1m})$	0.0096	0.0126
C_d $(U = V_{davg})$	0.0042	0.0048
Mean z_0 (cm)	2.0	2.8

Table A.12.2: Drag coefficient, C_d, values at PP2. The values are separated into flood and ebb phases of the tide. Two different reference speeds were used – a theoretical estimate at $z = 1$ m (V_{1m}) and a depth averaged speed which was computed to 95 percent of the surface signal.

	A	**B**	**C**	**D**	**E**	**F**
Diameter (m)	8.0	10.0	12.0	8.0	10.0	12.0
Cut-in Speed (m/s)	1.0	1.0	1.0	1.0	1.0	1.0
Rated Power (kW)	-	-	-	500	500	500
Max Power Output (kW)	349	546	786	349	500	500
Avg. Energy Production (kWh/day)	2142	3347	4819	2142	3345	4730
Operating Time (%)	82.5	82.5	82.5	82.5	82.5	82.5

Table A.12.3: Turbine statistics for six configurations at PP2. All turbines are assumed to have a hub height of 10 m and a water-wire efficiency of 0.4.

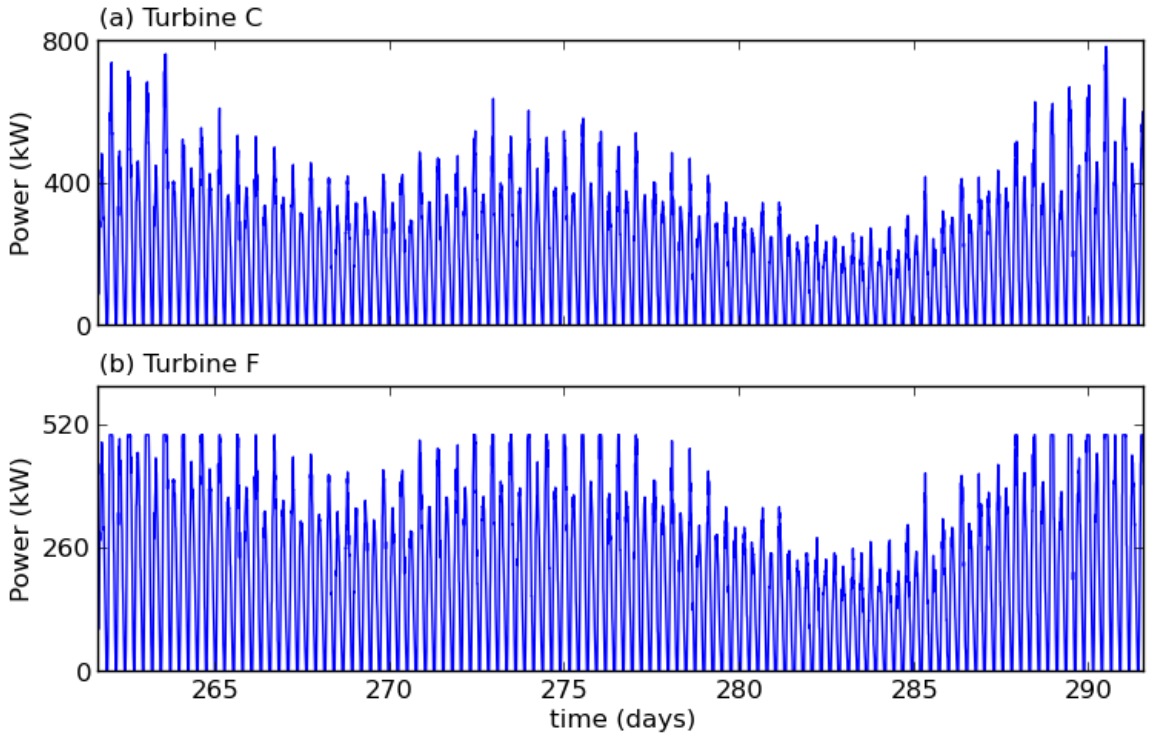

Figure A.12.8: A time series of the power output PP2 for the six turbine configuations listed in Table A.12.3. The power output was computed at a hub height of 10 m using the ten minute ensembled data.

A.13 PP3

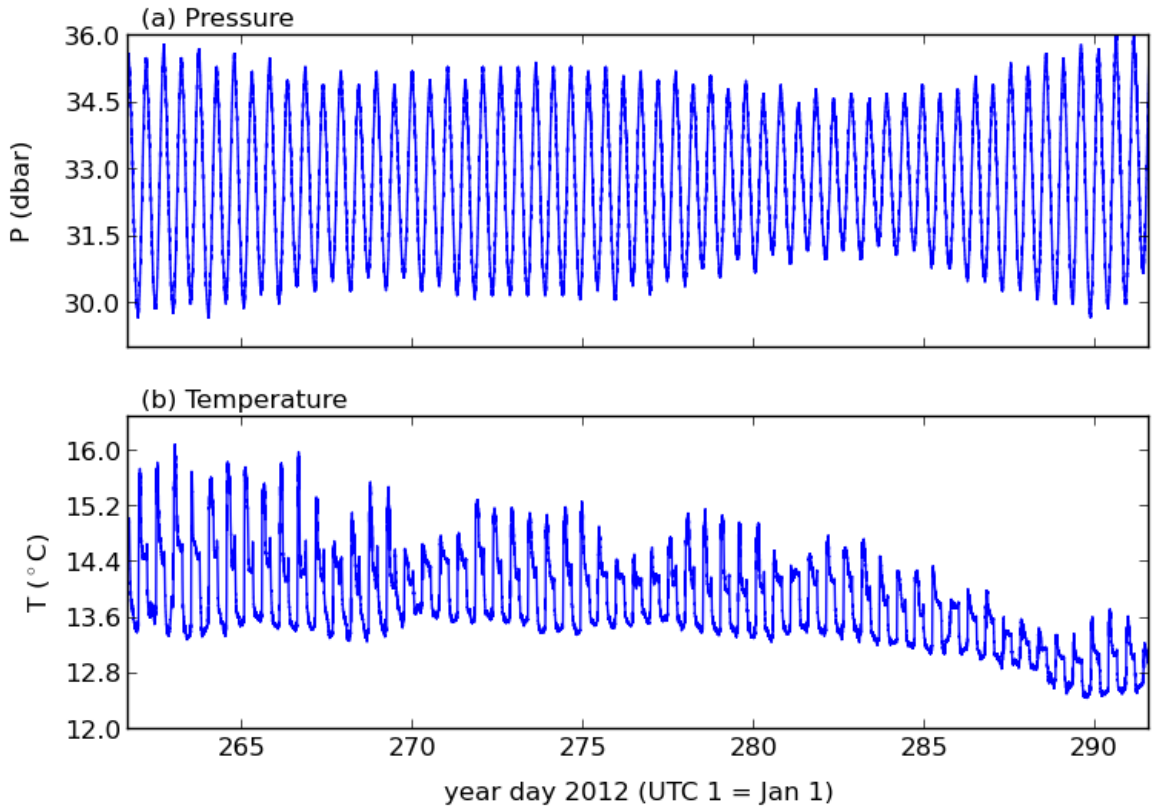

Figure A.13.1: Measurements of pressure and temperature at PP3.

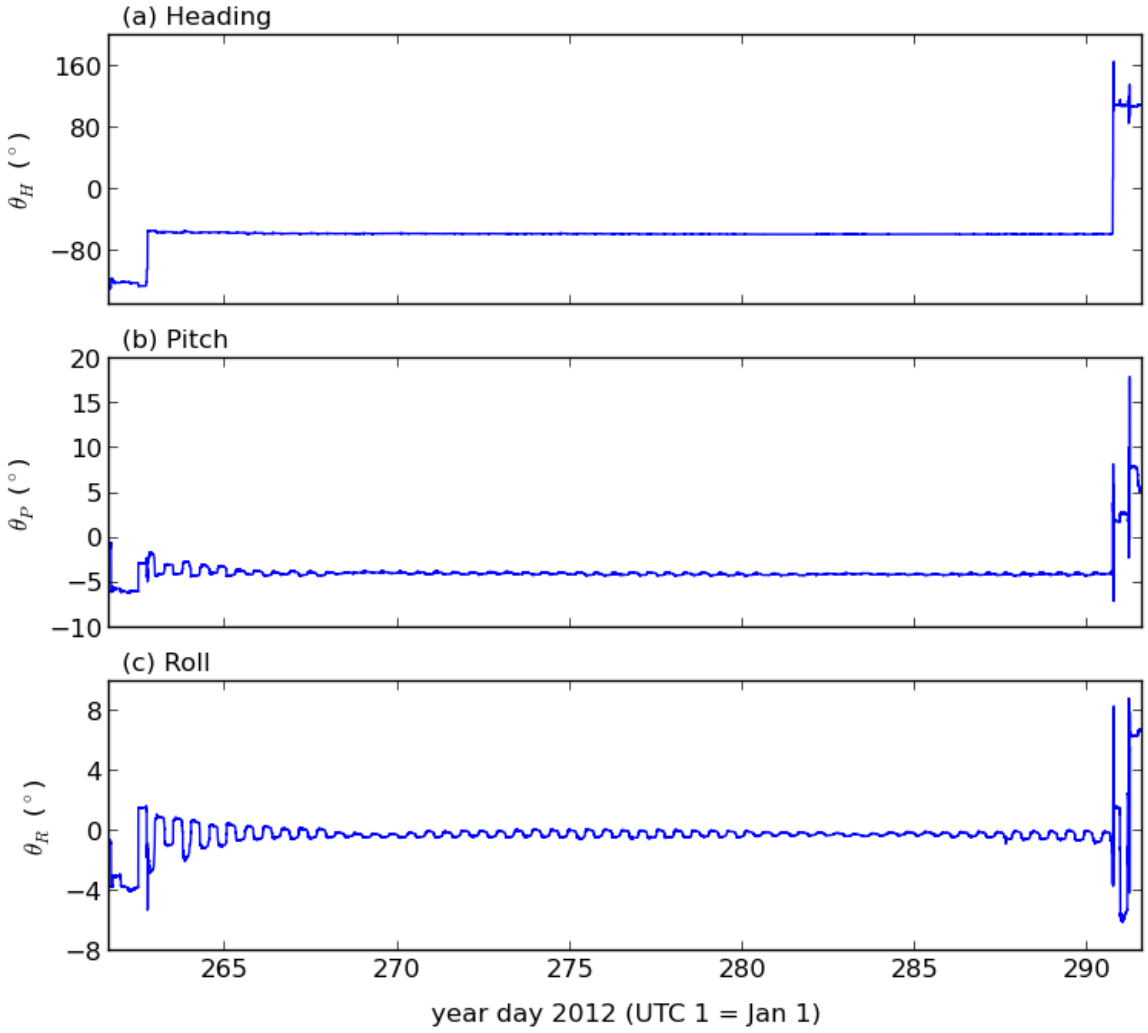

Figure A.13.2: Measurements of heading, pitch and roll at PP3.

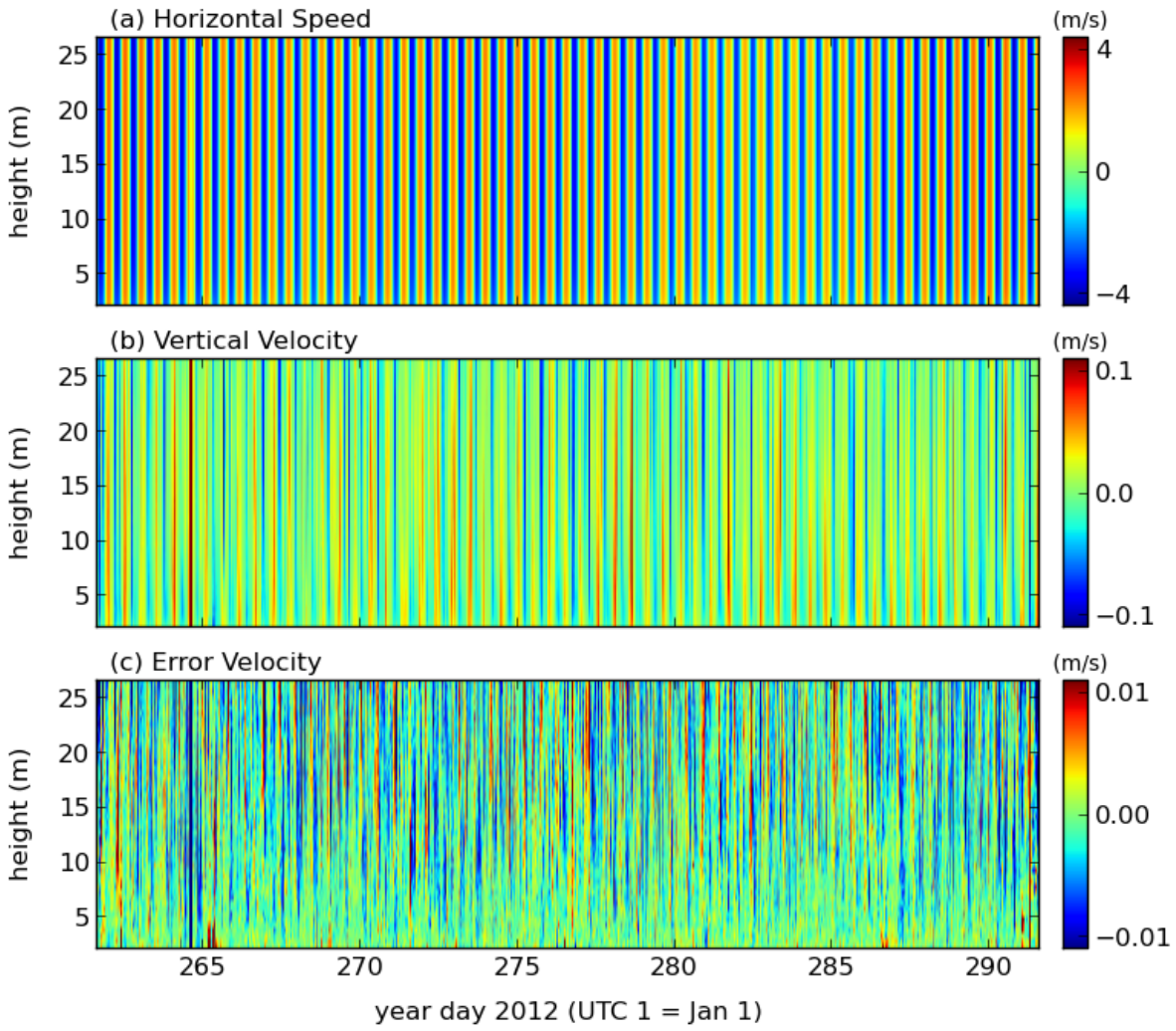

Figure A.13.3: Ten minute ensemble averaged horizontal current speeds, vertical velocities and error velocities for PP3. In panel (a), positive velocities correspond to the flood direction and negative velocities correspond to the ebb direction. The maximum depth is equivalent to 95% of the lowest low water.

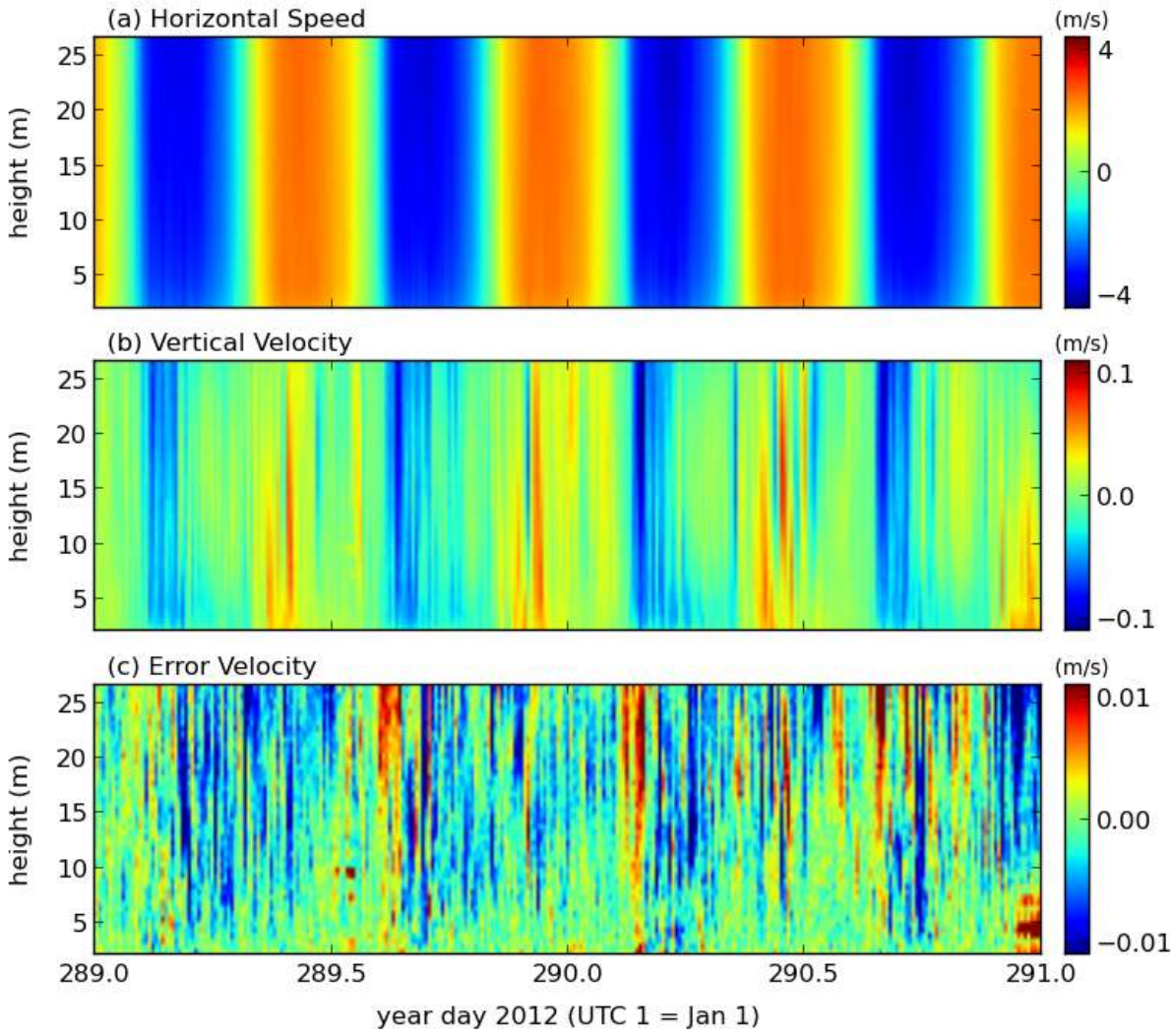

Figure A.13.4: As above, but during a 2-day period.

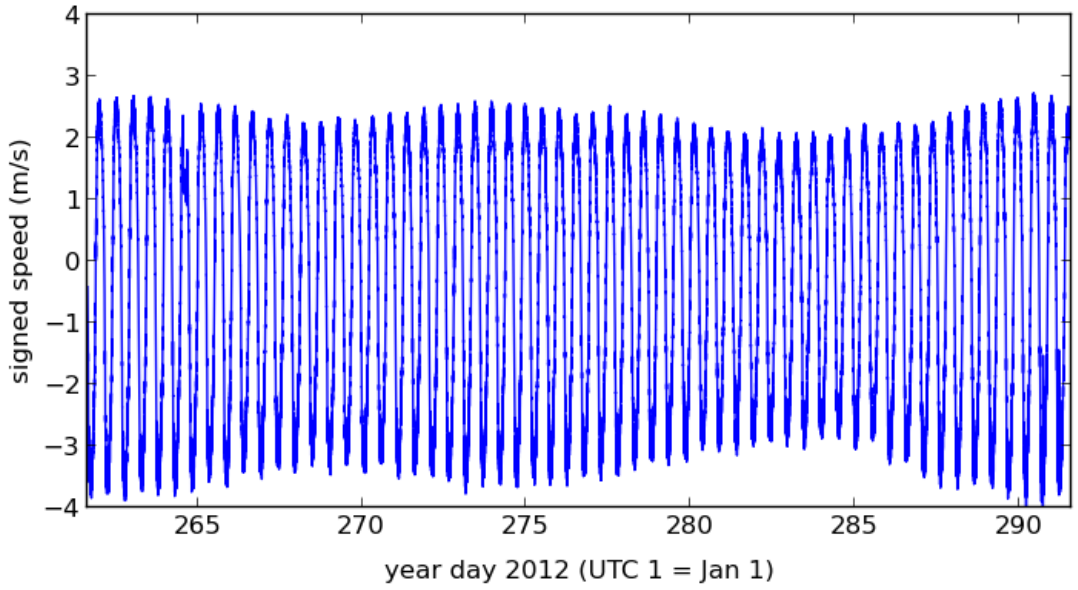

Figure A.13.5: Time series of the depth averaged velocity at PP3. The averages were computed to 95% of the surface signal. Positive velocities correspond to the flood direction and negative velocities correspond to the ebb direction.

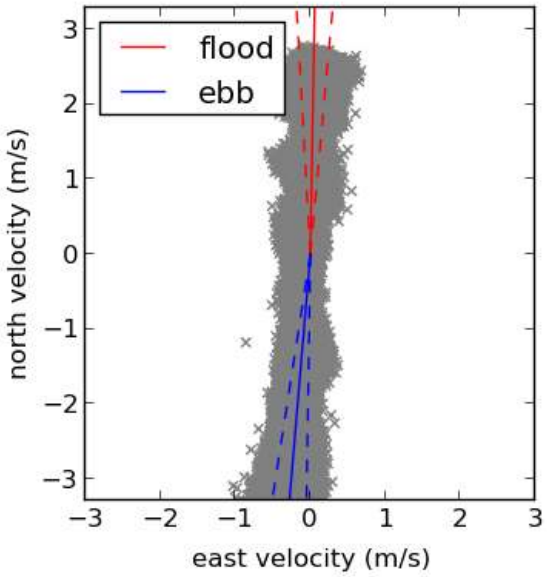

Figure A.13.6: The principal flow directions at PP3 are shown by the solid red and blue lines for the flood and ebb tides, respectively. The dashed lines indicate ±1 standard deviation from the mean. Individual values are plotted as grey x markers.

Constituent	Period	Elevation		Velocity			
	(hr)	Amplitude (m)	Phase (°)	Major (m/s)	Minor (m/s)	Inclination (°)	Phase (°)
M2	12.42	2.15	74	2.76	-0.03	87	330
N2	12.66	0.44	59	0.44	-0.00	87	318
S2	12.00	0.38	101	0.42	0.00	87	4
K1	23.93	0.12	165	0.02	0.00	87	67
M4	6.21	0.12	94	0.16	-0.03	80	110
O1	25.82	0.11	167	0.02	-0.00	85	28

Table A.13.1: Harmonic Analysis at PP3. The elevation fits were done over a period of 30 days and the velocity fits were done over a period of 30 days. The RMS amplitude of the residual elevation was 17 cm and the RMS amplitude of the residual current speed was 42 cm/s.

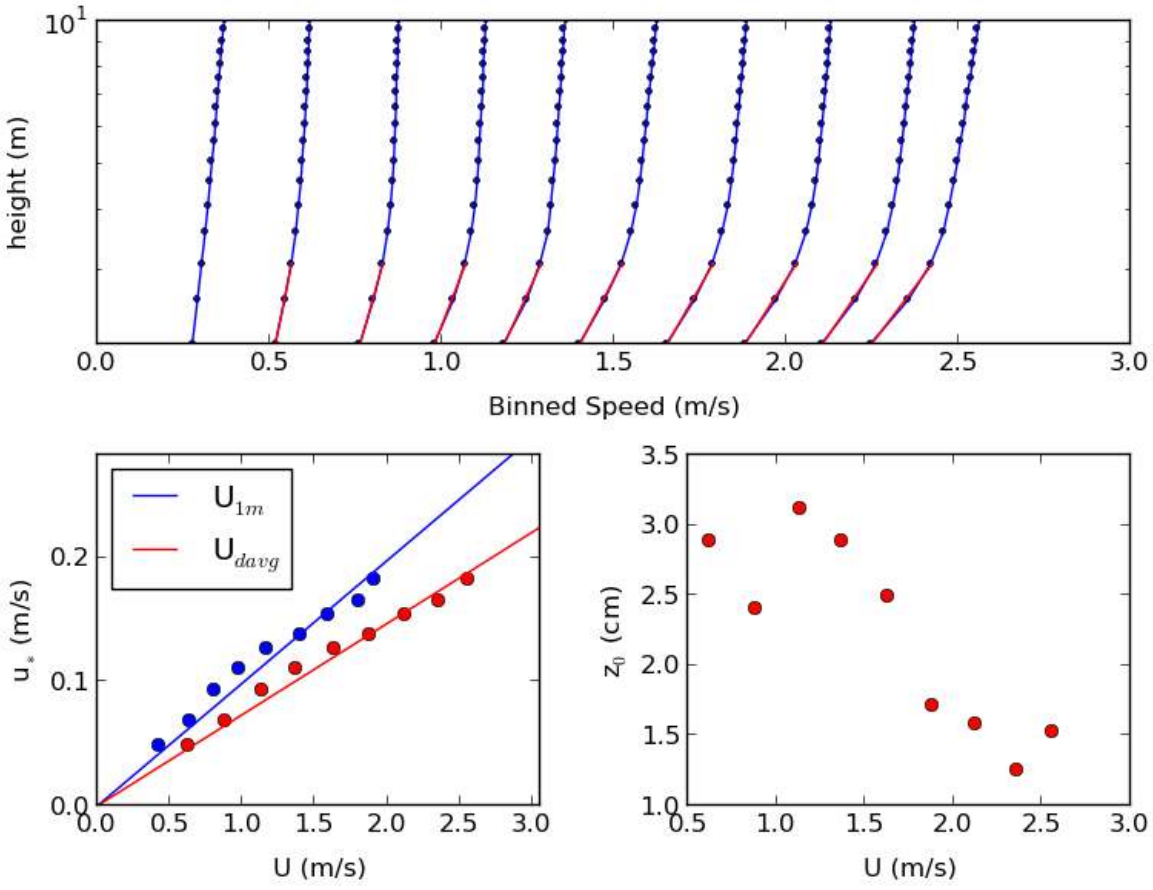

Figure A.13.7: The top panel shows the binned speed profiles during the flood tide at PP3. The red lines correspond to the law of the wall fits. The lower left panel plots u_* as determined from the law of the wall versus a reference speed. Since $u_*^2 = C_d U^2$, C_d is the is the square of the slope of the fitted line. These values are given in the table below. The lower right panel shows the estimates of z_0 from the law of the wall fits.

	Flood	Ebb
C_d $(U = V_{1m})$	0.0098	0.0083
C_d $(U = V_{davg})$	0.0054	0.0037
Mean z_0 (cm)	2.2	1.5

Table A.13.2: Drag coefficient, C_d, values at PP3. The values are separated into flood and ebb phases of the tide. Two different reference speeds were used – a theoretical estimate at $z = 1$ m (V_{1m}) and a depth averaged speed which was computed to 95 percent of the surface signal.

	A	B	C	D	E	F
Diameter (m)	8.0	10.0	12.0	8.0	10.0	12.0
Cut-in Speed (m/s)	1.0	1.0	1.0	1.0	1.0	1.0
Rated Power (kW)	-	-	-	500	500	500
Max Power Output (kW)	537	839	1208	500	500	500
Avg. Energy Production (kWh/day)	2800	4375	6300	2800	4217	5364
Operating Time (%)	82.0	82.0	82.0	82.0	82.0	82.0

Table A.13.3: Turbine statistics for six configurations at PP3. All turbines are assumed to have a hub height of 10 m and a water-wire efficiency of 0.4.

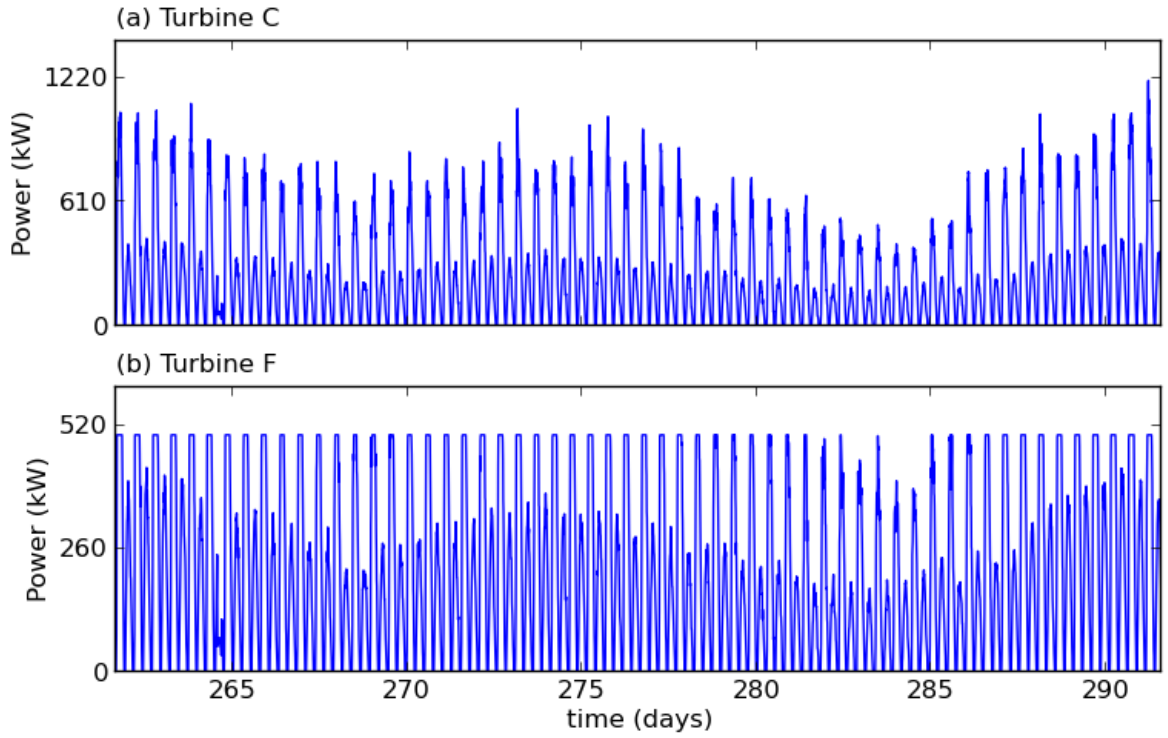

Figure A.13.8: A time series of the power output PP3 for the six turbine configuations listed in Table A.13.3. The power output was computed at a hub height of 10 m using the ten minute ensembled data.

A.14 PP4

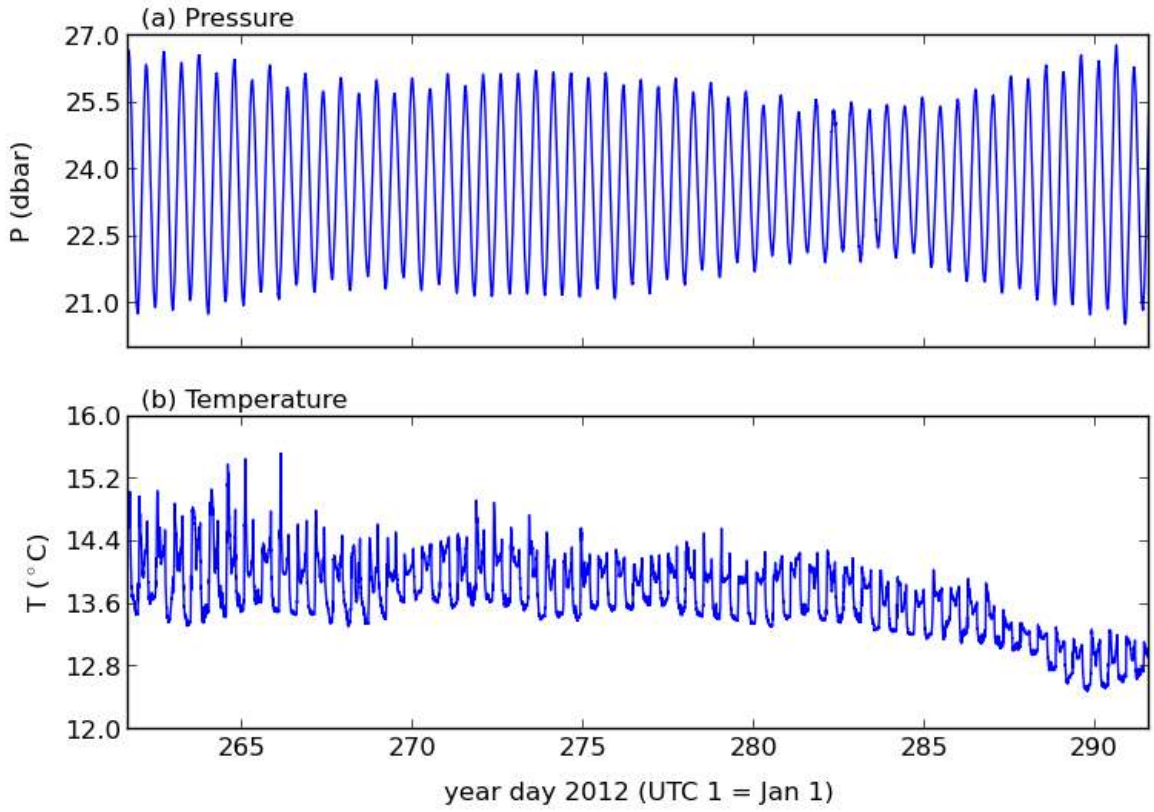

Figure A.14.1: Measurements of pressure and temperature at PP4.

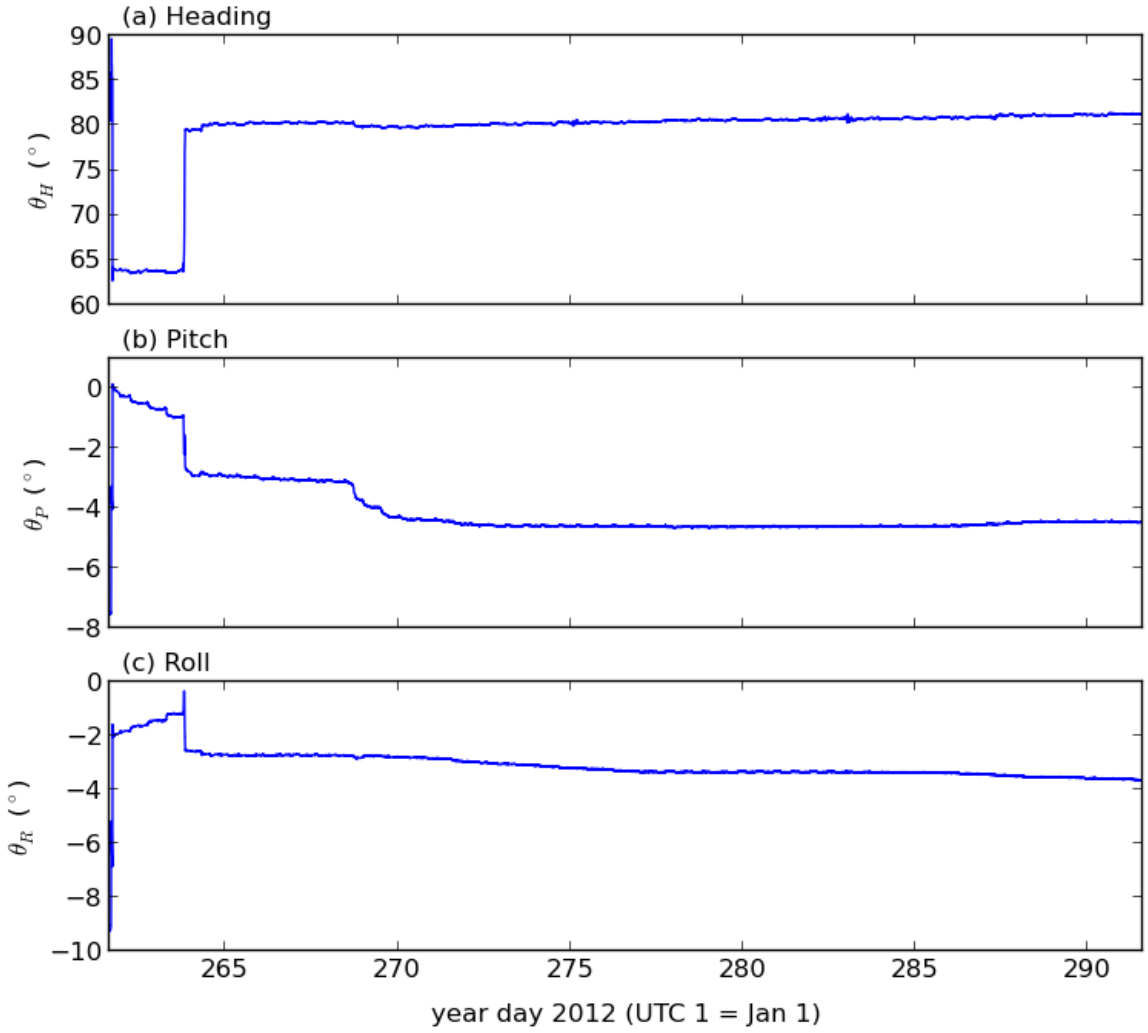

Figure A.14.2: Measurements of heading, pitch and roll at PP4.

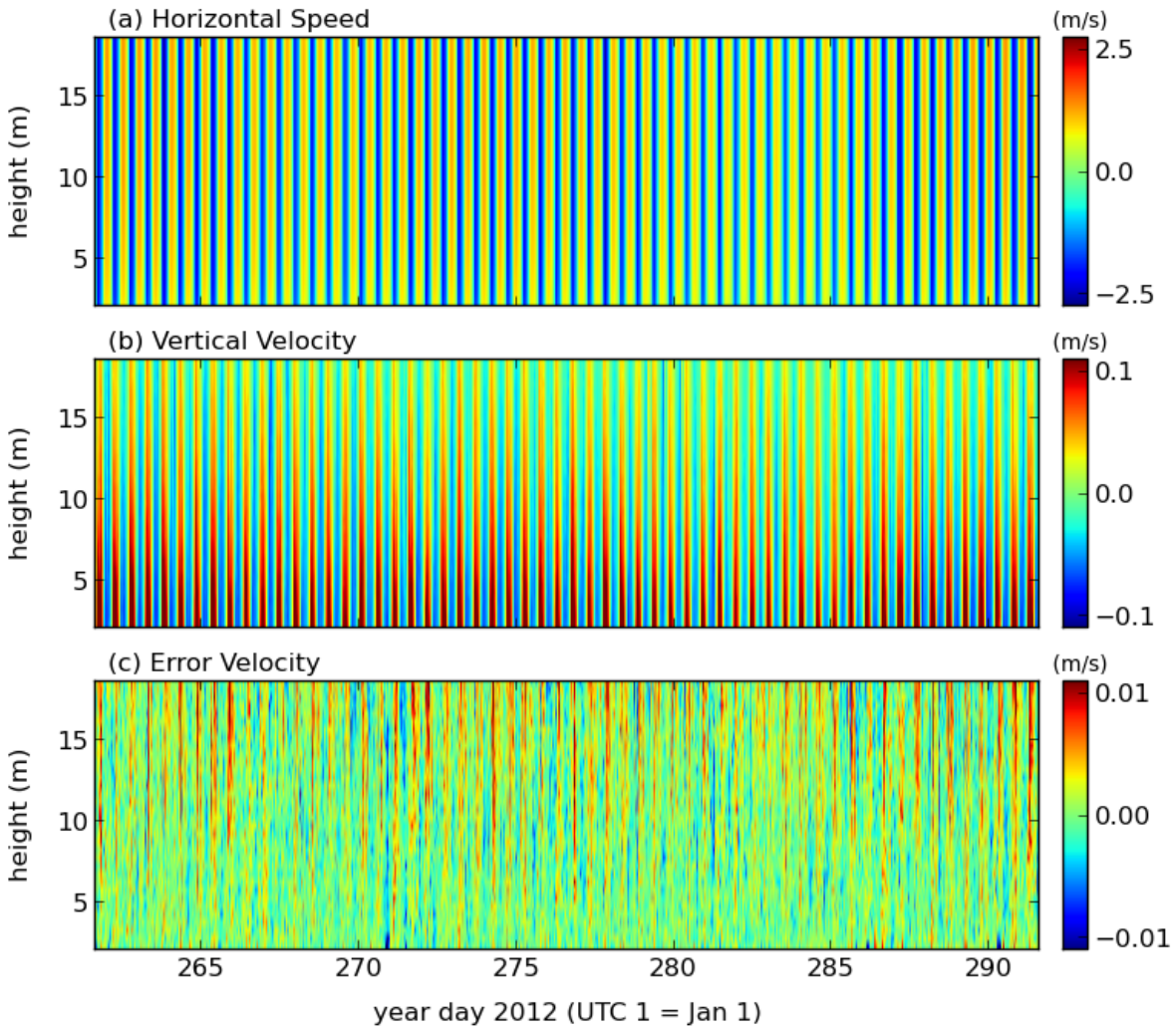

Figure A.14.3: Ten minute ensemble averaged horizontal current speeds, vertical velocities and error velocities for PP4. In panel (a), positive velocities correspond to the flood direction and negative velocities correspond to the ebb direction. The maximum depth is equivalent to 95% of the lowest low water.

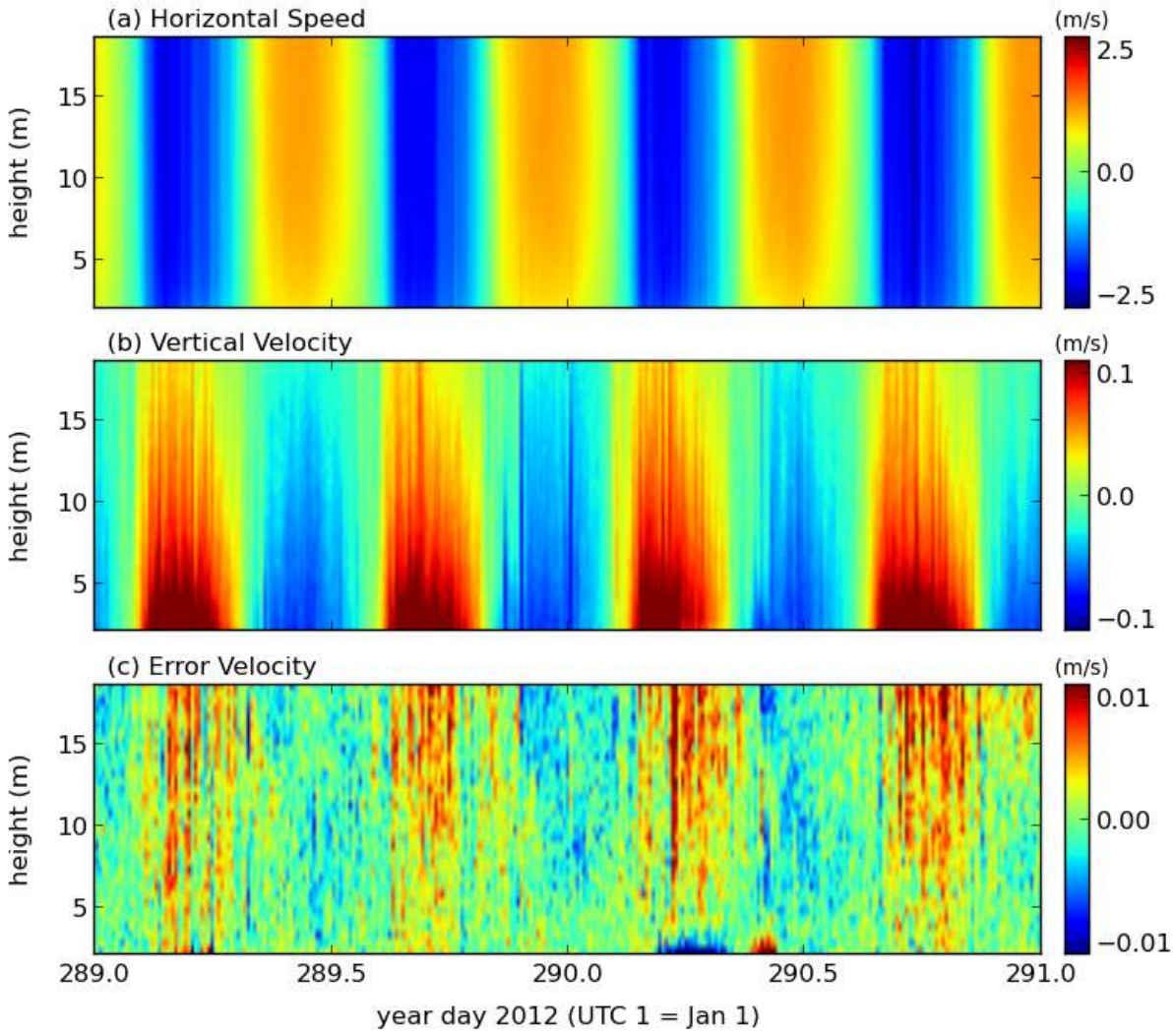

Figure A.14.4: As above, but during a 2-day period.

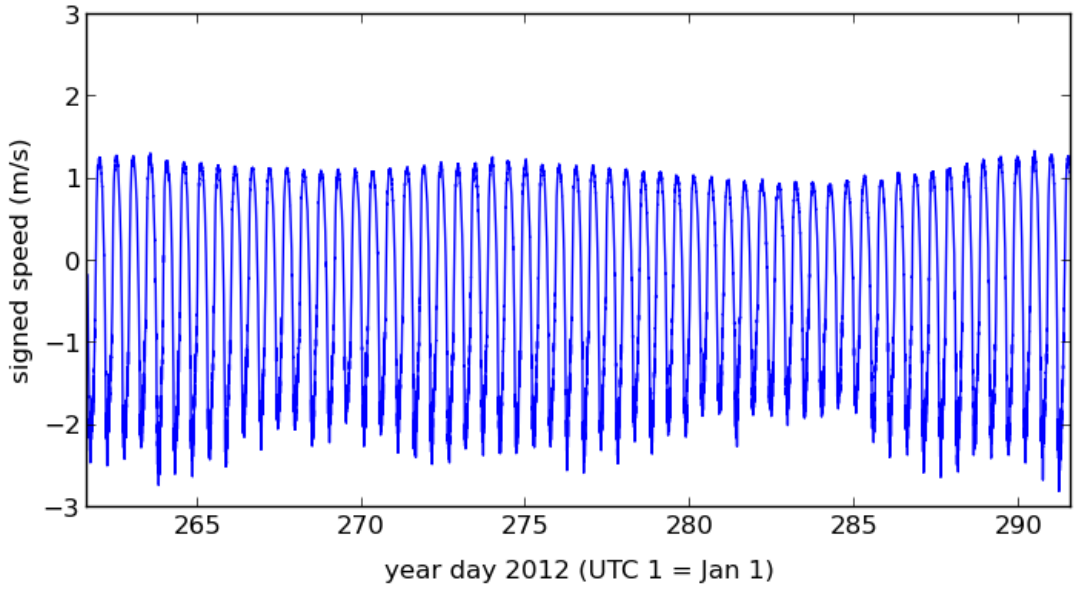

Figure A.14.5: Time series of the depth averaged velocity at PP4. The averages were computed to 95% of the surface signal. Positive velocities correspond to the flood direction and negative velocities correspond to the ebb direction.

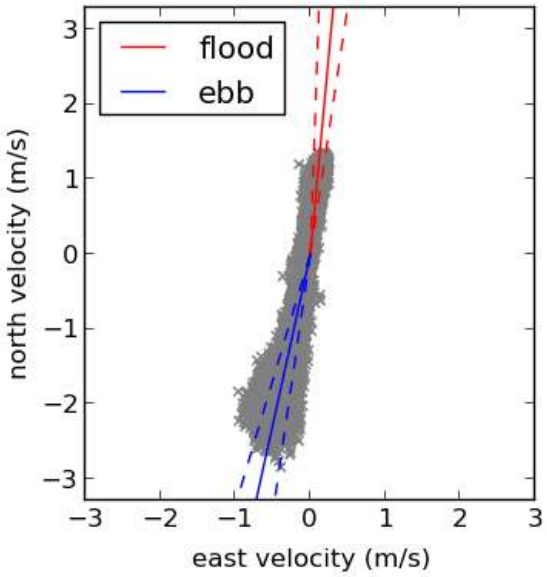

Figure A.14.6: The principal flow directions at PP4 are shown by the solid red and blue lines for the flood and ebb tides, respectively. The dashed lines indicate ±1 standard deviation from the mean. Individual values are plotted as grey x markers.

Constituent	Period (hr)	Elevation		Velocity			
		Amplitude (m)	Phase (°)	Major (m/s)	Minor (m/s)	Inclination (°)	Phase (°)
M2	12.42	2.11	73	1.51	0.01	80	330
N2	12.66	0.44	57	0.24	-0.00	81	318
S2	12.00	0.39	101	0.24	0.00	81	3
K1	23.93	0.12	171	0.02	-0.00	70	50
O1	25.82	0.11	175	0.01	-0.00	94	52
M6	4.14	0.03	212	0.12	-0.02	74	152

Table A.14.1: Harmonic Analysis at PP4. The elevation fits were done over a period of 30 days and the velocity fits were done over a period of 30 days. The RMS amplitude of the residual elevation was 11 cm and the RMS amplitude of the residual current speed was 30 cm/s.

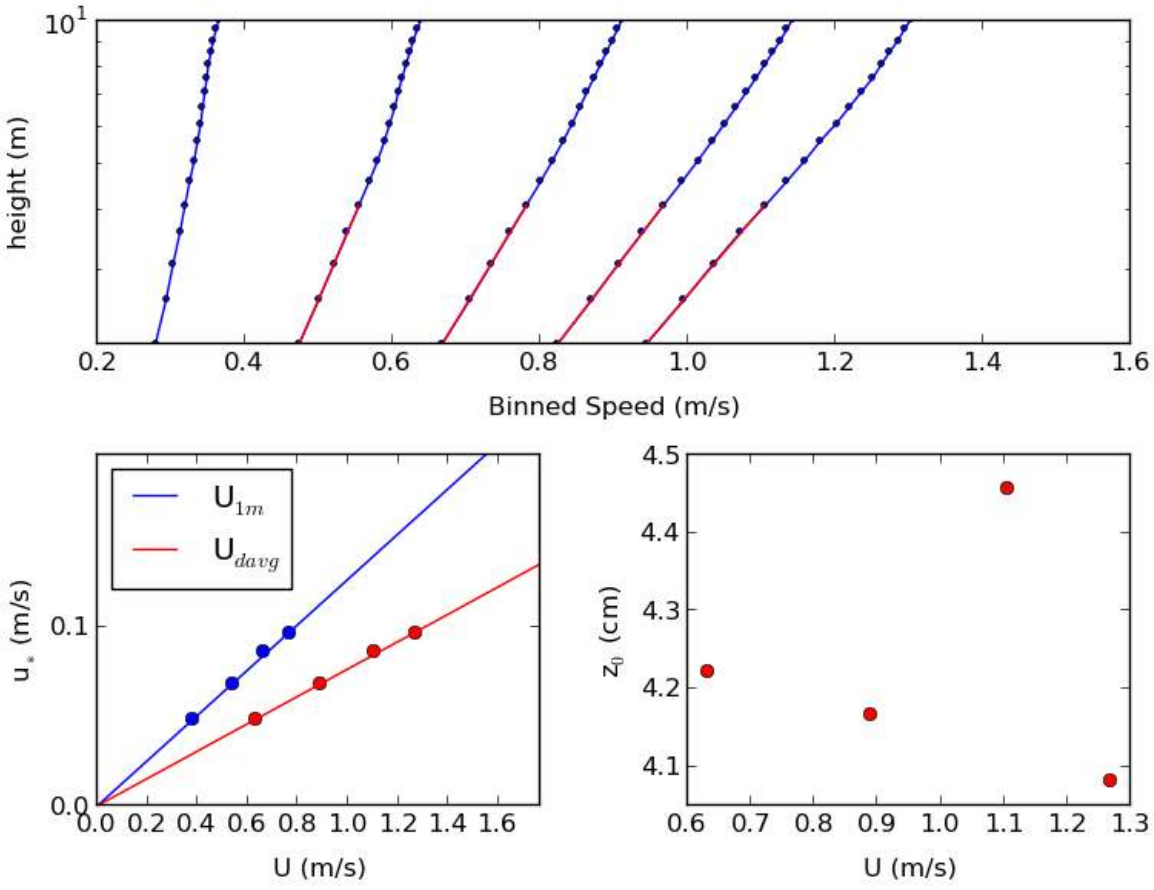

Figure A.14.7: The top panel shows the binned speed profiles during the flood tide at PP4. The red lines correspond to the law of the wall fits. The lower left panel plots u_* as determined from the law of the wall versus a reference speed. Since $u_*^2 = C_d U^2$, C_d is the is the square of the slope of the fitted line. These values are given in the table below. The lower right panel shows the estimates of z_0 from the law of the wall fits.

	Flood	**Ebb**
C_d $(U = V_{1m})$	0.0160	0.0033
C_d $(U = V_{davg})$	0.0058	0.0020
Mean z_0 (cm)	4.2	0.1

Table A.14.2: Drag coefficient, C_d, values at PP4. The values are separated into flood and ebb phases of the tide. Two different reference speeds were used – a theoretical estimate at $z = 1$ m (V_{1m}) and a depth averaged speed which was computed to 95 percent of the surface signal.

	A	**B**	**C**	**D**	**E**	**F**
Diameter (m)	8.0	10.0	12.0	8.0	10.0	12.0
Cut-in Speed (m/s)	1.0	1.0	1.0	1.0	1.0	1.0
Rated Power (kW)	-	-	-	500	500	500
Max Power Output (kW)	163	254	366	163	254	366
Avg. Energy Production (kWh/day)	535	836	1204	535	836	1204
Operating Time (%)	52.8	52.8	52.8	52.8	52.8	52.8

Table A.14.3: Turbine statistics for six configurations at PP4. All turbines are assumed to have a hub height of 10 m and a water-wire efficiency of 0.4.

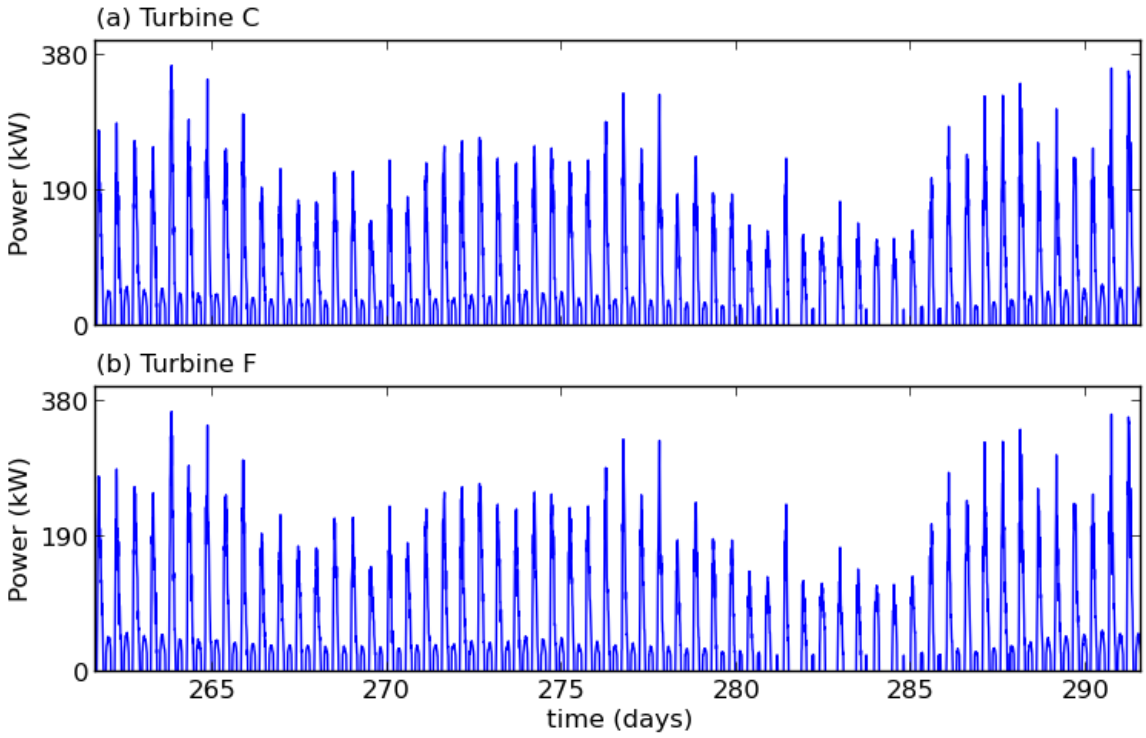

Figure A.14.8: A time series of the power output PP4 for the six turbine configuations listed in Table A.14.3. The power output was computed at a hub height of 10 m using the ten minute ensembled data.

A.15 PP5

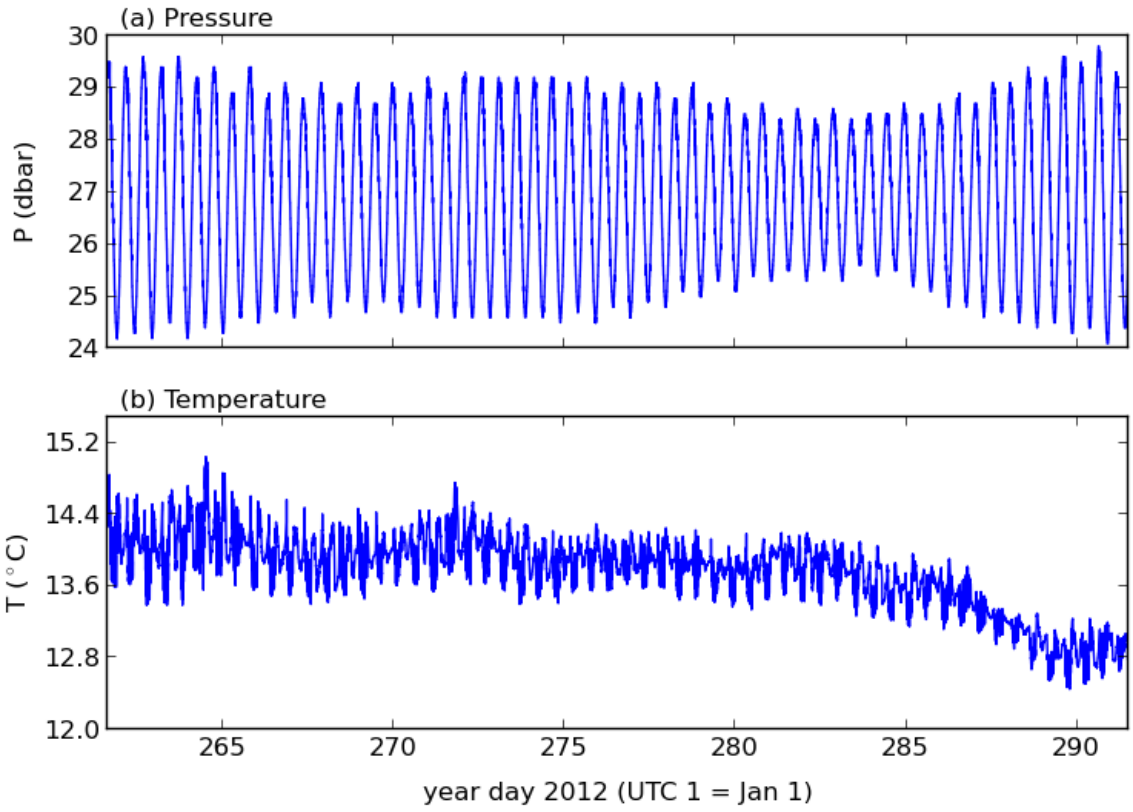

Figure A.15.1: Measurements of pressure and temperature at PP5.

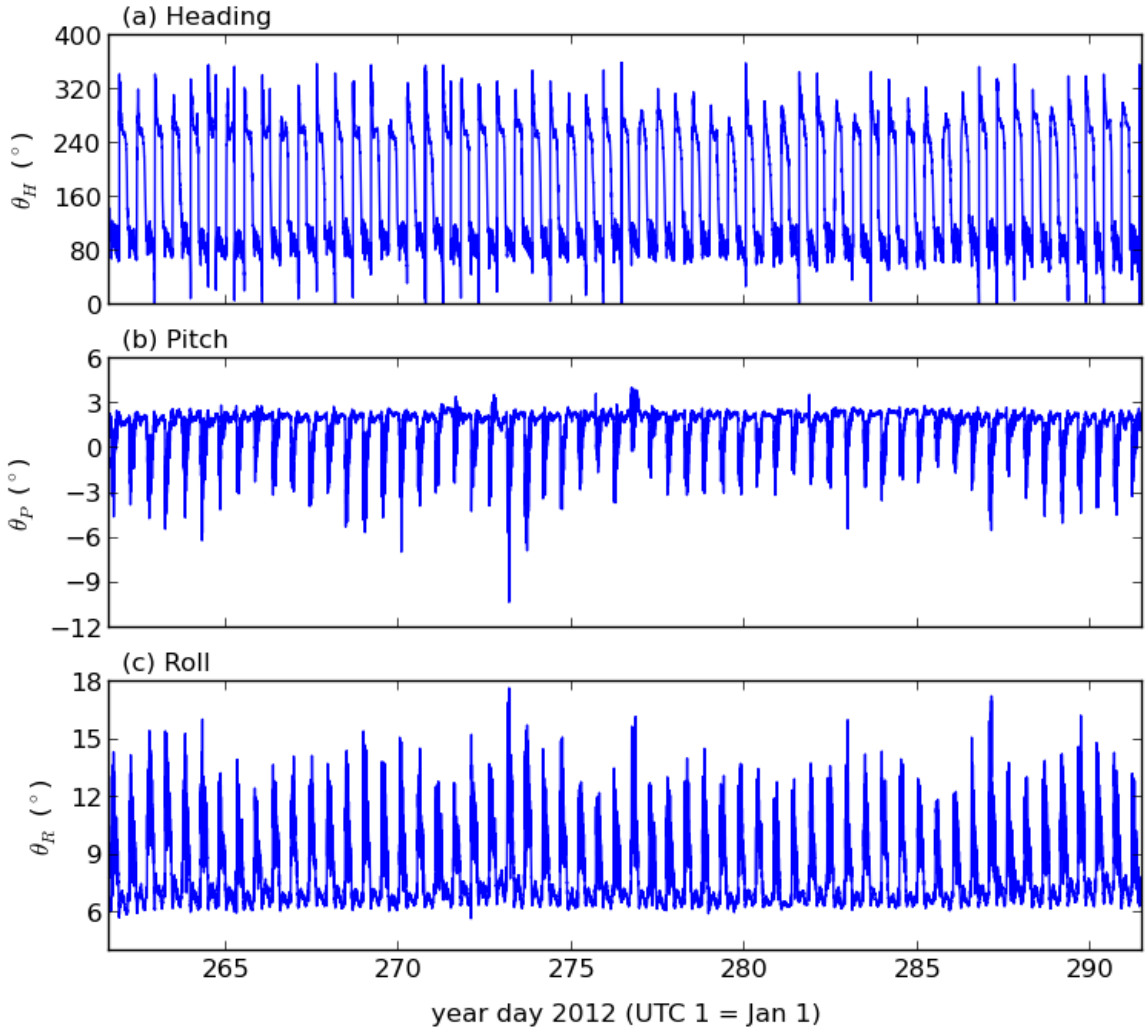

Figure A.15.2: Measurements of heading, pitch and roll at PP5.

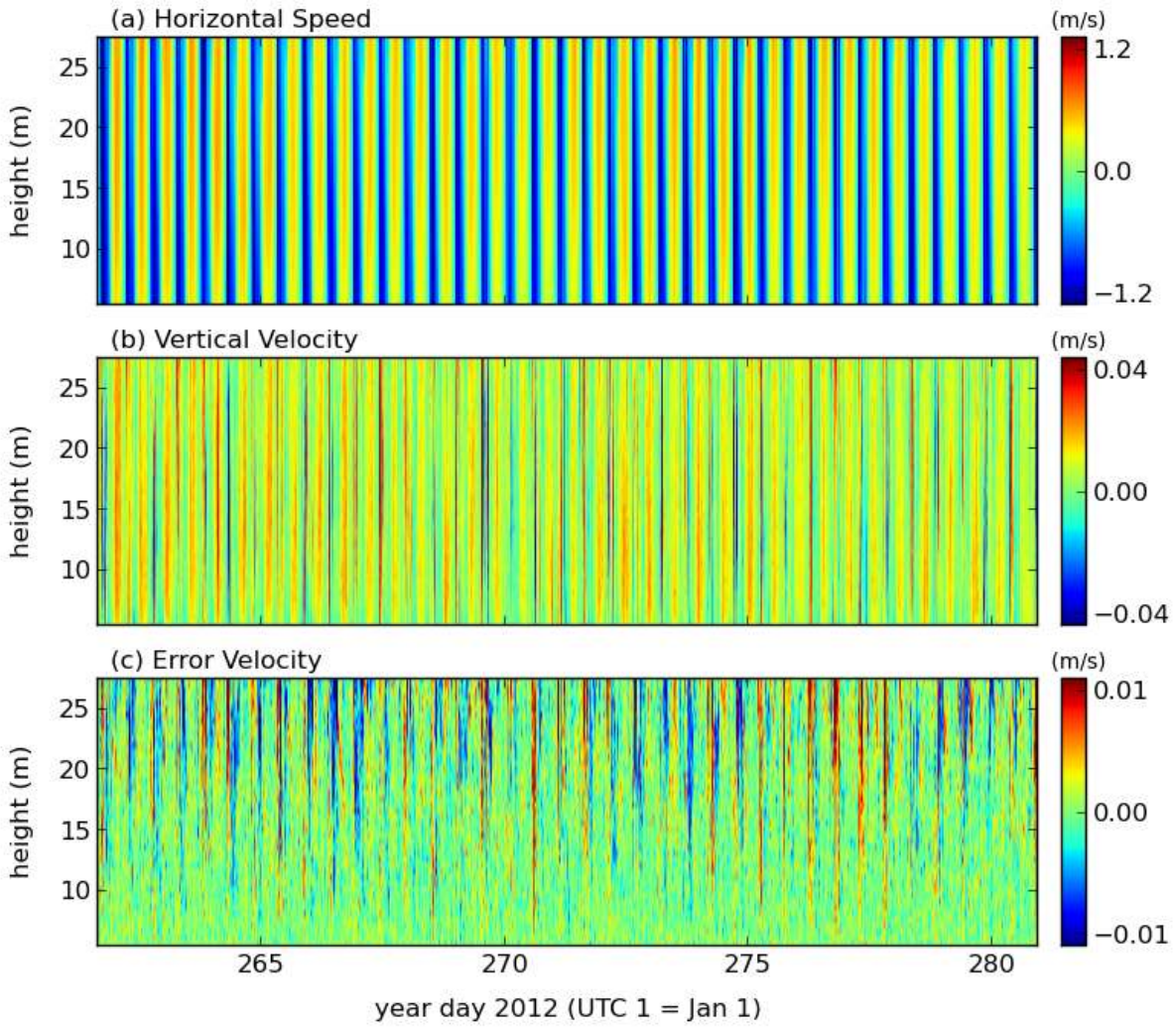

Figure A.15.3: Ten minute ensemble averaged horizontal current speeds, vertical velocities and error velocities for PP5. In panel (a), positive velocities correspond to the flood direction and negative velocities correspond to the ebb direction. The maximum depth is equivalent to 95% of the lowest low water.

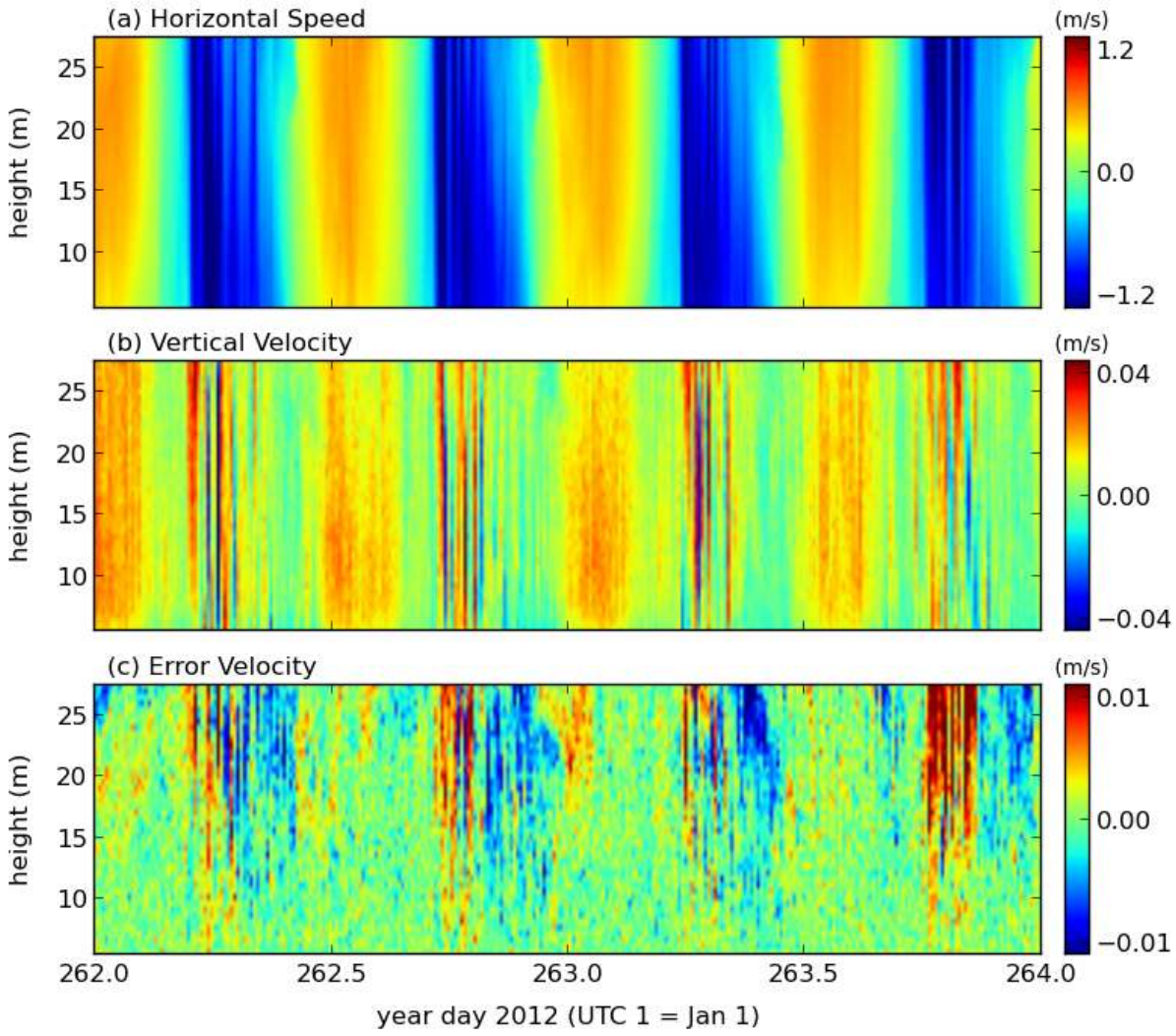

Figure A.15.4: As above, but during a 2-day period.

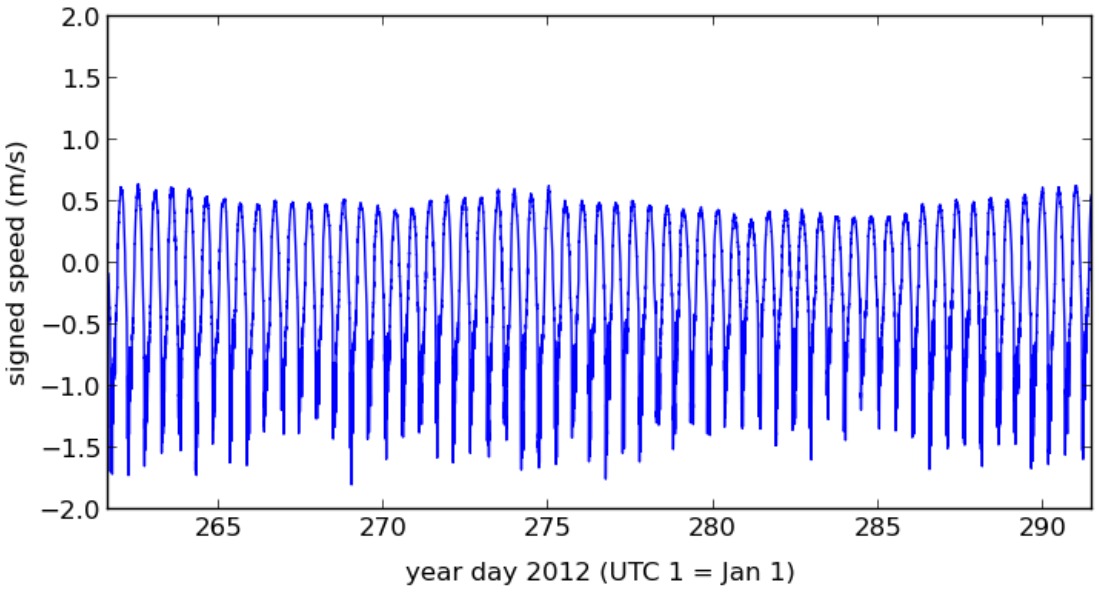

Figure A.15.5: Time series of the depth averaged velocity at PP5. The averages were computed to 95% of the surface signal. Positive velocities correspond to the flood direction and negative velocities correspond to the ebb direction.

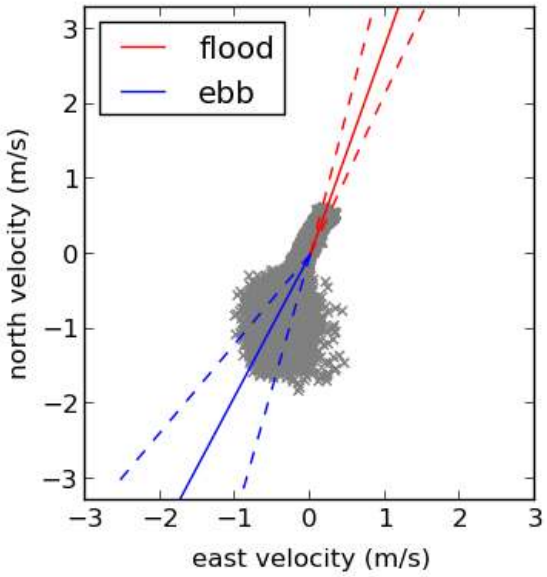

Figure A.15.6: The principal flow directions at PP5 are shown by the solid red and blue lines for the flood and ebb tides, respectively. The dashed lines indicate ±1 standard deviation from the mean. Individual values are plotted as grey x markers.

	A	B	C	D	E	F
Diameter (m)	8.0	10.0	12.0	8.0	10.0	12.0
Cut-in Speed (m/s)	1.0	1.0	1.0	1.0	1.0	1.0
Rated Power (kW)	-	-	-	500	500	500
Max Power Output (kW)	43	68	98	43	68	98
Avg. Energy Production (kWh/day)	58	91	131	58	91	131
Operating Time (%)	13.1	13.1	13.1	13.1	13.1	13.1

Table A.15.1: Turbine statistics for six configurations at PP5. All turbines are assumed to have a hub height of 10 m and a water-wire efficiency of 0.4.

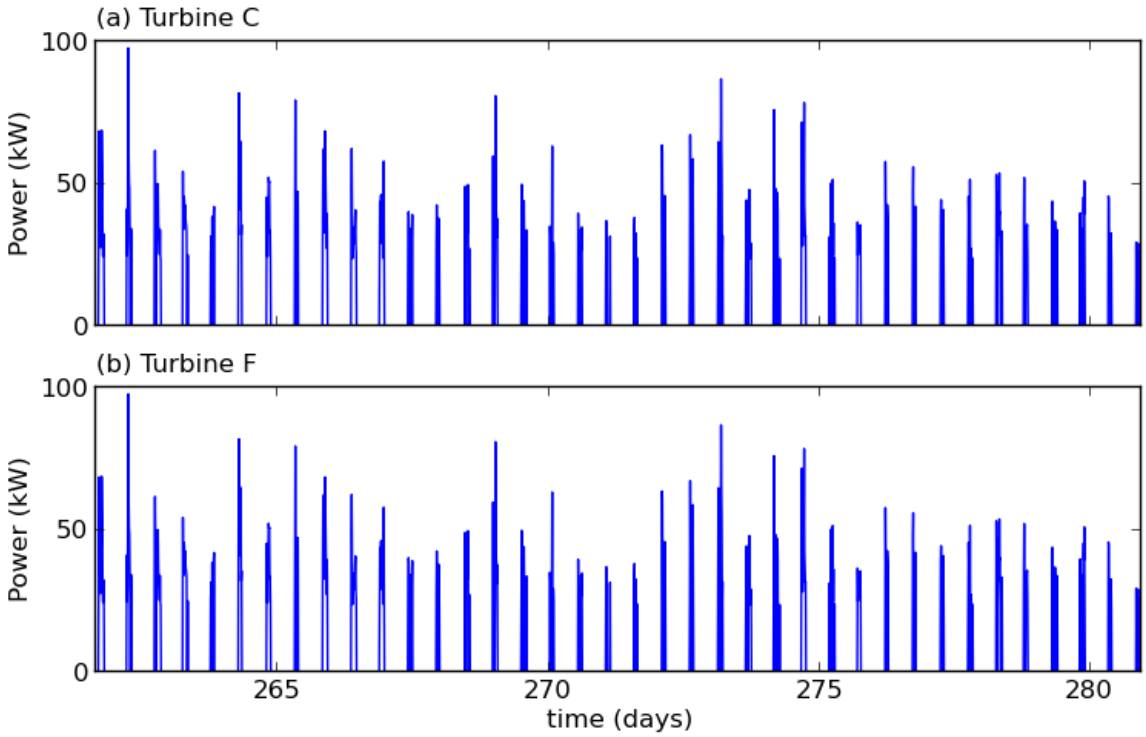

Figure A.15.7: A time series of the power output PP5 for the six turbine configuations listed in Table A.15.1. The power output was computed at a hub height of 10 m using the ten minute ensembled data.

A.16 IS1

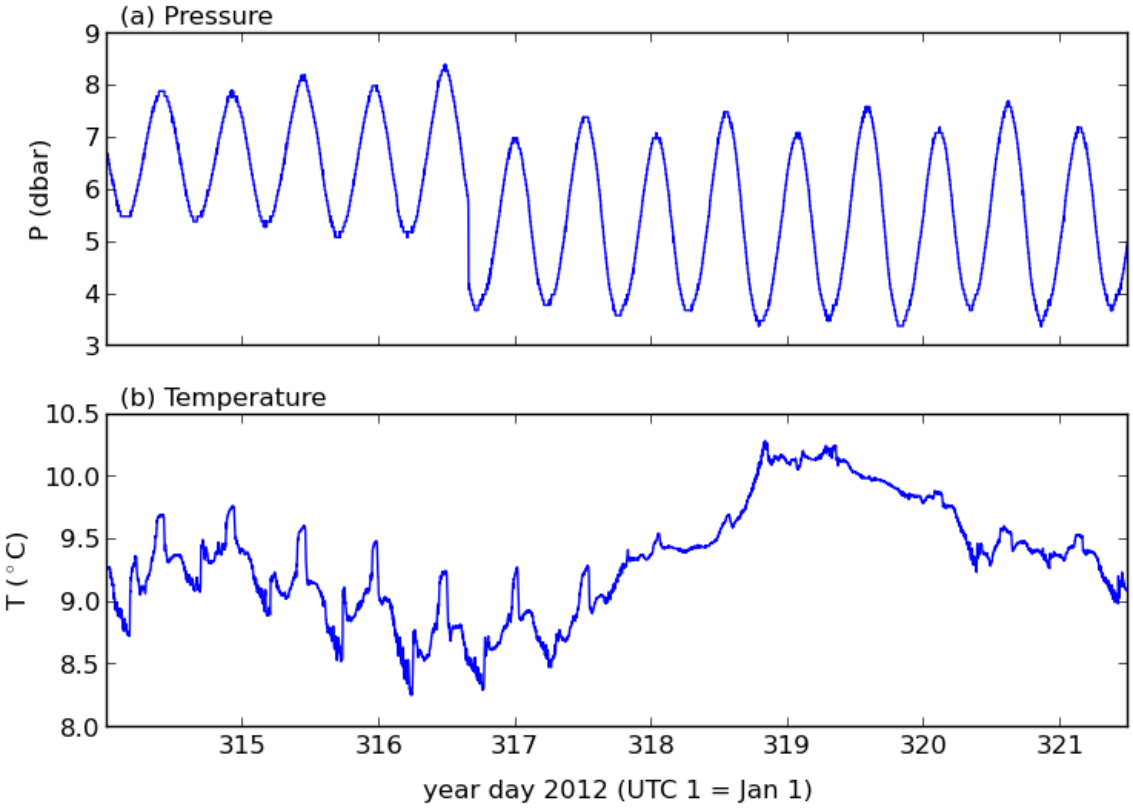

Figure A.16.1: Measurements of pressure and temperature at IS1.

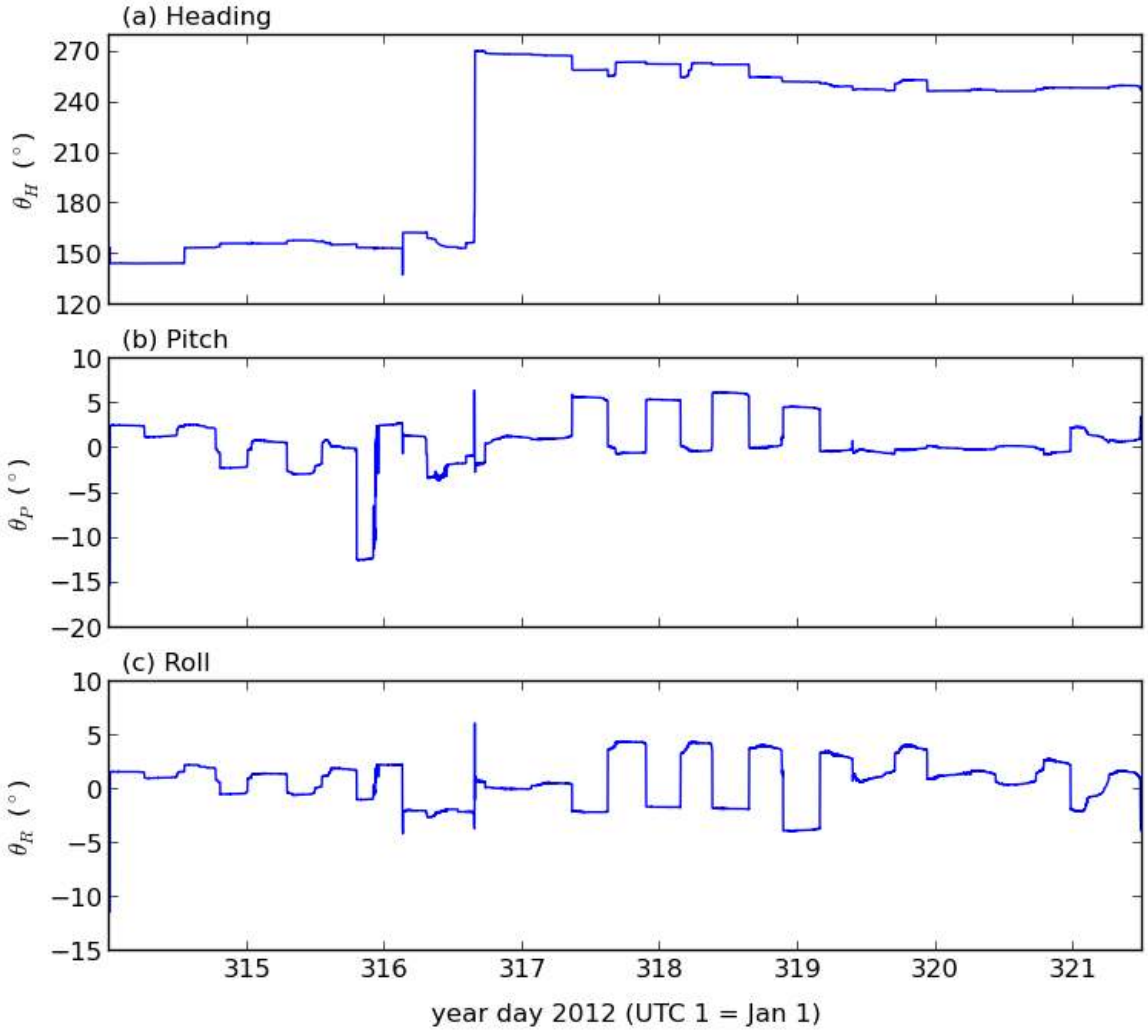

Figure A.16.2: Measurements of heading, pitch and roll at IS1.

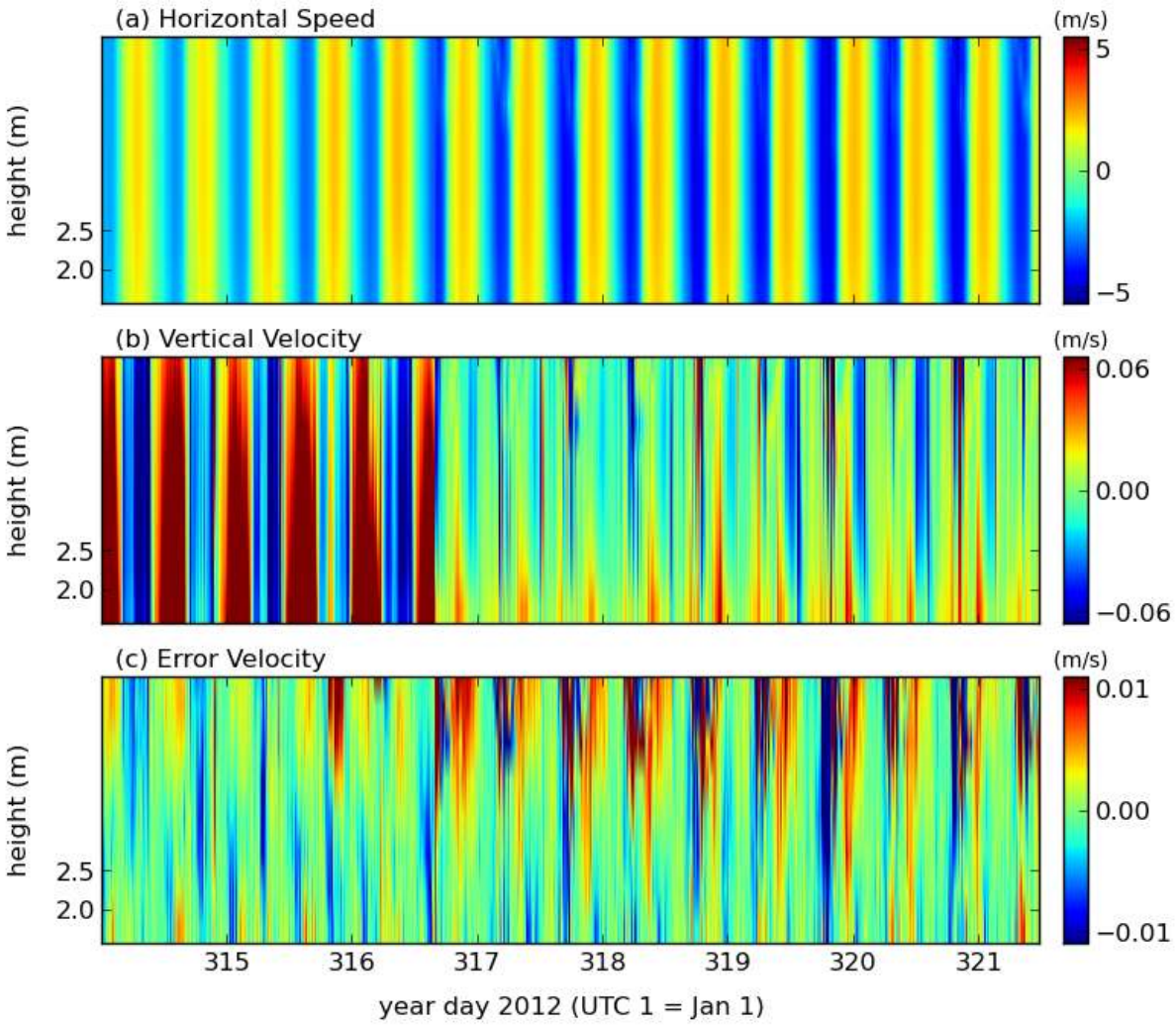

Figure A.16.3: Ten minute ensemble averaged horizontal current speeds, vertical velocities and error velocities for IS1. In panel (a), positive velocities correspond to the flood direction and negative velocities correspond to the ebb direction. The maximum depth is equivalent to 95% of the lowest low water.

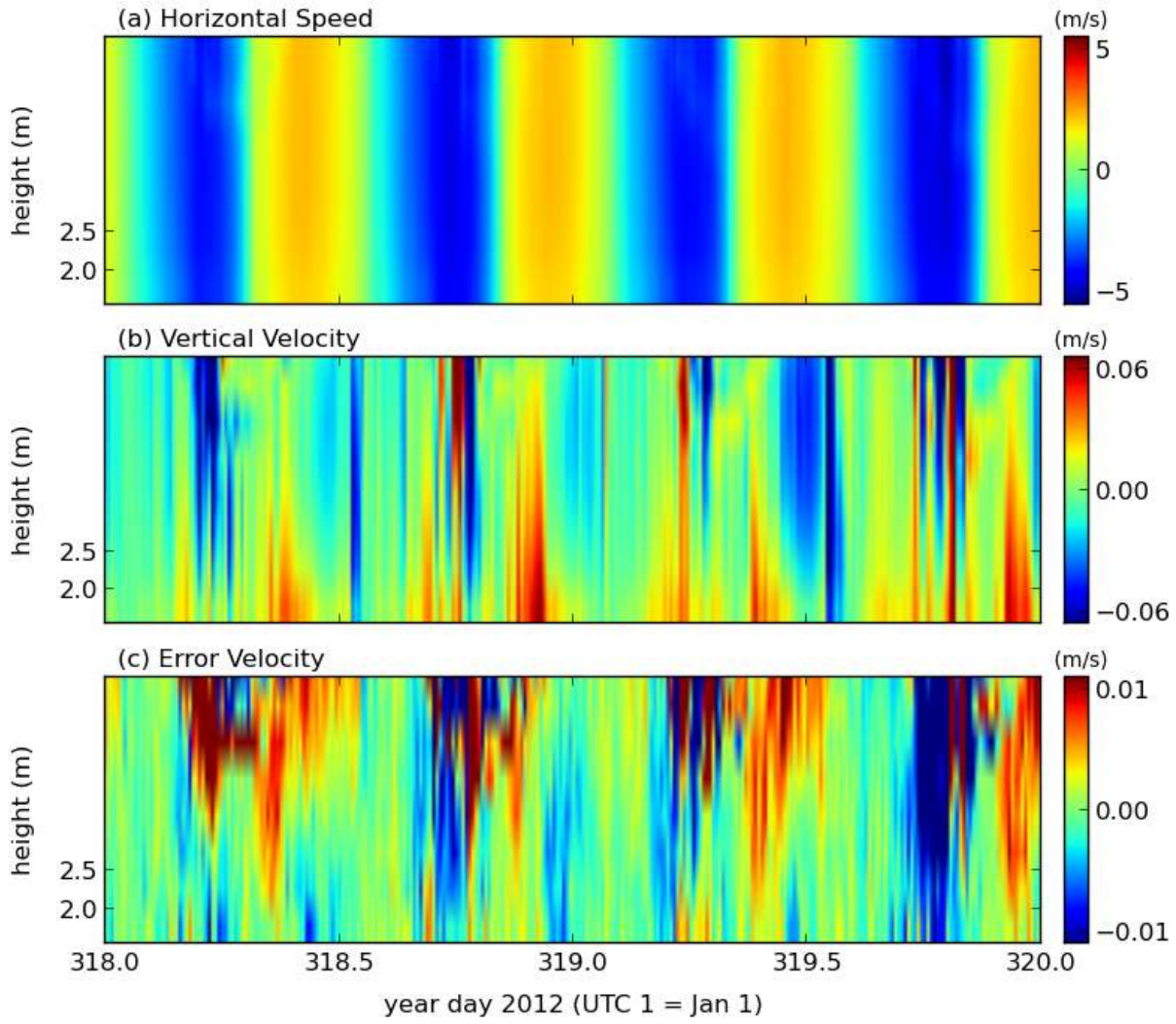

Figure A.16.4: As above, but during a 2-day period.

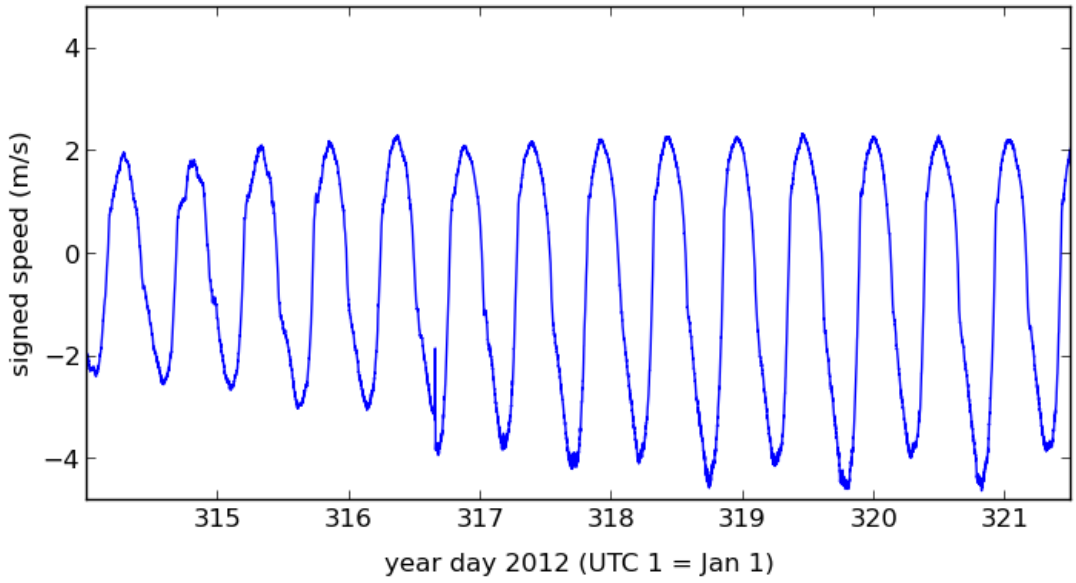

Figure A.16.5: Time series of the depth averaged velocity at IS1. The averages were computed to 95% of the surface signal. Positive velocities correspond to the flood direction and negative velocities correspond to the ebb direction.

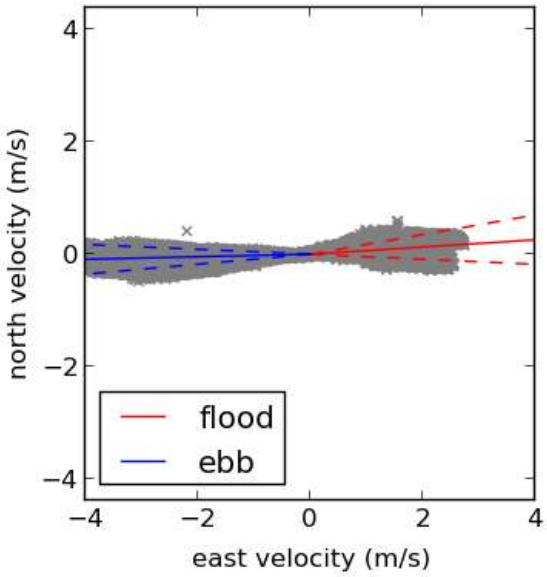

Figure A.16.6: The principal flow directions at IS1 are shown by the solid red and blue lines for the flood and ebb tides, respectively. The dashed lines indicate ±1 standard deviation from the mean. Individual values are plotted as grey x markers.

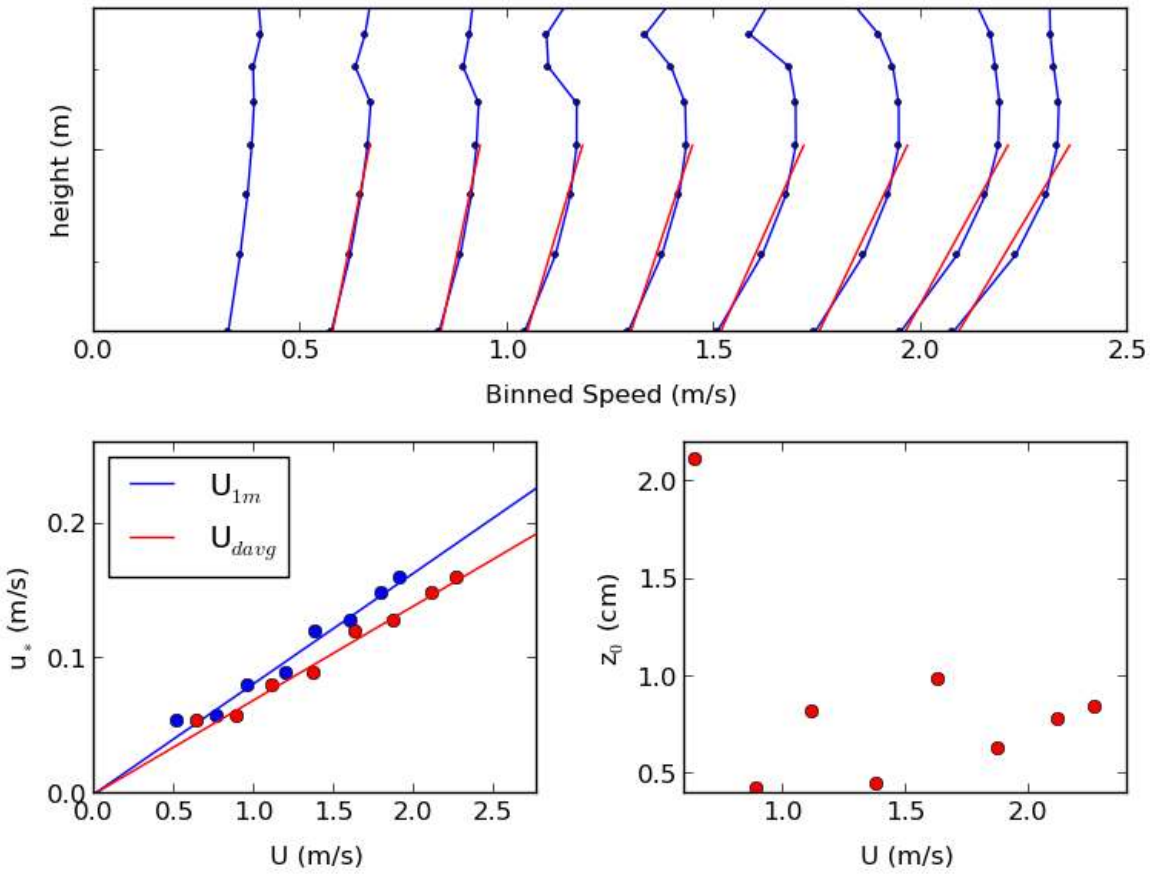

Figure A.16.7: The top panel shows the binned speed profiles during the flood tide at IS1. The red lines correspond to the law of the wall fits. The lower left panel plots u_* as determined from the law of the wall versus a reference speed. Since $u_*^2 = C_d U^2$, C_d is the is the square of the slope of the fitted line. These values are given in the table below. The lower right panel shows the estimates of z_0 from the law of the wall fits.

	Flood	**Ebb**
C_d $(U = V_{1m})$	0.0067	0.0050
C_d $(U = V_{davg})$	0.0049	0.0038
Mean z_0 (cm)	0.9	1.2

Table A.16.1: Drag coefficient, C_d, values at IS1. The values are separated into flood and ebb phases of the tide. Two different reference speeds were used – a theoretical estimate at $z = 1$ m (V_{1m}) and a depth averaged speed which was computed to 95 percent of the surface signal.

	A	B	C	D	E	F
Area (m^2)	10.0	20.0	30.0	10.0	20.0	30.0
Effective Diameter (m)	3.6	5.0	6.2	3.6	5.0	6.2
Cut-in Speed (m/s)	1.0	1.0	1.0	1.0	1.0	1.0
Rated Power (kW)	-	-	-	500	500	500
Max Power Output (kW)	190	380	569	190	380	500
Avg. Energy Production (kWh/day)	702	1404	2106	702	1404	2090
Operating Time (%)	83.4	83.4	83.4	83.4	83.4	83.4

Table A.16.2: Turbine statistics for six configurations at IS1. All turbines are assumed to be horizontally orientated cross-flow turbines with a hub height of 2 m and a water-wire efficiency of 0.4.

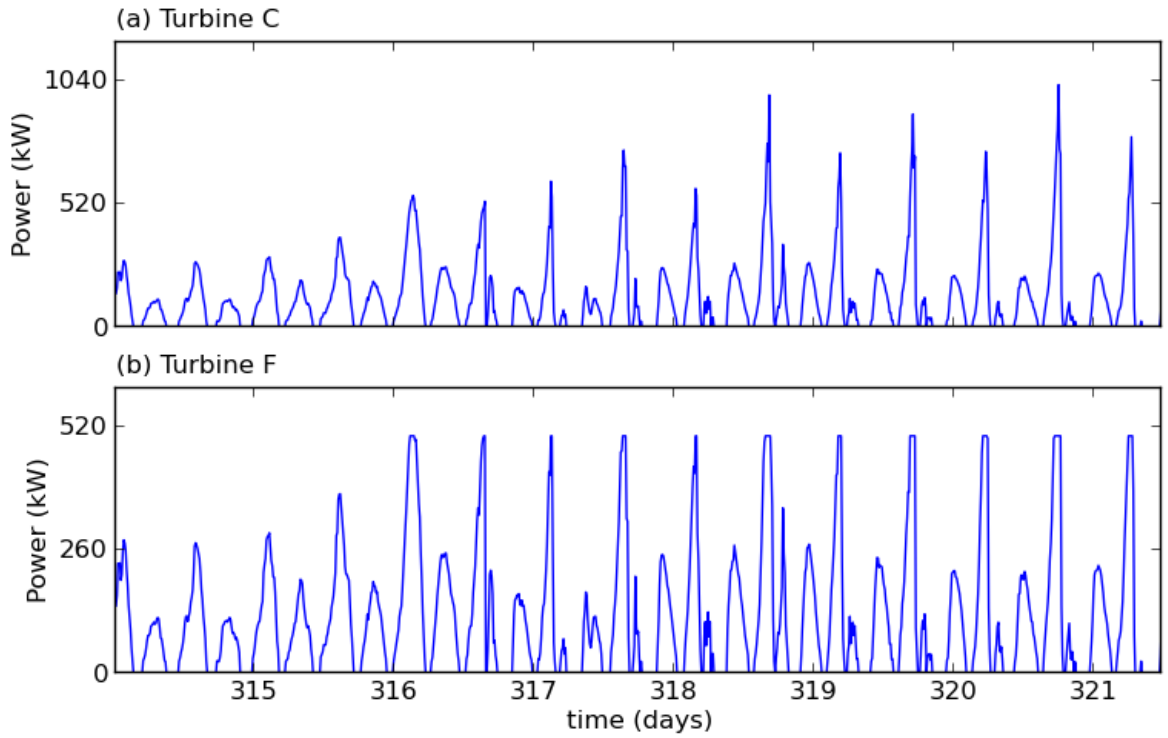

Figure A.16.8: A time series of the power output IS1 for the six turbine configuations listed in Table A.16.2. The power output was computed using the ten minute ensembled data. For this site, the turbines were assumed to be horizontally orientated cross-flow devices with a hub height of 2 m.